Comparison of methods to estimate fuel moisture content in different forest stand types in central British Columbia

By

Rulan Xiao

B.Sc., Simon Fraser University, 2020

A THESIS SUBMITTED IN PARTIAL FULFILMENT OF THE REQUIREMENTS FOR THE DEGREE OF MASTER OF SCIENCE IN

The Natural Resources and Environmental Studies Graduate Program

(Geography)

Supervisor: Dr. Joseph Michael Shea

Committee members: Drs. Phil Burton and Ché Elkin

UNIVERSITY OF NORTHERN BRITISH COLUMBIA

May 2023

Abstract

Wildfires are a growing threat due to climate change, and they often leave unburned forest patches called fire refugia. While young forests in some regions burn more severely, preliminary observations in central British Columbia suggest that managed juvenile forests exhibit lower fire severity, potentially influenced by fuel moisture conditions, and stand characteristics. To identify the role of fuel moisture in the formation of juvenile stand fire refugia, this research collects and examines ground-based, empirically modelled, and remote sensing indices of greenness, moisture, and fire severity.

This thesis investigates the fuel moisture contents (FMC) of duff, fine woody debris, and foliage at six locations near Prince George and Smithers, British Columbia (BC), over two summers (2021 and 2022). A total of 6116 individual samples of foliage, fine woody debris, and duff were collected from open, juvenile, and mature conifer forest stands and analysed for moisture content (MC). On average, the MC of duff and fine woody debris samples was higher in juvenile and mature forests than open sites. In contrast, open forests had higher foliage MC than the other forests. Observations of FMC were used to evaluate the accuracy of FMC estimates extracted from the Canadian Forest Fire Weather Index (FWI) system. Observations of FMC were also compared with remote sensing indices to assess the utility of using spaceborne (Landsat 8&9, Sentinel 2) remote sensing to predict local FMC.

Three versions of the FWI model were used to estimate FMC: the original FWI model which uses the closest fire weather station, and versions that used updated parameters based on local fuel conditions and in-stand weather data. When estimating fine woody debris MC, the best statistical results are obtained with locally calibrated models at open stands. However, the original FWI model provides better estimates of duff MC in juvenile stands.

For remote sensing of foliar MC in juvenile stands, the Normalized Difference Moisture Index (NDMI) had a higher R^2 value (0.334) and a lower RMSE than other indices, while the NDMI gave the best result for foliar MC in mature forests (R^2 = 0.160). For fine woody debris and duff MC in open stands, none of the remote sensing indices

tested have $R^2 > 0.1$ when estimating duff and fine woody debris MC. However, the RMSE of using empirical models from FWI to estimate duff (lowest at 59.95% RMSE) and fine woody debris (21.13%) MC was higher than remote sensing (41.64% for duff, 17.50% for fine woody debris).

Remote sensing indices such as NDMI and GNDVI (Green Normalized Difference Vegetation Index) were used to estimate pre-burn FMC, and the estimated FMC results were found to be generally higher at juvenile stands than mature forest from a case study area from Plateau Complex Wildfire of 2017. Lower remote sensing estimates of FMC in mature stands corresponded to higher burn severities.

Acknowledgments

I like to take this opportunity to express my gratitude to Dr. Joseph Shea, my supervisor, for providing me with the chance to work on such an important project. This study is a side extension of Dr. Phil Burton's project, which already had a good quantity of material for me to work with. Dr. Phil Burton and Dr. Ché Elkin, members of my committee, have provided numerous helpful comments regarding my thesis work process. Vanessa Foord provided and installed weather sensors for this research, which was extremely important for data collection.

Mackenzie McLean, Morgan Endacott, Dongxu Piao, Shiyuan Jing, Allie Golt at Prince George, and Clayton Rose and Trevor Schibli at Smithers have been invaluable in gathering fuel moisture data for the 2021 and 2022 summers.

My funding comes from the Natural Sciences and Engineering Research Council and Natural Resource Canada. Also, UNBC provided me with teaching assistant opportunities as well, which also helped this research proceed. My parents Shu Cong and Ruiqi Xiao have been understanding and supportive of my ongoing research journey.

I acknowledge my work is located on unceded Lheidli T'enneh and Wet’suwet’en territory.

Table of contents

Figures:

Tables:

Appendix:

1. Introduction

Wildfires are a serious threat to humans, infrastructure, and industry (McGee et al., 2015). They are expected to increase in frequency and severity as a result of climate change (Flannigan et al., 2000). In the western Cordillera of North America, wildfires frequently leave unburned blocks of forest known as fire refugia or fire islands (Krawchuk et al., 2016). According to a prior study in southwestern Oregon, USA, young forests burn more severely, and many old forests were left largely unburned as wildfire refugia (Zald & Dunn, 2018). However, preliminary observations from central British Columbia (BC) showed that some juvenile forests burn less severely than mature forests (Burton et al., 2019). Typically, distinct from naturally regenerating forests, young forests planted after logging in central BC are characterised by a dense uniform structure of a single tree species (Wang et al., 2019). Managed juvenile forest stands in central BC have several plantation features: uniform tree species (often lodgepole pine, *Pinus contorta* var. *latifolia* trees) and tight spacing between them (Burton, 2022). The difference between fire refugia in central BC and other regions could be caused by a disparity in fuel moisture conditions, the effects of the stand characteristics on the factors that influence fire spread, or both. Previous research has shown that fuel components in different stand types can influence fire behaviour (Kane et al., 2015; Dunn & Bailey, 2016).

Specific approaches have used remote sensing and weather data to estimate the fuel moisture content (FMC) of flammable materials found in nature. Fuel moisture content is a strong determinant of wildfire susceptibility and behaviour (Scott & Burgan, 2005, Krawchuk et al. 2009). The Canadian Forest Fire Weather Index (FWI) system is widely used to measure and communicate forest fire danger in Canada (Van Wagner, 1987). Parts of FWI can be used to estimate the moisture content (MC) of fine woody debris and duff around fire weather stations, which were located in forest openings (Van Wagner, 1987; De & William, 1998). Previous research has used remote sensing to estimate MC in broadleaf (Danson & Bowyer, 2004) and coniferous foliage in western Montana, USA (Qi et al., 2014). Previous studies have also used remotely sensed burn severity indices to help understand fire behaviour from historical fires (Parks et al., 2014). Due to the challenge of diverse, complex and interacting fire effects, there is a limitation in using remote sensing indices to assess burn severity (Penelope et al., 2014). However, there needs to be more research to accurately estimate FMC in different forest stands. It is necessary to compare methods to estimate selected FMC attributes in central BC and determine whether differences in FMC might explain why juvenile forests sometimes remain as wildfire refugia in central BC, in contrast to patterns observed in southwestern Oregon (Zald & Dunn, 2018).

This study includes ground-based observations of fuel moisture levels against directly measured weather conditions, standard empirically based modelling approaches, and remote sensing data. Weather conditions, empirical models and remote sensing methods are tested to estimate FMC in different forest stands. Estimated FMC from these alternative data sources were also used to analyse observed burn severity differences in the Plateau Complex Wildfire in central BC in 2017. Pre-fire evaluation and prevention could be accomplished by using the methods determined by this research, with monitoring and assessing FMC on a larger scale for different stand types (Chuvieco et al., 2003).

1.2 Thesis statement

There are two statements I aimed to prove in this research: 1. Empirical models and remote sensing can be used to estimate fuel moisture contents on a larger scale (Central BC) 2. High fuel moisture contents played a role in juvenile stand fire skips in a recent wildfire. To accomplish the research stated above, this study has:

1) Developed and tested empirical models of the FWI system to estimate duff and fine woody debris MC from regional weather conditions and on-site fire weather station data with field observation data.
2) Collected and analysed remote sensing imagery, calculated greenness and MC indices, and compared them with field observations and empirically modelled FMC values.
3) Compared burn severities calculated with remote sensing imagery for a historical wildfire with remote sensing indices related to FMC and evaluated the role of FMC in fire severity and fire refugia.

2. Literature review

In Canada, wildfires consume more than two million hectares of forest yearly (McGee et al., 2015). Fires have an impact on forested areas around the world and contribute significantly to greenhouse gas emissions (Chuvieco, 2008). Many ecosystems are well adapted to fire cycles, and fire has historically been used as a tool for land use management (Chuvieco et al., 2010). However, recent changes in the climate and societal factors can alter traditional fire regimes, potentially magnifying the adverse effects of fire on vegetation, soils, and human values (Chuvieco et al., 2010).Based on inflation-adjusted insurance claims, the most expensive wildfire disasters in Canada include the Kelowna wildfires in British Columbia in 2003 (costing $252 million), the Slave Lake wildfires in Alberta in 2011 ($864.67 million), the Horse River Wildfire in northeastern Alberta in 2016 (the costliest natural disaster in Canadian history, at $3.84 billion), and the British Columbia wildfires in 2017 ($137.3 million) (Tymstra et al., 2020). When the costs of suppression, recovery, lost revenue, and other effects (such as on the air and water quality) are also considered, the overall cost of wildfire disasters listed above is significantly higher (Tymstra et al., 2020).

Wildfires are a common disaster with substantial consequences, necessitating research on wildfire prevention and mitigation (Tymstra et al., 2020). The most comprehensive indicator of the potential for fire ignition and spread is fuel moisture content (FMC), which is expressed as the ratio of water to dry mass (Blackmore & Flanner, 1968; Fosberg & Schroeder, 1971; Paltridge & Barber, 1988; Pompe & Vines, 1966; Trowbridge & Feller, 1988; Viegas et al., 1992). The FMC strongly impacts the time to ignition and the manner of fire development (Nelson, 2001).

It has been historically observed that old forests often functioned as fire refugia that experienced lower severity burns in stand-replacing fires (Meigs et al., 2020). However, according to observations from recent fires in central BC, some juvenile forest stands escaped wildfire while mature forest burned around them, a phenomenon that occurred more frequently than could be expected by chance (Burton et al., 2019). Studies in California and Oregon have demonstrated that the fuel components in different stand types of influence fire intensity and behaviour (Kane et al., 2015; Dunn & Bailey, 2016). While there are many factors that can influence fire behaviour, fuel moisture content (FMC) is an important measure of moisture in forest fuels that can have a significant impact (Anderson 1982, Jolly et al. 2015). Other factors that can affect fire behaviour include differences in tree species, site preparation (e.g., soil types), and the specific area, level, and stage of fire initiation and spread (Byram 1959, White et al. 1996). Nonetheless, FMC remains a crucial variable in assessing fire risk and developing effective fire management strategies (Anderson 1982, Jolly et al. 2015).

Field observations of FMC provide accurate observations on one fire risk factor but are time-consuming and only represent conditions in the sample collection area at specific points in time (Caccamo et al., 2011). The FWI system has been used to estimate weather-driven fire risk and local fuel moisture contents such as fine woody debris and the forest floor or duff (Van Wagner, 1987). The associated Canadian Forest Fire Danger Rating System (CFFDRS) is widely used to measure and report forest fire danger across Canada today (Wang et al., 2017). Unfortunately, FWI needs accurate weather conditions from weather stations, which can limit its application in sparsely instrumented and topographically complex landscapes (Van Wagner, 1987). Remote sensing has been suggested as an alternative approach to estimating FMC on a larger scale. However, satellite image resolution (20-200 m), quantity (image collection frequency), and quality (cloud cover) are challenges in operationalizing this research (Yang et al., 2018). The following literature review examines the principles and background of the three main components of this study: ground-based FMC observations, empirical modelling of FMC, and remote sensing for FMC and wildfire severity.

2.1 Field Observations of Fuel Moisture Content

Duff (forest floor organic matter consisting of fermentation and humus layers, typically at 5-10 cm below the surface) and fine woody debris (small dead fuel such as twigs and branches with diameter of 2-7mm), play a role in wildfire intensity and spread (Ryan, 2002, Norum et al., 1984). In regions where the ground cover has high duff and woody debris composition, fires burn several hours longer than in regions with widespread mineral soil exposure, and this increases the chances of fire spreading to foliage (Ryan, 2002; Hartford & Frandsen, 1992).

Fuel moisture content can substantially affect ignition probability and the severity of forest fires, as low fuel moisture levels can be necessary for wildfire initiation and spread (Dennison et al., 2008; Chuvieco et al., 2009; Nolan et al., 2016). Fuel moisture estimation is thus necessary for fire risk assessment and prevention (Dennison et al., 2008; Yebera et al., 2013).

Fuel moisture content is calculated as the percent difference between a sample's fresh weight and dry weight (Equation 1, Chuvieco et al. 2003):

$$\boldsymbol{FMC} = \left(\frac{\boldsymbol{FW-DW}}{\boldsymbol{DW}}\right) * 100\% \quad \text{[Eq. 1]}$$

where *FW* is the fresh weight, and *DW* is the dry weight after oven-drying at 100 ℃ for at least 24 hours. The typical ranges of FMC vary with fuel type, forest age, and recent weather conditions and events. In FWI models, the MC of fine woody debris can range between 0 to 250 %, and the MC of duff is between 20 to 300 % (Van Wagner, 1987). The FWI model is based on observations from boreal and eastern Canada dominated by pine stands of various ages and structures, so fuel conditions may respond differently to weather in central BC (Wagner, 1987).

2.2 Fuel moisture inferred from weather station data

The FWI system uses weather station data to estimate fire risk and FMC of fine fuels and duff for the area adjacent to the index weather station (Van Wagner, 1987; De & William, 1998). The system includes a Fine Fuel Moisture Code (FFMC) and a Duff Moisture Code (DMC), which are empirically calibrated estimates of the cumulative fuel drying/wetting effects of recent weather behaviour (Viegas et al., 2001). The FFMC and DMC indices (Figure 1), which are unitless, can be used to convert back to the MC of fine woody debris and duff, respectively, by using formulas based on an empirical model or by creating local formulas (Wotton, 2009).

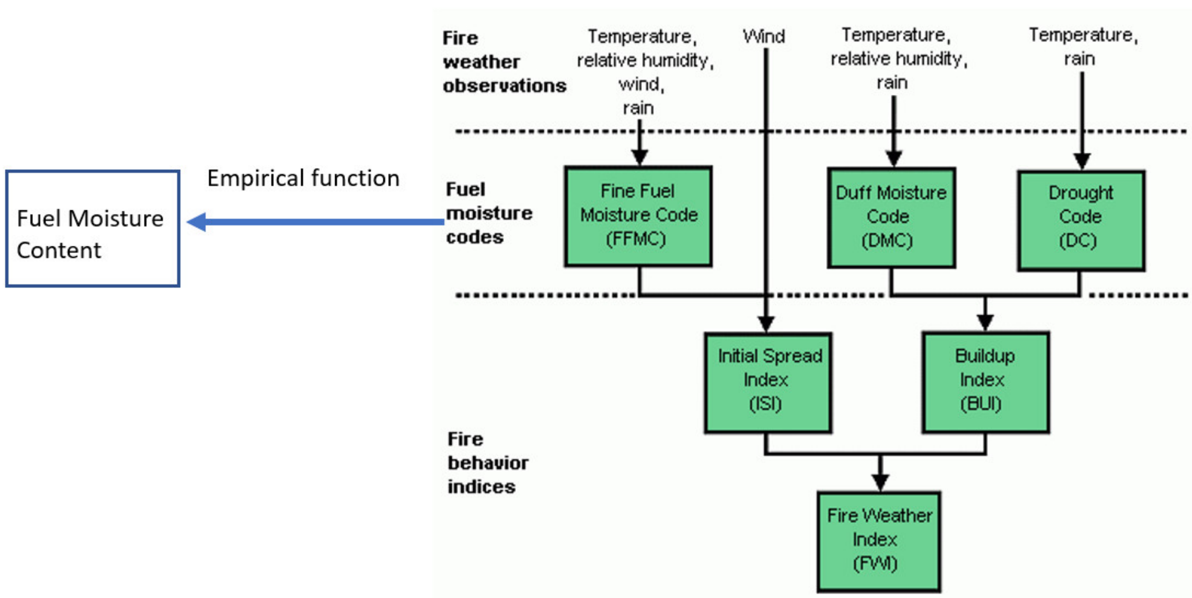

Figure 1:Schematic of FWI, modified from (Natural Resources Canada, accessed May 2023)

The calculation of FFMC requires inputs of accumulated daily precipitation (mm), relative humidity (%), wind speed (km hr^{-1}), and temperature (^{o}C) at noon, and the previous day's value of FFMC (Van Wagner, 1987; Wotton, 2009). As the duff layer is found beneath the surface of the forest floor, it is unaffected by wind. The calculation of

DMC requires daily precipitation (mm), relative humidity (%), temperature (°C), and day length (h) and the previous day's DMC (Van Wagner, 1987; Wotton, 2009).

2.2.1 Fine Fuel Moisture Code (FFMC)

The Fine Fuel Moisture Code (FFMC) assesses the flammability and ease of ignition of fine fuels, such as fine woody debris, which typically have a dry weight of around 0.25 kg m^{-2} (Van Wagner, 1987). It estimates the MC of litter and other cured fine fuels within a forest stand during mid - afternoon (Van Wagner, 1987). FFMC calculations require input data of temperature, relative air humidity, wind speed at noon, and precipitation from 24 hours measured at a nearby fire weather station. Wetting by rain and drying is also considered in FFMC calculations. The FFMC index is calculated from equations 2 to 11 as follows (Van Wagner & Pickett, 1985):

Calculation of the current day's FFMC ($FFMC_t$) requires the previous day's (t-1) moisture content (*MC*, %), which is a function of the previous days $FFMC_{t-1}$:

$$\boldsymbol{MC_{t-1} = 147.2 * \frac{101 - FFMC_{t-1}}{59.5 + FFMC_{t-1}}} \quad \text{[Eq. 2]}$$

Precipitation (*P*, mm) is measured from noon of the previous day to noon of the current day. If the precipitation amount is greater than 0.5 mm, the wetting effect from rain is added to the previous day's fine fuel moisture content (MC_{t-1}) to get today's fine fuel moisture content (MC_t). The wetting effect is estimated empirically as follows:

$$\boldsymbol{MC_t = MC_{t-1} + 42.5 * P * \left(e^{\frac{-100}{251 - M_{t-1}}}\right)\left(1 - e^{\frac{-6.93}{P}}\right)}, \text{ for } \boldsymbol{MC_{t-1}} < 150 \quad \text{[Eq. 3]}$$

$$\boldsymbol{MC_t = Eq.3` + 0.0015(MC_{t-1} - 150)^2 P^{0.5}}, \text{ for } \boldsymbol{MC_{t-1}} \geq 150 \quad \text{[Eq. 4]}$$

In the FFMC model, the maximum fine fuel MC is 250%. If a moisture content calculated from Eq.3 or 4 is higher than 250%, then it is converted back to 250. Then a drying effect (E_d) considers air temperature (*T*, °C) and relative humidity (*H*, %) measured at noon on the current day, and is calculated as follows:

$$\boldsymbol{E_d = 0.09428H^{0.679} + 11 * e^{\frac{H-100}{10}} + 0.18(21.1 - T) * (1 - e^{0.115H})} \quad \text{[Eq.5]}$$

If E_d is less than MC_{t-1}, the fine fuel moisture content MC_t is calculated by including the wind speed (*W*):

$$\boldsymbol{K = 0.424\left(1 - \left(\frac{H}{100}\right)^{1.7}\right) + 0.0694W^{0.5}\left(1 - \left(\frac{H}{100}\right)^{8}\right)0.581e^{0.0365-T}} \quad \text{[Eq.6]}$$

$$MC_t = E_d + (M_{t-1} - E_d) * 10^{-K}$$ [Eq.7]

If E_d is greater than MC_{t-1} then Eq. 7 would lead to a negative moisture content. So instead, a wetting effect E_w that considers temperature and humidity is used to calculate MC_t:

$$E_w = 0.618H^{0.753} + 10e^{\frac{H-100}{10}} + 0.18(21.1 - T)\left(1 - e^{0.115*H}\right)$$ [Eq.8]

If $E_w > MC_{t-1}$, then MC_t can be calculated as following equations:

$$MC_t = E_w - (E_w - MC_{t-1})10^{-K}$$ [Eq.9]

If $E_w \leq MC_{t-1} \leq E_d$, then there is no drying effect on the previous day's moisture content and M_{t-1} is equal to MC_t . Finally, the current day's moisture content MC_t is converted back to FFMC following:

$$FFMC = 59.5\frac{250 - MC_t}{147.2 + MC_t}$$ [Eq. 10]

In areas where snow is typically present in the winter, the calculation of FFMC begins on the third day after the disappearance of snow. When snow cover is not a prominent characteristic in a region, the calculation begins on the third day in a row that the noon temperature is over 12°C (Lawson and Armitage 2008). The FFMC index is set to 85 as its initial value.

2.2.2 Duff Moisture Code (DMC)

Another fuel moisture code from the Canadian forest fire weather index (FWI) system is the Duff Moisture Code *(*DMC). Duff consists of loosely packed, decomposing organic matter in the fermentation and humus layers (Norum et al., 1984) of forest soils, and it has a dry weight of around 5 kg m^{-2} (Van Wagner, 1987). Similar to FFMC, the calculation of DMC considers the wetting and drying phases. Required inputs to the DMC calculation are temperature, relative air humidity, daily precipitation (at noon), the previous day's DMC, and day length (Van Wagner, 1987). DMC is calculated from equations 12 to 19 as follows (Van Wagner & Pickett, 1985):

Duff requires daily precipitation (P) greater than 1.5 mm to achieve a wetting effect; rainfall effect (P_e) is calculated by:

$P_e = 0.92P - 1.27$, for P >1.5 mm [Eq.11]

The wetting variable (b) for previous day's DMC (DMC_{t-1}) is calculated for three different DMC_{t-1} ranges (less than 33, between 33 to 65, higher than 65):

$\boldsymbol{b = \frac{100}{0.5+DMC_{t-1}}}$ for $DMC_{t-1} \leq 33$ [Eq.12]

$\boldsymbol{b = 14 - 1.3\ln(DMC_{t-1})}$, for $33 < (DMC_{t-1}) \leq 65$ [Eq.13]

$\boldsymbol{b = 6.2\ln(DMC_{t-1}) - 17.2}$, for $DMC_{t-1} > 65$ [Eq.14]

Once wetting effect *b* is calculated, it can use the previous day's duff moisture content ($MC_{duff\ t-1}$) to get the current day's duff MC (M_{duff}), first estimating $MC_{duff\ t-1}$ from DMC_{t-1} :

$$\boldsymbol{MC_{duff_{t-1}} = 20 + e^{5.6348-\left(\frac{DMC_{t-1}}{43.43}\right)}} \quad \text{[Eq.15]}$$

$$\boldsymbol{MC_{duff} = MC_{duff_{t-1}} + \frac{1000P_e}{48.77+bP_e}} \quad \text{[Eq.16]}$$

MC_{duff} is then converted back to the current day's *DMC* for the next day continuous calculation:

$$\boldsymbol{DMC = 244.72 - 43.43\ln(MC_{duff}} - 20) \quad \text{[Eq.17]}$$

As DMC can not go below 0, if *DMC* from Eq.18 is lower than 0, it will be set to 0 for the continuous calculation. If *P* is less than 1.5 mm, the above calculation is not used and *DMC* = DMC_{t-1}. After calculating the *DMC* with the rainfall effect, a drying effect will also be added to get the final *DMC* (DMC_f) for the current day as follows:

$$\boldsymbol{DMC_f = DMC + 100 * (1.894 * (T + 1.1) * (100 - H) * DL * 10^{-6})} \quad \text{[Eq.18]}$$

where *T* is temperature, *H* is relative humidity measured at noon, and DL is the day length; notice the minimum temperature is set as -1.1 ℃, and any inputs lower than -1.1℃ will be set as -1.1℃. The DMC computation begins on the third snow-free day in areas typically covered in snow throughout the winter. When snow cover is not prominent in a region, the calculation begins on the third day in a row that the noon temperature is over 12 °C (Lawson & Armitage, 2008). The index's initial value must be set to 6.

Though the fine fuels and duff moisture codes can be used to estimate the MC of woody debris and duff layers, the accuracy will vary with the distance between the site and the fire weather stations, as temperature, relative humidity, wind speed, and precipitation will vary. The drying and wetting corrections for FFMC and DMC are empirical corrections based on data collected from major eastern pine forests around Ontario (Van Wagner, 1987). In contrast, fuel conditions might differ in other regions and forest types. Fire weather stations are usually located in open spaces close to a highway. Previous research has used FFMC and DMC in old-growth forests in Australia, with in-stand weather stations, where it was shown that the microclimate is moister in the mature forest than in open and younger forests (Furlaud et al., 2021).

2.3. Fuel moisture from remote sensing

Remote sensing and spectral reflectance in different band combinations have been widely used to retrieve information on the biophysical properties of vegetation by using wavelengths of reflected radiation that capitalise on the spectral signatures of healthy versus diseased vegetation or moisture (Ceccato et al., 2002). Band combinations such as the Normalised Difference Vegetation Index (NDVI) (Tucker, 1979) and the Normalised Difference Moisture Index (NDMI) have been calculated with Landsat 8 data to estimate FMC, as they contain bands that are most sensitive to the water content of plant tissue (Rao et al., 2020; Table 1 and 2). The Visible Atmospherically Resistant Index (VARI) provides an alternative estimate of greenness based on visible wavelengths and has been used previously to estimate FMC in southern California (Schneider et al., 2008) as well as monitor water content (Gitelson et al., 2002, bands information in Tables 1&2). The NDVI indicator and the normalised multi-band drought index (NMDI) can be used to estimate soil MC, as those indices exhibited strong relationships with soil moisture data in previous studies (Wang & Qu, 2007, Tables 1&2). Green Normalized Difference vegetation index (GNDVI) was used in estimating grassland MC in previous research (Bao et al. 2022), which can be expanded to estimate FMC in this research (Tables 1&2).

The MODIS (Moderate Resolution Imaging Spectroradiometer) satellite platform provides daily imagery and has been used previously to monitor FMC. However, its spatial resolution (250-1000 metres) limits its application in this research because the planted forest blocks are relatively small compared to other studies (Caccamo et al., 2011; Yang et al., 2018). Landsat 8/9 and Sentinel 2 have been used to study forest FMC content in previous research, with their higher spatial resolution data (10 -30 metres resolution), but at the expense of less frequent data acquisition for a given location (Wang & Qu, 2007; Zhang & Zhou, 2016) (Table 1).

Pre- and post-wildfire imagery can be used to distinguish between burned and unburned forests and can help assess wildfire burn severity and help understand historical fire behaviours (Key et al., 2006). Due to its 30 m spatial resolution, approximately 16-day temporal resolution, and extensive library of freely accessible images dating back to 1984, imagery from the Landsat TM and ETM+ sensors has been widely used to estimate and map burn severity (Parks et al., 2014). Sentinel 2 imagery has also been used in burn severity studies (Quintano et al., 2018), and it has higher spatial (10-30 metres) and temporal resolution (5 days). In the previous research, differenced Normalised Burn Ratio (dNBR) (Key et al., 2006) and its related form, the relativized dNBR (RdNBR) (Miller et al., 2007) are the two most used band ratios for estimating burn severity (Table 2). Instead of using differenced Normalised Burn Ratio (dNBR), Relativized Burn Ratio (RBR) has been proved as a more appropriate index to use when comparing burn severity across diverse western US forests, as it uses the surrounding surviving forest pre- fire conditions as a parameter to adjust the scale of burn ratio (Parks et al., 2014) (Table 2).

Table 1:Satellite sensors used in this study (Data source: USGS, Sentinel Hub)

Satellite name	Band	Resolution	Central Wavelength	Description
Sentinel 2	B1	60 m	443 nm	Ultra blue (Coastal and Aerosol)
Frequency (Day)	B2	10 m	490 nm	Blue
5	B3	10 m	560 nm	Green
	B4	10 m	665 nm	Red
	B5	20 m	705 nm	Visible and Near Infrared (VNIR)
	B6	20 m	740 nm	Visible and Near Infrared (VNIR)
	B7	20 m	783 nm	Visible and Near Infrared (VNIR)
	B8	10 m	842 nm	Visible and Near Infrared (VNIR)
	B8a	20 m	865 nm	Visible and Near Infrared (VNIR)
	B9	60 m	940 nm	Short Wave Infrared (SWIR)
	B10	60 m	1375 nm	Short Wave Infrared (SWIR)
	B11	20 m	1610 nm	Short Wave Infrared (SWIR)
	B12	20 m	2190 nm	Short Wave Infrared (SWIR)
Satellite name	**Band**	**Resolution**	**Wavelength**	**Description**
Landsat 8/9	B1	30 m	0.433 - 0.453 µm	Coastal / Aerosol
Frequency (Day)	B2	30 m	0.450 - 0.515 µm	Visible blue
16	B3	30 m	0.525 - 0.600 µm	Visible green
	B4	30 m	0.630 - 0.680 µm	Visible red
	B5	30 m	0.845 - 0.885 µm	Near-infrared
	B6	30 m	1.56 - 1.66 µm	Short wavelength infrared
	B7	60 m	2.10 - 2.30 µm	Short wavelength infrared
	B8	15 m	0.50 - 0.68 µm	Panchromatic
	B9	30 m	1.36 - 1.39 µm	Cirrus
	B10	100 m	10.3 - 11.3 µm	Long wavelength infrared
	B11	100 m	11.5 - 12.5 µm	Long wavelength infrared

Table 2: Band indices used in this study (Data source: USGS, Sentinel Hub)

Remote sensing indices/Application	Satellite	Bands Combination
NDVI: Measure live green vegetation	Landsat 8/9	(B5-B4)/(B5+B4)
	Sentinel 2	(B8-B4)/(B8+B4)
NDMI: Measure crops water stress level	Landsat 8/9	(B5-B6)/(B5+B6)
	Sentinel 2	(B8-B11)/(B8+B11)
NMDI: Measure soil/vegetation moisture	Landsat 8/9	(B5-(B6-B7))/(B5+B6-B7)
	Sentinel 2	(B8a-(B11-B12))/(B8a+(B11-B12))
VARI: Estimate vegetation fraction	Landsat 8/9	(B3-B4)/(B3-B4-B2)
	Sentinel 2	(B3-B4)/(B3-B4-B2)

GNDVI: Measure vegetation greenness	Landsat 8/9	(B5-B3)/(B5+B3)
	Sentinel 2	(B8-B3)/(B8+B3)
dNBR: Estimate burn severity	Sentinel 2	Δ(B8-B12)/(B8+B12)
	Landsat 8/9	Δ(B5-B7)/(B5+B7)
RBR: Estimate burn severity	Sentinel 2	dNBR/(prefire(B8-B12)/(B8+B12)+1.001)
	Landsat 8/9	dNBR/(prefire(B5-B7)/(B5+B7)+1.001)

3. Study Areas

3.1 Prince George and Smithers

The Biogeoclimatic Ecosystem Classification (BEC) zone of the surrounding forests of Prince George and Smithers is generally classified as the Sub-Boreal Spruce (SBS) zone (Klinka et al., 1999). The SBS zone is dominated by mature coniferous forests, including species such as spruce (*Picea glauca, Picea engelmannii, Picea mariana*), fir (*Abies lasiocarpa*), and pine (*Pinus contorta*) (Natural Resources Canada, 2017). Other tree species found in this zone include larch (*Larix laricina*), aspen (*Populus tremuloides*), and birch (*Betula papyrifera)* (Natural Resources Canada, 2017). Cool and moist climates characterise this region, mean annual temperature in the SBS zone typically ranges from 0°C to 5°C, while mean annual precipitation ranges from 500 mm to 1,500 mm (Ministry of Forests, Lands, Natural Resource Operations and Rural Development, 2014). However, there can be significant variation within the zone, with some areas receiving much higher or lower levels of precipitation depending on elevation, latitude, and local topography (Ministry of Forests, Lands, Natural Resource Operations and Rural Development, 2014). The terrain is characterised by rolling hills, flat plateaus and gentle slopes, with well-drained soils and scattered wetlands (Ministry of Forests, Lands, Natural Resource Operations and Rural Development, 2014).

Six research locations (Figures 2 and 3) near Prince George and Smithers in central BC were selected for this research. The sites were selected for (a) proximity to Prince George and Smithers; (b) proximity to provincial fire weather stations; and (c) access to three stand types (open, juvenile, and mature) in close proximity to each other. The locations selected for this study are approximately 50 km apart in different directions from Prince George or Smithers, with a provincial fire weather station located approximately 3.21 – 27.3 km away (Figure 2 and 3). Each research location has three stand types (Figure 4) that close to each other, with the following characteristics (Burton, 2022):

- Juvenile: Lodgepole pine (*Pinus contorta* var. *latifolia*), and interior white spruce (*Picea engelmannii* x *glauca*) have been planted after the primary forest had been logged. Juvenile forests are dense, with only 2-3 metres separating each tree; stands are 20–40 years old.
- Open: recently logged, relatively open land with widely space, recently established pine trees that are less than 5-7 years old.
- Mature: stands that have never been logged; they are characterised by a preponderance of trees older than 120 years, with various tree species (lodgepole pine, interior white spruce, subalpine fir and interior Douglas-fir (*Pseudotsuga menziesii* var. *glauca*), with lesser amounts of broadleaf species such as trembling aspen (*Populus tremuloides*), black cottonwood (*Populus balsamifera* ssp. *trichocarpa*) and paper birch (*Betula papyrifera*), at low densities, and with irregular spatial arrangements.

Each stand's latitude, longitude, and elevation are shown in Appendix 1. The name of closest fire weather station to each research location is also provided in Appendix 2, with its latitude, longitude, elevation, and distance to the research location presented as well.

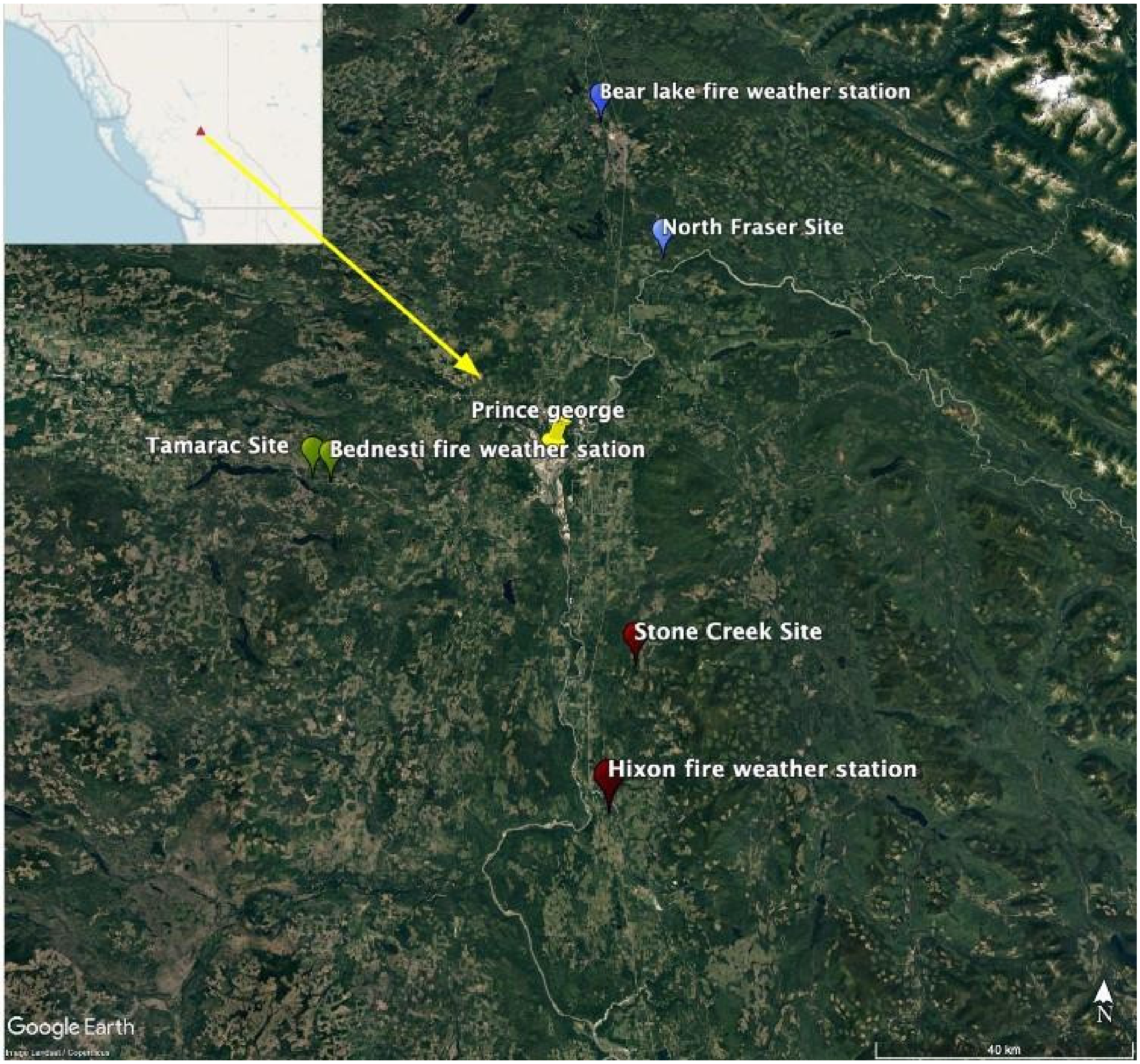

Figure 2: Prince George field sites (imagery from Google Earth™)

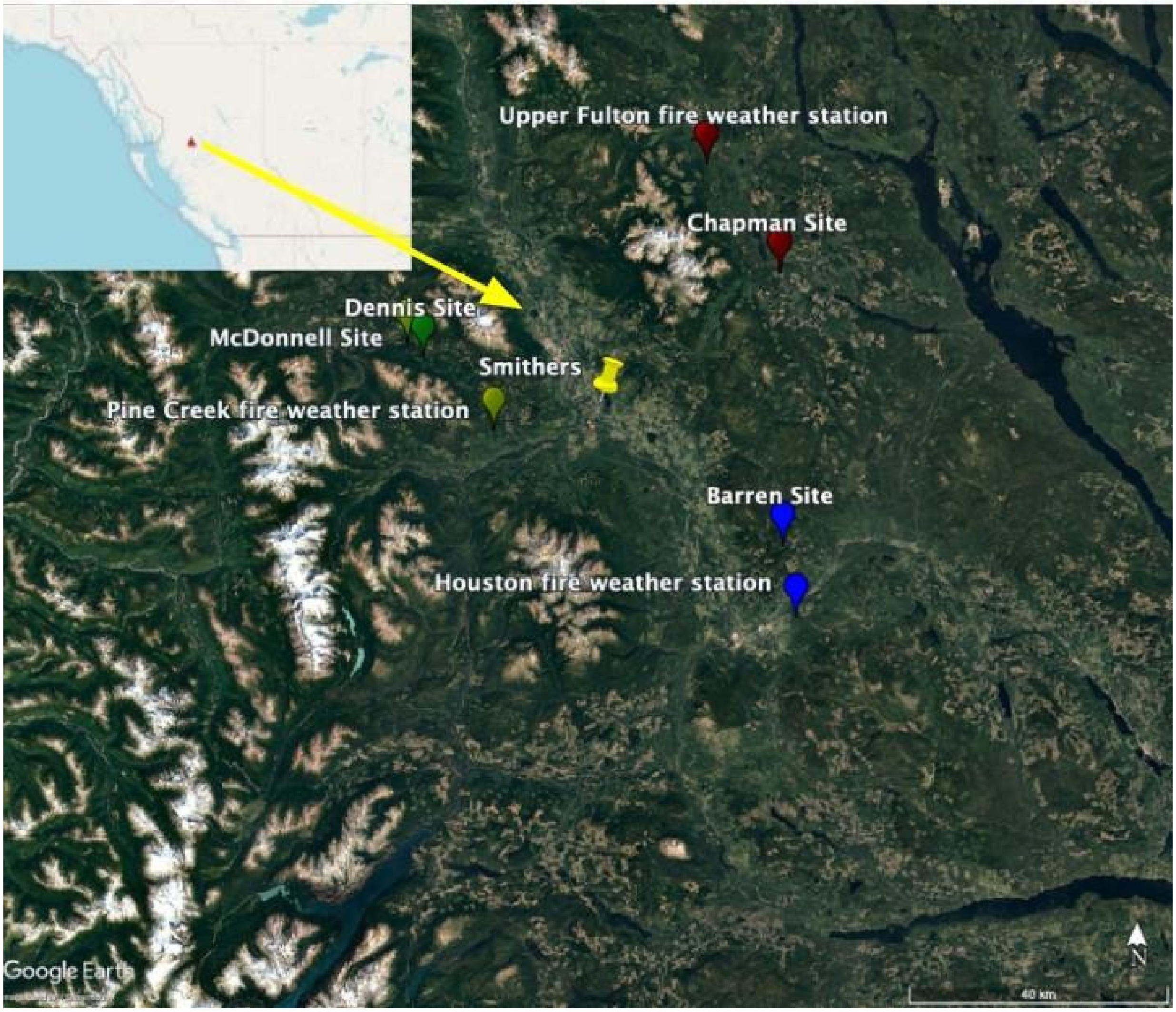

Figure 3: Smithers field sites (Image clipped: Google Earth™)

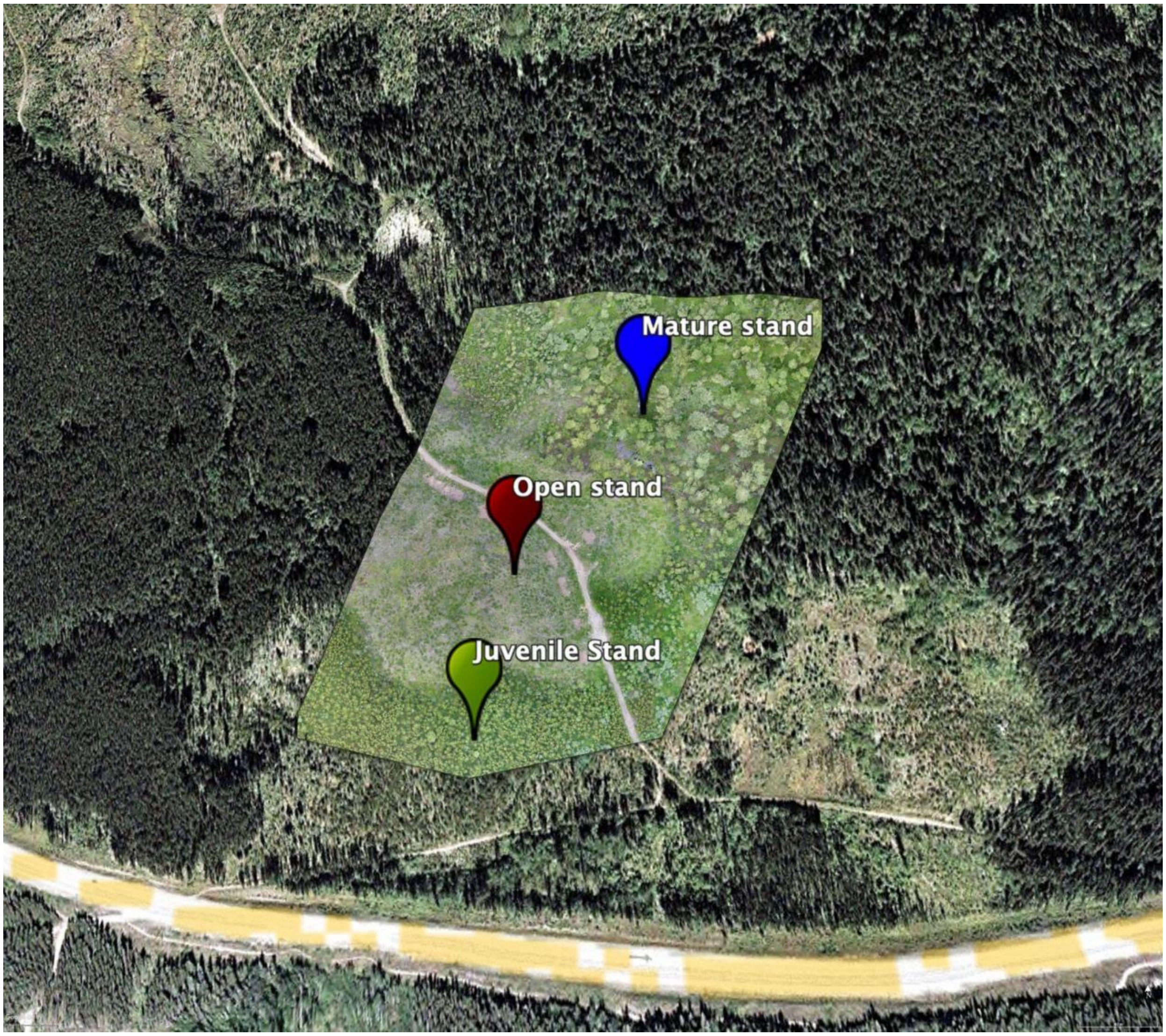

Figure 4: Tamarac sampling locations near the BCWS Bednesti fire weather station, showing three stand types (Image clipped: Google Earth™, RPAS image: Dr.Joseph Shea)

3.2. Plateau Complex Wildfire, Williams Lake

The Plateau Complex Fire occurred in the Cariboo Regional District of British Columbia, Canada, approximately 60 kilometres northwest of Williams Lake, and 150 kilometres southwest of Prince George (Figure 5). The fire burned over a distance of approximately 135 kilometres (84 miles) from south to north, and 70 kilometres (43 miles) from east to west (BC Wildfire Service, 2022). Between 7th July and 1st September 2017, a few wildfires merged to burn a total of 521,012 hectares covering a broad range of stand types and ages (BC Wildfire Service, 2022). Due to logging and replanting activities in the area, the wildfire covered a mix of recently harvested open sites, juvenile replanted sites, and some mature forest blocks (Williams Lake Community Forest, 2022).

The Plateau Complex Fire provides a suitable case study in which to test applications of this research, as it covered similar stand types (open, juvenile, and mature, much of it dominated by lodgepole pine) to the Smithers and Prince George field sites in central BC. For this case study, the method and results from FMC observations and remote sensing indices, were used to examine how fire severity corresponds to areas that exhibited low moisture content/greenness immediately before the wildfire.

A small subset of the Plateau Complex Fire was selected for this research, as wildfire conditions can vary substantially across such a large fire perimeter, and smoke conditions prevented suitable image acquisitions across the entire fire complex. The subset area included open, juvenile, and mature forests located near each other, similar to the Prince George and Smithers observation sites, for which suitable pre- and post-fire imagery was available for the calculation of fire severity indices. The proximity of these stands also suggests they would have experienced similar fire weather conditions.

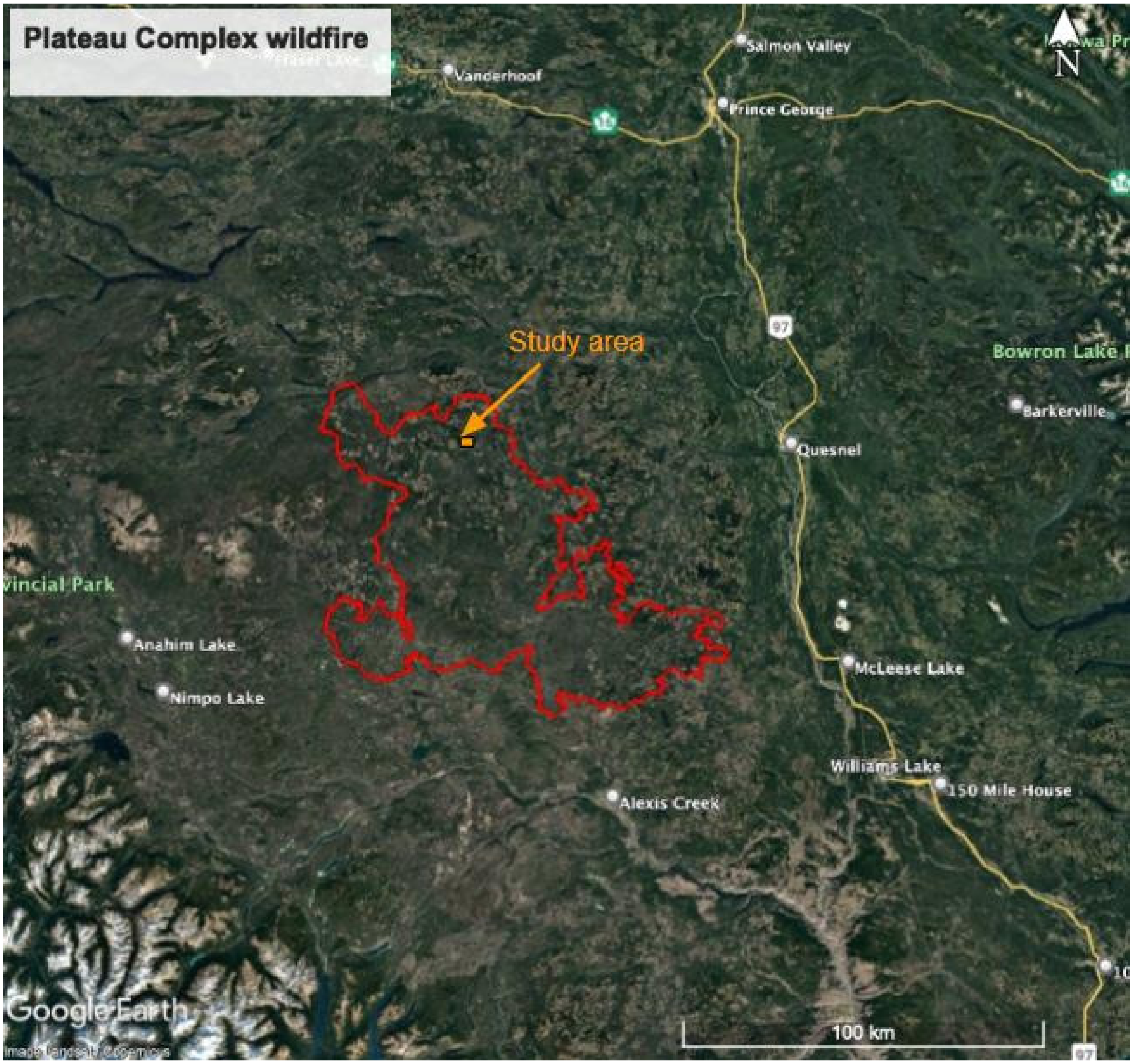

Figure 5: Plateau Complex Wildfire map and study area (image captured in Google Earth™).

Figures 6 and 7 show pre- and post-fire near-infrared composite images of the Plateau Complex northwest of Williams Lake, where intense red indicates the vigour of greenness (juvenile and mature forests), and green/brown indicates the lack of vegetation (open stands) or burnt areas. The false color composite images in Figures 6 and 7 use the combination of Sentinel-2 bands 8 (near-infrared), 4 (red), and 3 (green). Note in Figures 6 and 7, that some juvenile forests appeared to act as wildfire refugia, which remain bright red in both pre-and post-fire images. A comparison of the remote sensing indices and fuel moisture conditions in the pre-fire area between different stand types can serve as a reference guide for future wildfire vulnerability assessment and prevention and could help demonstrate the relationship between fire activity and FMC/remote sensing indices.

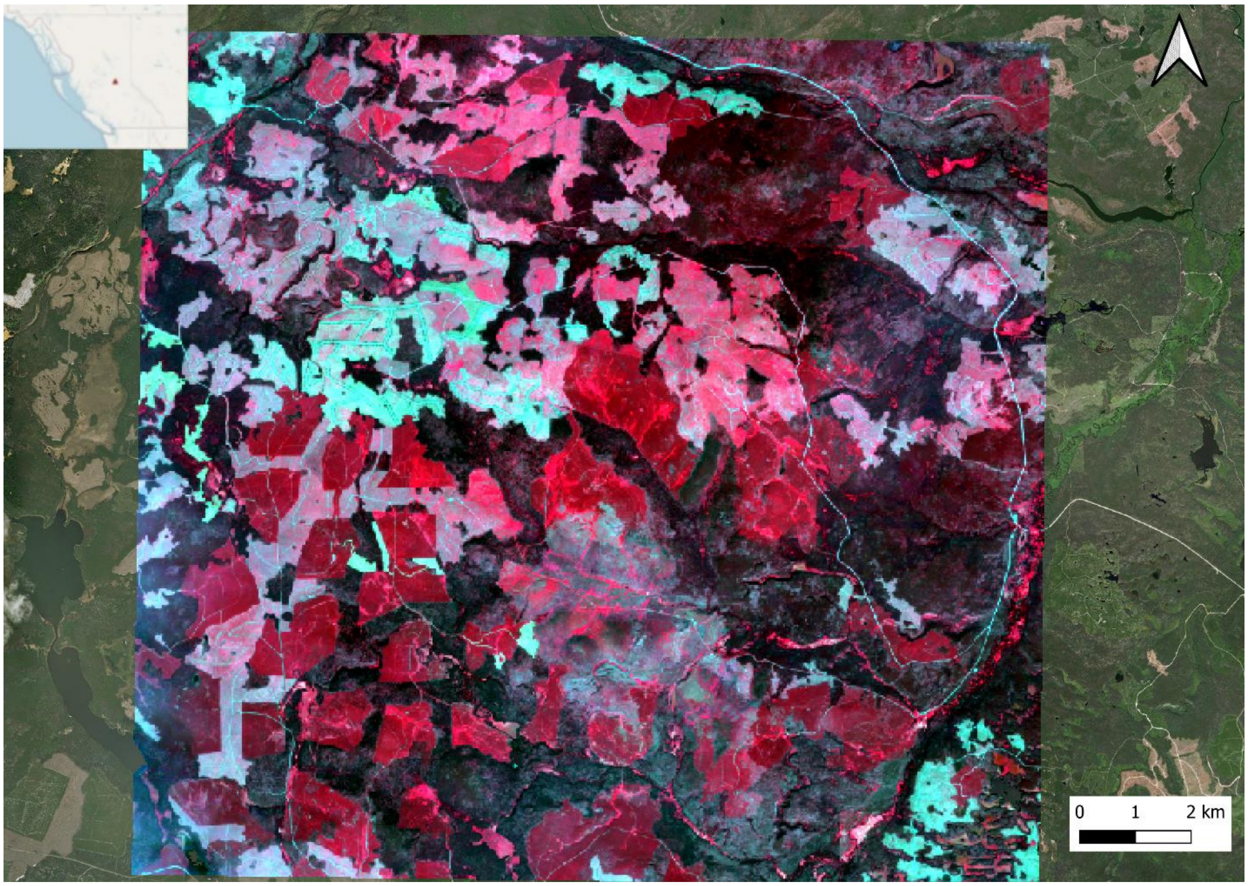

Figure 6: False colour composite pre-fire map at Plateau Complex, image captured on June 11th, 2017, centred on 52.94105 N, -124.01571 W.

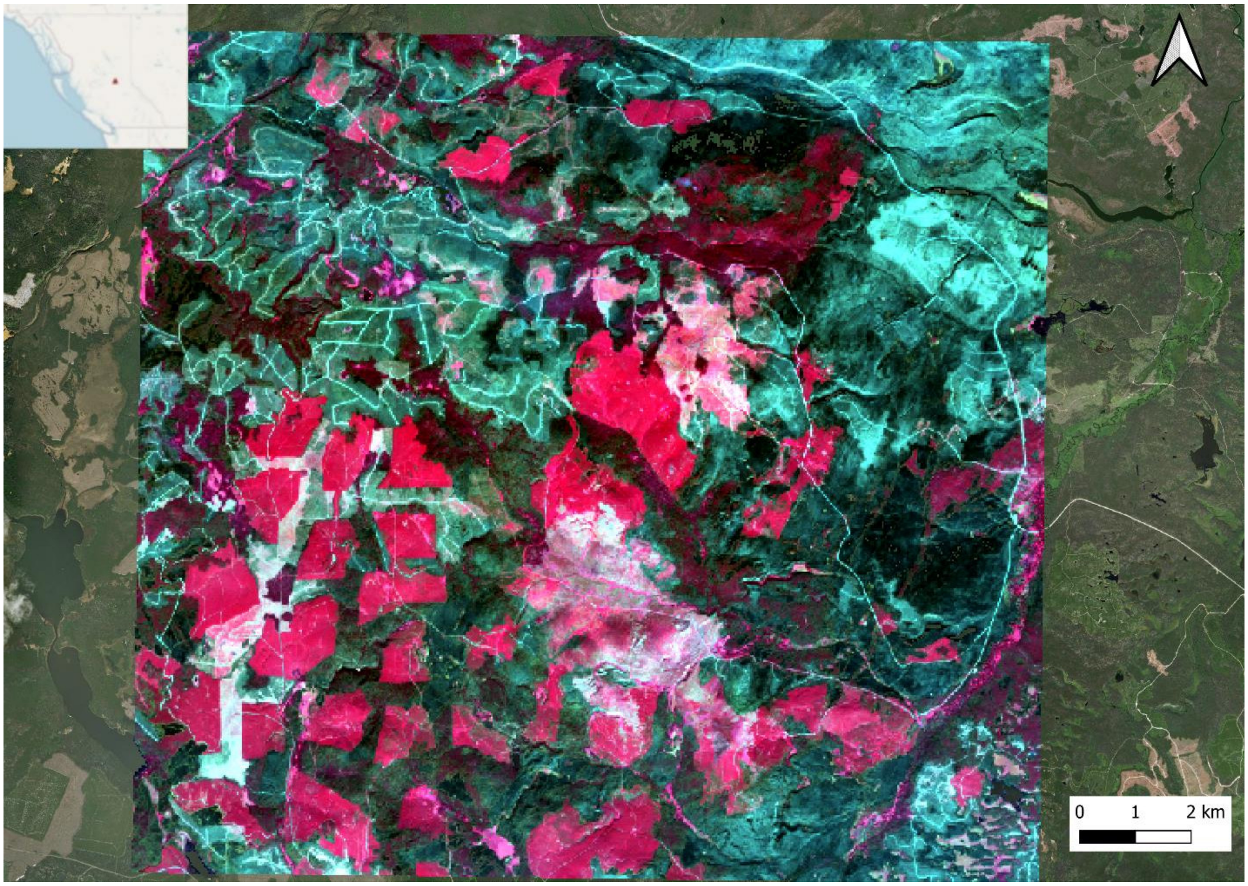

Figure 7: False colour composite postfire map at Plateau Complex, image captured on September 4th, 2017, centred on 52.94105 N, -124.01571 W.

4. Methods

4.1 Fuel Moisture Observations

4.1.1 Sample collection

In the summers of 2021 and 2022, samples of foliage (older than 1 year), fine woody debris, and duff were collected from six research locations near Prince George and Smithers for this project (Figures 2 and 3). Each sampling location contains three stand types located near each other. Field samples were taken from open (dominated new grown pine), juvenile (pine dominated, with some spruce), and mature forests (mix of pine, spruce, and fir). Higher foliage was collected at heights 4-6 m above the ground with cutting poles at the juvenile and mature sampling sites to compare with lower foliage. Lower foliage was collected at a height of 1-2 metres. Duff and fine woody debris were typically picked with a mix of sun-exposed and shaded areas at the Prince George sites. At the Smithers sites, duff and fine woody debris were collected from multiple diverse spots in each stand to ensure consistency and obtain a mixture of moisture data from sun-exposed and shaded areas. Replication of sample trees cannot be excluded as the sites were chosen randomly at each visit.

In the summer of 2021, at Prince George, twelve samples were collected at each visit to the juvenile and mature sites: three samples of duff, three of fine woody debris, and three each for higher (4-6 m) and lower (1-2 m) foliage. Nine samples were collected for open sites, as there is no higher foliage at open sites. Samples collected at the start of 2021 were transported in plastic sandwich bags prior to oven drying, and then were oven-dried in aluminium baking cups. After mid-summer 2021, different sizes of metal tins with lids were used to collect samples, and these were subsequently stored and transported in a cooler to reduce moisture loss from the samples, with the same tins used for sample drying in the oven.

In the summer of 2022, lower-level foliage was not collected due to the increased sampling frequency and lack of sample tins. Additional characteristics such as tree species and fuel exposure to the sunlight were documented while collecting the samples, as they can influence plant water conditions.

Ideally, field sample collection dates would coincide with satellite overpasses to directly compare field-observed FMC with remote sensing data (Sentinel 2; Landsat 8 and 9). Landsat 8 and 9 (launched in 2022) capture images at 10:00 am local time, whereas Sentinel 2 collects data at noon local time (USGS, 2022). The sample collecting period is aimed to be close around noon, as DMC and FFMC are also calculated at noon (Van Wagner, 1987). However, the collection times often varied due to weather conditions, transportation time, schedules, and labour constraints. Generally, samples were collected between 10:30 am and 3:00 pm Pacific Standard Time (PST).

4.1.2 Moisture content measurement

In previous studies, samples of duff, fine woody debris, and foliage were set in an oven for 48 hours at 60 degrees to dry (Viegas et al., 1992). Before the sample collection began, foliage from the forests at UNBC was collected and tested for two drying approaches. In the first approach, twelve test samples were measured after drying for 24 hours at 100 °C and another three days at 100 °C. The MC results from both approaches were approximately identical, with less than 0.06% moisture change for foliage and fine woody debris and 0.01% moisture change for duff, compared with the average dry weight of 5 g for foliage and fine woody debris and 40 g for duff. Due to a lack of tins and time-saving purposes, samples in this study were dried for 24 hours at 100 °C.

The weight of field samples was measured and recorded in tins after they arrived at UNBC's Enhanced Forestry Lab (EFL) (Figure 8), and they were sent to dry in an oven for roughly 24 hours. Tins with dried samples were weighed and recorded on another day. The weight of the empty tins and lids was subtracted from the dry and wet weight to get their mass, then Eq.1 was used to calculate FMC. At Prince George, the scale used to measure woody debris and duff was accurate to 0.01 g. A higher precision scale (0.001g) was used to measure the weight of the foliage. Samples collected at Smithers locations were measured with a scale that measured to 0.01 g for woody debris and duff, and 0.001 g for foliage. Measurements were recorded in field notebooks and transferred to a spreadsheet along with information on fuel types, tree species, sunlight exposure, and weather conditions.

Figure 8: Drying process at UNBC EFL lab

4.1.3 Moisture content analysis

Observations collected while it was raining, or collected immediately after rainfall were filtered out as there was water attached to the fuel surface. Foliage from tree species other than pine, spruce, fir, or Douglas-fir were removed from this analysis as well. Only juvenile and mature forests were analysed with the remote sensing method for its correlation with foliage, as their canopy was dense enough to cover the ground. Foliage data from two summers of fieldwork was separated by species, and their mean, maximum and minimum values were determined. Using remote sensing to estimate fine woody debris MC and duff MC was only applied at the open sites, where the forest floor was fully exposed.

Once two years of data collection were completed, the 3 subsample FMC values collected for each of foliage, fine woody debris, and duff from each stand at each date were averaged, then plotted as time series and boxplots to visualize changes through time and differences between fuel types. Statistical tests (Kruskal-Wallis one way analysis of variance) were conducted to determine whether the FMC levels varied significantly among different stands throughout the summers of 2021 and 2022. The seasonal evolution of FMC in different stands and fuel types may help explain the existence of juvenile fire refugia. Time-series of FMC values were plotted for each stand to understand the seasonal evolution of moisture contents in different stand types. Meanwhile, FMC at different stands and sites was compared with the results from empirical meteorological models and remote sensing indices, as explained in the following sections.

4.2 Regional and on-site meteorological data

4.2.1 Fire weather stations

The BC provincial fire weather stations observe several weather parameters related to fire behaviour. For this research, temperature, relative humidity, wind speed, and precipitation data were used from fire weather station data. The temporal frequency of the data collected by these fire weather stations can vary. Generally, the observations are taken at least once per day, usually in the afternoon. However, during periods of high fire risk or active fire events, the frequency of observations may increase to multiple times per day or even hourly, depending on the situation. This more frequent monitoring allows for better tracking of changing fire weather conditions and enhances the accuracy of fire danger ratings and fire behaviour predictions. Fire weather station data were obtained from the Pacific Climate Impacts Consortium website (https://www.pacificclimate.org/data/bc-station-data-disclaimer-0).

4.2.2 In-stand meteorological observations

HOBO™ U23 Pro v2 (Onset Computer Corporation, Bourne, Massachusetts) temperature and relative humidity sensors (Appendix 3) were installed at all six sampling locations and in each of the three different stand types. Each HOBO was mounted on a metal rebar about 30 cm above the forest ground, and their location is given in Appendix. Full weather stations were also installed at the open sites, measuring hourly air temperature, relative humidity, precipitation and wind speed at approximately two metres high (Appendix 4). Open site weather stations had a tipping bucket (except North Fraser) to collect precipitation data in 2021, though open site weather station installation occurred after the start of field sampling (July 8th-10th for Smither sites, June 6th – 8th for Prince George sites). Therefore, on-site precipitation and wind speed was not used to estimate duff and fine woody debris MC in 2021.

For the analysis of 2021 data, in-stand HOBO sensor data (temperature and relative humidity) were combined with nearby fire weather station data (precipitation and/or wind speed). In the summer of 2022, tipping buckets (event data only) and wind speed sensors (recorded every 15 mins) were installed in all stands. Meteorological and microclimate data will be archived in an open-source repository.

4.2.3 Meteorological data analyses

Daily averages of temperature, relative humidity, and wind speed, as well as daily accumulated precipitation, were calculated for in-stand and fire weather station data (Appendix 3).As the data are not normally distributed, Kruskal-Wallis one-way analysis of variance tests were applied to identify any significant differences between fire weather station and in-stand s weather station data (Section 5.2). As the meteorological data are not normally distributed, the non-parametric Kruskal-Wallis test was used to compare means between sites. The null hypothesis is that there is no significant difference between populations, and a significance threshold of 0.05 was used to accept ($p > 0.05$) or reject ($p < 0.05$) the null hypothesis. Data variance was also calculated following Eq. 19: (Section 5.2),

$$(\sigma^2) = \Sigma[(x_i - \mu)^2] / n \qquad \text{[Eq.19]}$$

where x_i represents each individual data point in the dataset, μ represents the mean of the dataset, and n is the number of observations. Variances are also reported in Sec 5.2.

4.3 FWI empirical model

To test the accuracy of the moisture contents generated by the FWI model in the study region, four versions of the model used in this research. First, the original FWI model (Model 1) was used to calculate FFMC and DMC from nearby fire weather station data to estimate MC with Eq.2 and Eq.17. The second approach (Model 2) used meteorological data from nearby fire weather stations locally calibrated and stand-specific fine woody debris and duff start MC values to estimate MC. The third approach used partial (Model 3) or full on-site meteorological data (Model 4) from the different stands and constrained parameters based on local moisture observations to estimate MC.

4.3.1 Model 1: Fire weather stations and empirical coefficients

The FWI system described in section 3.2 was used with nearest fire weather station data to estimate the MC of duff and fine woody debris in coniferous stands (Van Wagner, 1987). This approach is consistent with the current operational use of the FWI system, and a flow chart outlining this stage of the research is shown in Figure 9. In 2021, FFMC and DMC values from nearby fire weather stations were provided, while in 2022 they were calculated nearby fire weather station data (Figures 2 and Figure 3). daily expected values of FMC for fine woody debris and duff can be calculated based on Eq. 2 and 16 with their FFMC and DMC (Viegas et al., 2001, Wotton, 2009).

Daily FMC estimates from empirical models, and local/regional meteorological inputs are compared with the field-based observations of FMC. To compare the estimated and observed FMC, RMSE and MBE were calculated. The goodness of fit (R^2 and p value) for each site and stand type were calculated based on observed MC and MC predicted from the regression line.

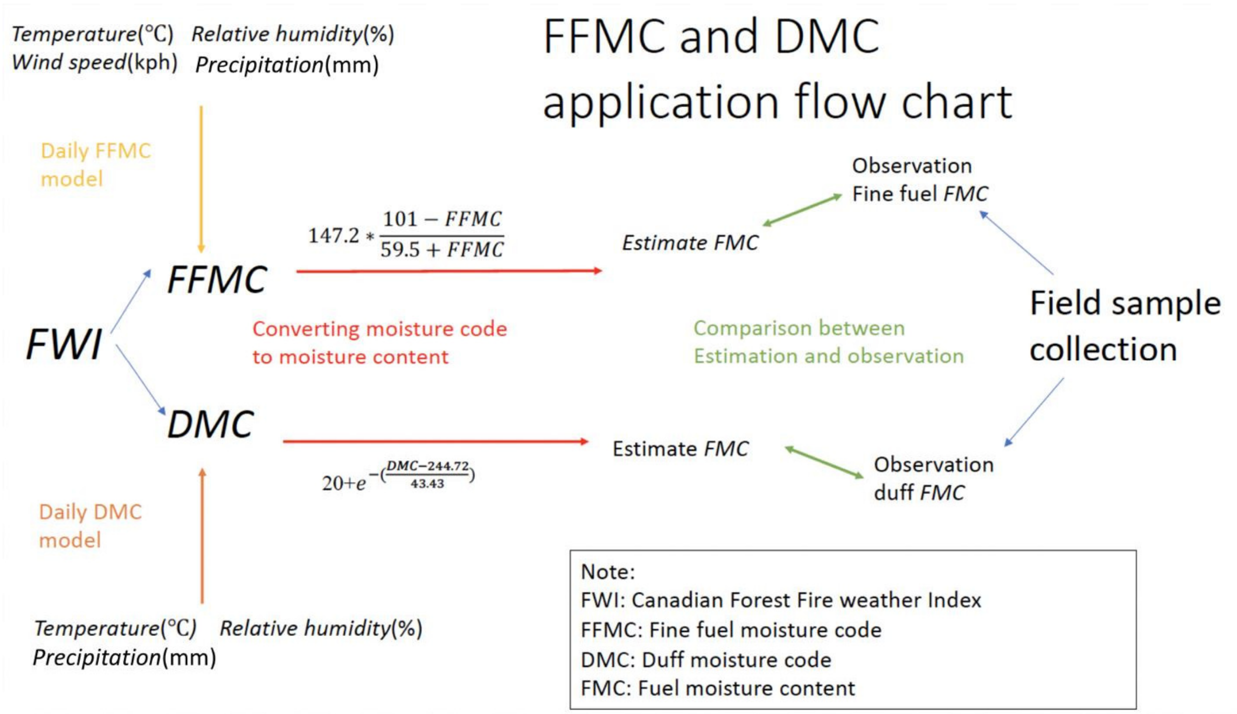

Figure 9: FFMC and DMC application flow chart

4.3.2 Model 2: FFMC and DMC corrected for local moisture contents.

As the FWI model is based primarily on eastern Canada forest types and climates, previous research has updated parts of the DMC and FMC based on local conditions (Wotton, 2009). Both DMC and FFMC models require the previous day's DMC and FFMC value, to which the drying and wetting effects are added to calculate the current day's DMC and FFMC (Eq.2 to Eq.18). To initialise the DMC and FFMC models at the start of the season, default values of 85 for FFMC and 6 for DMC have been used in the original model (Van Wagner, 1987). Using Eqs. 2 and 15, this gives initial moisture contents of 16.3% for fine woody debris and 264.7% for duff. Errors in the initial MC values used in the FFMC and DMC models would lead to accumulated errors throughout the summer season.

Averaged initial duff and fine woody debris MC at each stand and location subsamples for 2021 and 2022 are shown in Table 3. In 2021, the average initial MCs observed in mature stands was 181.7% for duff and 19.2% for fine woody debris, while for open stands it was 119.1% for duff and 13.3% for fine woody debris. For juvenile stands, the average initial MC was 137.7% for duff and 26.1% for fine woody debris. In 2022, the average initial MC for mature stands was 281.0% for duff and 61.6% for fine woody debris, while for open stands it was 193.6% for duff and 28.1% for fine woody debris. For juvenile stands, the average initial MC was 225.6% for duff and 58.5% for fine woody debris. While average observed initial values may be similar to those derived from Eqs. 2 and 15, there is variability between sites and years that may be important for model estimation.

Table 3: Initial FMC at different sites and stand around Prince George and Smithers in 2021 and 2022, where FWD means fine woody debris.

		Duff 2021	FWD 2021	Duff 2022	FWD 2022
Location	Stand	Initial FMC (%)	Initial FMC (%)	Initial FMC (%)	Initial FMC (%)
Tamarac	Mature	199.37	17.64	107.6	31.85
North Fraser	Mature	205.23	26.51	281.04	35.7
Stone Creek	Mature	122.47	19.54	246.31	57.78
Chapman	Mature	105.72	13.80	218.65	77.04
McDonnell/Dennis	Mature	261.50	23.20	410.39	63.85
Barren	Mature	196.02	14.25	474.63	103.23
Average	Mature	181.72	19.16	288.77	61.58
Tamarac	Open	79.80	9.73	136.03	16.70
North Fraser	Open	214.29	15.43	185.70	24.49
Stone Creek	Open	104.56	22.06	184.06	9.60
Chapman	Open	152.51	10.13	206.53	30.26
McDonnell/Dennis	Open	62.03	14.21	323.98	14.41

Barren	Open	101.30	8.49	125.04	73.19
Average	Open	119.08	13.34	193.56	28.11
Tamarac	Juvenile	97.23	20.36	101.37	16.96
North Fraser	Juvenile	189.06	24.26	227.46	90.88
Stone Creek	Juvenile	191.63	44.96	224.94	83.97
Chapman	Juvenile	66.45	16.12	194.55	62.11
McDonnell /Dennis	Juvenile	128.33	35.59	303.97	40.24
Barren	Juvenile	153.28	15.45	301.38	57.10
Average	Juvenile	137.66	26.12	225.61	58.54

The start averaged duff MC range in central BC was found to vary from 62.0 – 474.6% across different forest stand types, seasons, and weather conditions. As the DMC was originally developed for pine forests in the eastern US and Canada (Wotton, 2009) and fuel components vary in different regions, Eq. 19 was updated to use the local in-stand maximum FMC for MC_{max} and the local in-stand minimum FMC for E_t.

By replacing all the parameters "*DMC*" in the DMC model with Eq.19, duff MC can be calculated directly from weather conditions. Values of MC_{max} and E in Eq. 19 were updated based on local measurements of duff MC through summer of 2021 and 2022. Instead of entering default initial DMC to calculate the following, averaged first observed duff *MC* from different stands at different locations were entered to calculate their following MC. With local duff MC values as starting points and updated maximum/minimum values, it provides an opportunity to monitor the surrounding different forests' MC based on local conditions.

The previous day's FFMC is used to estimate to fine woody debris MC with Eq. 2, then drying and wetting effects are used to calculate the current day's MC (Van Wagner, 1987). In the FFMC wetting rate, the maximum fine woody debris MC value is set to 250% (Van Wagner, 1987), whereas it may differ in central BC. For the samples collected around Prince George and Smithers, the maximum daily averaged fine woody debris

MCs at the open stand is 228.4%, 192.0% in the mature stands, and 195.0% in the juvenile stands, all of which are less than 250%.

Although FFMC does not require minimum fine woody debris MC, like DMC, FFMC also has a default initial value to start the estimation, which is 16.3%. The initial averaged fine woody debris MC varies between 8.5 - 103.2% in different stands (Table 3). Resetting maximum MC values in the FFMC model and entering local observation data as a starting point from Table 3 can provide an opportunity to better estimate fine woody debris MC locally. These maximum duff MC values, starting DMC, and starting FFMC as applied to run locally customized FWI indices in each stand type at each location are presented in Table 6. Subsequent calculations of daily DMC and FFMC used the standard meteorological data from the nearest fire weather station.

Similar to the analysis of the original FWI model (Section 4.3.1), duff and fine fuel MC estimated with the updated model parameters were compared with on-site FMC observations. To evaluate the model skill, R^2, p-value, RMSE and MBE were calculated.

4.3.3 Model 3: FWI with local temperature and relative humidity

Model 1 and 2 presented in sections 4.3.1 and 4.3.2 estimate MC with data measured at a regional fire weather station. However, as fire weather stations are sited with specific requirements (open areas, measurement heights), and often some distance away, these cannot be expected to reflect the actual in-stand weather conditions. On-site relative humidity is higher (particularly at night-time), and wind speed is lower than observed at the fire weather station. Some of these differences are likely due to measurement heights: wind speed data were collected at approximately 2.5 meters height for this study, while fire weather station wind speeds are collected at 10 meters height. Total precipitation over the observation period is similar, though individual event totals vary. Distances between fire weather stations and sampling sites range between 3.2 and 27.3 km. Hence, the use of regional weather stations potentially introduces an additional source of error in the estimation of FMC.

In-stand temperature and humidity data were used in Model 3, combined with nearby fire weather station data for wind speed and precipitation to reduce errors caused by weather differences. While the FWI formulas were developed to empirically predict in-stand fuel moisture conditions using standardized observations from fire weather stations, the third empirical model tested here relies partially on-site weather conditions (temperature and relative humidity), locally updated model parameters and initial conditions, and is combined with the closest fire weather station data to estimate in-stand duff and fine woody debris MC.

4.3.4 Model 4: FWI with local weather conditions

Differences in microclimate between juvenile/mature stands and open stands are also expected, as various forest tree densities and canopy cover lead to different wind blocking, exposure to sunlight, and interception of rainfall (Karki & Chaudhary, 2018). Forest stands and their canopy can also influence wind speed and precipitation, which requires in-stand sensors to capture accurate in-stand data.

In the summer of 2022, wind speed sensors and tipping buckets were installed in most sites to capture on-site wind speed and precipitation. The new wind speed sensors and tipping buckets were installed at a height of 2.5 m in all stands and were located near the 30-cm HOBO sensors (monitoring temperature and relative humidity). In-stand wind speed data were combined with in-stand temperature and relative humidity to calculate a localized “in-stand” estimate of fuel moisture contents from FWI indices (Model 4). RMSE, MBE and goodness of fitting (R^2 and p value) from Model 4 were calculated and compared with other models to check if there is any improvement statistically.

4.4 Remote sensing and GIS

Multispectral data and remote sensing indices were collected and analysed with Google Earth Engine (GEE), which provides access to historical satellite images. Harvested Areas of BC and Vegetation Results Inventory (VRI) data (Government of British Columbia, accessed May 2023) from the BC data catalogue and Government of Canada was used in QGIS to select and filter the various forest types based on their recorded year of logging/ project ages, which can help to determine the forest condition before wildfires. Although combining Landsat 8 & 9 and Sentinel 2 data will increase the image capture frequency, there are challenges that prevent the combination of the different platforms (Zhu et al., 2019). Differences between Landsat and Sentinel 2 data, such as spatial and spectral resolutions, can also limit the usage and introduce errors when combining them (Zhu et al., 2019).

Bands and remote sensing indices mentioned above from Landsat 8 & 9 and Sentinel-2 are listed in Tables 1 and 2. Band descriptions, wavelength, and remote sensing index band combinations are also shown in Tables 1 and 2.

4.4.1 Remote Sensing Indices For FMC

During the first field observation period from late May to September 2021, Sentinel 2 satellite imagery was collected using Google Earth Engine (GEE). A buffer with a 30-metre radius was applied to the site of each sampling location, which was within the range of sample collection, and bands were clipped to the buffered area. Quality assessment (QA) bands were used to filter out images with clouds and cloud shadows that could affect the band ratio analysis for Landsat 8 & 9. As Sentinel 2 does not have a cloud shadow mask, a 2 x 2 km polygon was applied to identify the possible presence of clouds over the study area, but not directly over the site, as this could produce cloud shadows. Sentinel 2 scenes that have higher than 10% cloudy pixels in the 2 x 2 km polygons were considered to potentially contain cloud shadows, and they were removed from the analysis. The images retained after filtering were exported from GEE and visually inspected before analysis.

In 2021, the smoke created by wildfires reduced the available satellite images to use, and field samples were collected at different times than satellite acquisitions. Therefore, a Locally Weighted Scatterplot Smoothing (lowess) function was used to generate continuous remote sensing indices values (Moreno et al. 2014) throughout the summer to match the dates of field sampling. In 2022, sample collection was aimed to match satellite collection dates. However, the lowess smoothing function was still applied to avoid mismatches between field sampling data and remote sensing indices caused by clouds and shadows.

In 2022, Sentinel 2 underwent a shift in its bands and use Harmonized collection to match the same range as in older scenes (Earth Engine Data Catalog, 2022), which resulted in its cloud quality assessment (QA) filter not functioning as intended. To address this issue, a simple method of using NDVI to map clouds and cloud shadows was employed (Tucker, 1979). This method is based on the fact that vegetation reflects more in the near-infrared range than in the visible range, while clouds and shadows reflect relatively evenly across all wavelengths (Tucker, 1979; Fonseca & Andrade, 2019; Xiong et al., 2020). Therefore, pixels with low NDVI values are more likely to be clouds or shadows and can be masked or removed from the analysis. To remove cloudy pixels from the 2022 Sentinel 2 data, a threshold was first calculated (see below) and applied to NDVI values calculated for each scene: pixels with NDVI values below this threshold were classified as cloudy or shadowed.

To determine a NDVI threshold for the detection of cloud and cloud shadows, a series of clear, cloud/shadow, and cloudy images from the North Fraser site in June 2022 were exported and analysed. NDVI and true colour images were compared in Appendix 6 to Appendix 8, where A is the true colour image, and B is the NDVI image, with open (red polygons), old (blue polygon), and juvenile (purple polygon) separated. When there was no cloud (Appendix 6A), mature and juvenile forests have generally higher NDVI (0.6-0.8) than open forests (0.4-0.6). When it is cloudy, NDVI is generally lower than 0.2 (white colour), regardless of the stand types (Appendix 7 and Appendix 8). For cloud shadow, as shown in Figures 12-B, the shadow's NDVI was typically higher than 0.9 (black colour), which also matched the shadows in the true colour image. Consequently, when exporting remote sensing indices with 2022 Sentinel 2 data, pixels with NDVI lower than 0.2 or higher than 0.9 were removed on that image capture day.

Remote sensing indices (NDVI, NDMI, VARI, NMDI, GNDVI, Table 2) were calculated on an average of the extracted pixel values (partial pixels on edge included) for buffered areas from GEE (Figure 10). To compare remote sensing indices and observations of FMC, locally weighted smoothing (lowess) functions were used to interpolate remote sensing indices between satellite retrieval dates for the 2021 and 2022 summers, as there is a mismatch between sample observation and satellite visiting days. After applying lowess functions, remote sensing index values from lowess were paired with the same day averaged observation data at the exact location.

An example of NDMI indices and their lowess smoothers at Tamarac juvenile stands in 2022 summer is shown in Figure 11. NDMI values from the lowess smoother were compared with sample observation data with a smoothing parameter set to 0.5. The smoothing parameter controls the balance between the fit to the data and the degree of smoothing applied to the curve. A lower smoothing parameter corresponds to a more responsive curve that better fits the data, while higher parameter value corresponds to a smoother curve (Cleveland, 1974). As there were days with smoke that couldn't be removed with QA bands and the NDVI filter, a lowess smoother parameter set as 0.5 can help to avoid the influence of smoke days.

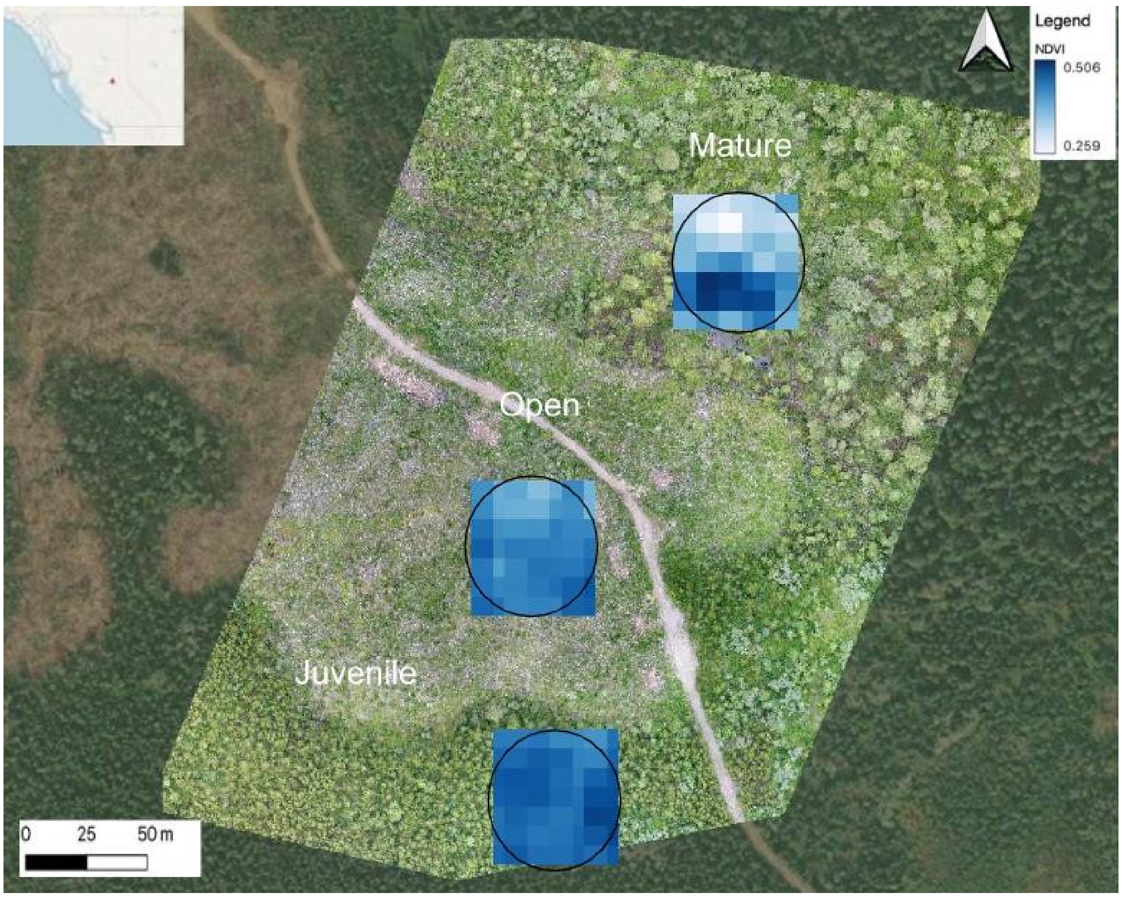

Figure 10: Tamarac NDVI in different stands in 30 metres pixels in three stand types, NDVI captured on July 20th, 2022.

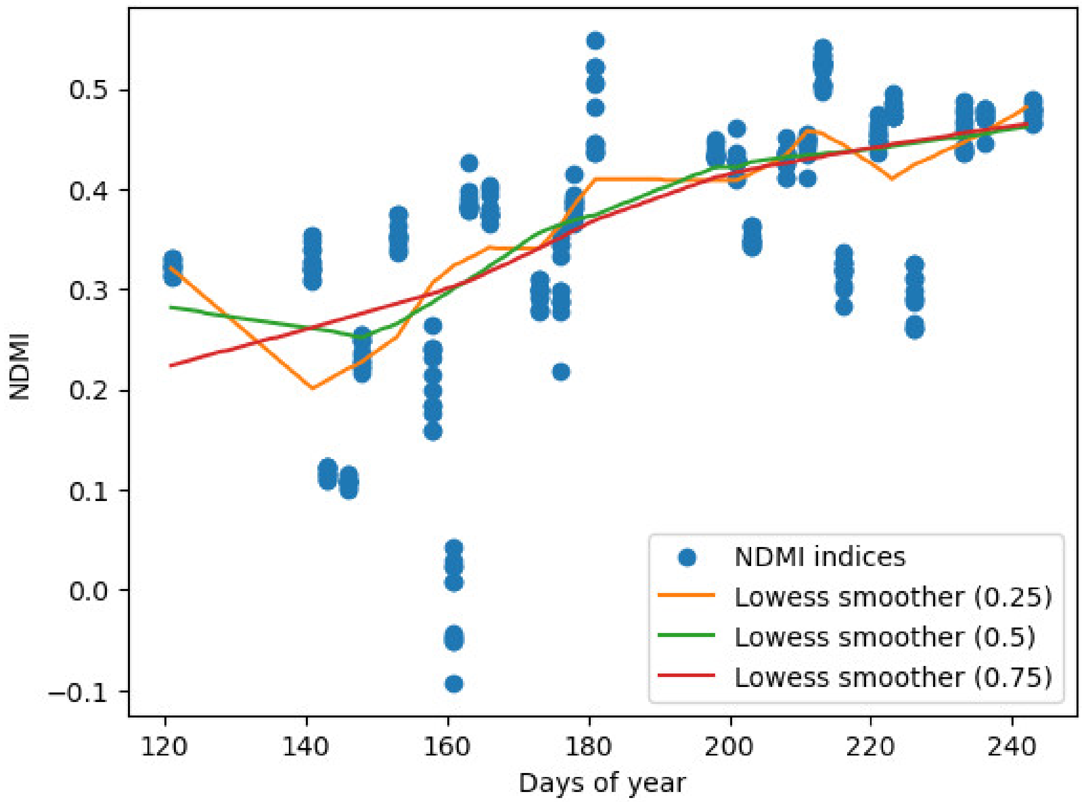

Figure 11: Example of lowess smoothing of NDMI, at Tamarac juvenile site in 2022 summer, with the smoothing parameter (degree of smoothing) set to 0.25, 0.5, and 0.75.

Remote sensing indices were compared to foliage MC observations at juvenile and mature sites, and duff and fine woody debris MC values at open sites, representing exposed/partially exposed ground. To test the performance of the model collaboration, 60% of the data was randomly selected as the training data set to generate linear regressions, and goodness of fitting (p-value and R^2) were calculated. The generated best-fitting line was then used to calculate the RMSE with the remaining 40% of data.

Randomly selecting training data and calculating the RMSE with the remaining test data is a common practice in remote sensing studies and has been previously used in related research (e.g., Zhou et al., 2016). This approach helps verify the results' reliability and consistency and comprehensively evaluates the remote sensing indices employed. This comparison can inform the development of empirical functions to estimate fuel conditions in different stands at a larger scale and help to understand the fire behaviour from historical wildfires.

For foliage in mature and juvenile stands, as well as duff and fine woody debris in open stands daily-averaged FMC observation data points were compared with index values from lowess smoothers for the same day; 60% were selected randomly as training data for the linear regression, their goodness of fit (R^2 and p-value) was also calculated, as well as their equations. The remaining 40% observations were used to test the model and generate error statistics (RMSE).

4.3.2 Mapping Forest types with GIS

Open, juvenile, and mature/old forests have different canopy covers and spectral characteristics (Cohen et al., 1995). To investigate the relationship between remote sensing indices and burn severity in stands of different ages, it is necessary to develop a method for mapping recently logged (open), juvenile, and mature forests prior to the occurrence of a wildfire. Forest harvest year data was used to map recently logged forests as it provided more recent and accurate information on logging activity. Meanwhile, VRI data was used to map juvenile and mature forests as it provided age information for most forests, including primary forests that have never been logged. For this study, mature forests were defined as stands older than 60 years, juvenile stands were logged 10-60 years before 2017, and recently logged areas were logged less than ten years before 2017. Figure 12 shows that most of the mature, juvenile, and recently logged forests were successfully mapped for the selected case study region.

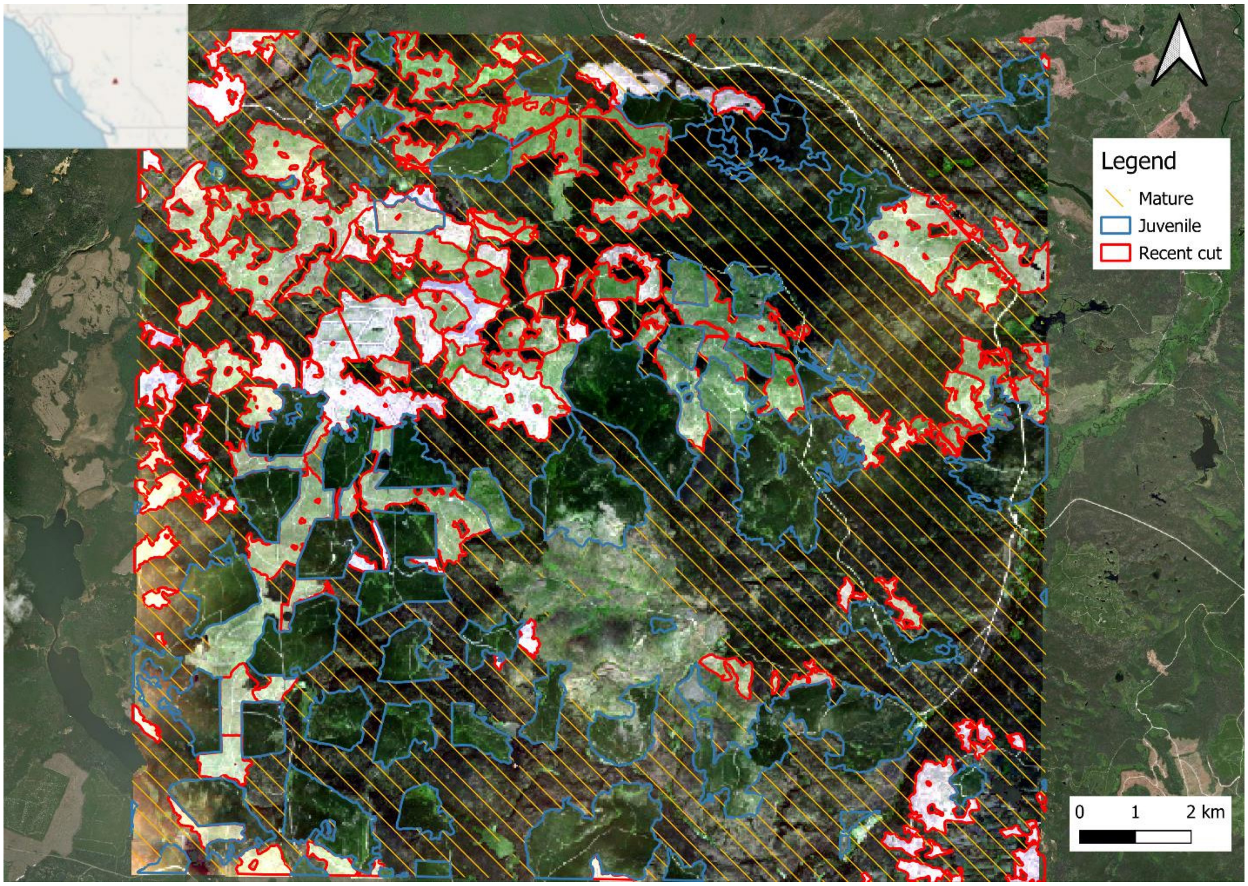

Figure 12: Stand ages with true colour image on 6th July 2017, centred on 52.94105 N, -124.01571 W.

4.3.3 Relations between dNBR/RBR and remote sensing indices

As mentioned in section 2.3, dNBR and RBR can both be used to estimate burn severity after wildfires. For this analysis, QA bands have been used to filter out the cloudy pixels, and Normalised Difference Water Index (NDWI) has been used to mask out water bodies such as lakes (Gao, 1996).

To extract the remote sensing indices representing the pre-fire forests/fuel condition, the image captured at the closest date before the wildfire started should be chosen. Sentinel 2 data was selected to use when extracting pre-fire indices, as Sentinel 2 visited the study area (Figure 4) from the Plateau Complex fire area on July 6th, the day before the wildfire started. As wildfires created much smoke, the first cloud-free image from Sentinel 2 after the fire was on September 4th, which was used as a post-fire image for burn severity calculations. A dNBR value range provided by the United States Geological Survey (USGS) was used to convert fire severities to burn severity categories (Table 4). In this research, dNBR were classified into five levels, which are Regrowth (-500 to -101), Unburned (-100 to +99), Low severity (+100 to +269), Moderate severity (+270 to +650) and High severity (+660). To match the dNBR range in Table 4, dNBR were scaled by 10^3.

Table 4: Burn severity levels obtained calculating dNBR, proposed by USGS (Key et al. 2006)

Severity level	dNBR range (scaled by 10^3)
Enhanced regrowth, high (post fire)	-500 to -251
Enhanced regrowth, low (post fire)	-250 to -101
Unburned	-100 to +99
Low severity	+100 to +269
Moderate-low severity	+270 to +439
Moderate-high severity	+440 to +659
High severity	+660 to +1300

As RBR was examined and evaluated with 18 different fires in the western USA, its range classification is different compared to dNBR (Parks et al. 2014). Table 5 shows the severity level and its averaged RBR range from the results in different fires (Parks et al., 2014), which was applied in this research as well.

Table 5: Burn severity levels obtained calculating RBR, proposed by Parks et al., 2014.

Severity level	RBR range
Unburned	<35
Low severity	35-130
Moderate severity	130-298
High severity	>298

Remote sensing indices such as NDMI and NDVI were extracted from the pre-fire image to compare fire severity among the different stands. As this method produces a large quantity of data points, hexbin plots of indices versus burn severity were plotted to show data density, frequency distribution (histograms at x and y axis), and relations between the two elements. Hexbin plots are commonly used to reduce noise in the data by showing the overall distribution and patterns in the data, rather than individual data points (Camacho, 2014). Linear or non-linear fits were not attempted in the analysis of estimated moisture content and fire severity, and this is discussed in Section 6.

5. Results

5.1 Fuel Moisture Contents

Summaries of the daily average MC for different observations sites, forest stands (juvenile, mature, and open), different types of fuel (duff and fine woody debris), as well as statistical results are presented in Table 6. Information on the total number of daily averaged observations for each category is also included in Table 9, along with the maximum and minimum FMC values. The maximum FMC for duff was 439.27 %, which was found in mature stand; the minimum MC for duff was 14.38 %, and it was in a mature stand (Table 6).

The daily averaged MC for duff was also listed in Table 6, and it was not normal distributed in all stands. At mature stand had 163.76 % MC compared with juvenile (143.56 %), and the difference was statistically significant ($p < 0.05$) with Kruskal-Wallis test. The daily averaged FMC for duff at open stands is 14.03 % lower compared with juvenile, and the difference was statistically significant ($p < 0.05$).

Information on the daily averaged FMC for fine woody debris was also in Table 6. The average fine woody debris MC for juvenile stands was 50.19 %, while for mature stands it was 1.17 % lower, which was not statistically significant ($p > 0.05$). However, for open stands, the daily averaged MC for fine woody debris was 20.11 % lower compared to juvenile stands, and this difference was statistically significant ($p < 0.05$). The maximum MC for daily averaged fine woody debris was 228.38 %, which was found in an open stand, and the minimum FMC was 2.17 %, also in an open stand.

Table 6: The maximum, minimum of daily averaged MC, variance, and averaged of daily averaged MC for duff and woody debris from different stands in 2021 and 2022.

Forest Stand	Juvenile	Mature	Open	Juvenile	Mature	Open
Fuel Type	Duff	Duff	Duff	Fine woody debris	Fine woody debris	Fine woody debris
Total Number	132	131	132	132	132	132
Maximum MC (%)	407.44	423.68	439.27	194.98	192.04	228.38
Minimum MC (%)	28.75	29.87	14.38	8.64	9.53	2.17
Averaged MC (%)	143.56	163.76	129.57	50.19	51.9	49.02
Variance ($\%^2$)	6918.07	8082.44	7514.89	1515.28	1428.62	1300.20

As different types of foliage species were collected during the summers of 2021 and 2022, daily average foliage MC, as well as maximum and minimum MC values for each stand and species type are shown in Table 7. Kruskal-Wallis tests were conducted to determine if there were any significant differences in daily averaged FMC among the different types of foliage species, as none of the dataset is normal distributed.

At the juvenile stand, where pine was the dominant species type, its daily averaged MC was compared with that of spruce and fir. Pine foliage had an average MC of 112.38%, which is 0.08% lower than fir and 8.45% higher than spruce (Table 7). However, the difference was not statistically significant, as both p-values were higher than 0.05. Fir was used as the reference species to compare with other species types at the mature stand (Table 7), and no statistically significant differences were observed, with all p-values higher than 0.05. At the open stand, pine was compared with spruce and fir (Table 7). Similar to the juvenile and mature stands, the p-values were both higher than 0.05, indicating no statistically significant difference in foliar among MC species.

Table 7: The maximum, minimum of daily averaged MC, and averaged of daily averaged MC for foliage from different stands around Smithers and Prince George in 2021 and 2022, where DFir means Douglas-fir.

Foliage type	Pine	Spruce	Fir	Pine	Spruce	Fir	DFir	Pine	Spruce	Fir
Forest	Juvenile	Juvenile	Juvenile	Mature	Mature	Mature	Mature	Open	Open	Open

stand										
Total Number	111	21	23	6	49	108	6	113	3	15
Maximum MC (%)	151.40	156.81	195.82	112.27	237.12	191.65	299.26	233.85	226.26	161.32
Minimum MC (%)	82.63	71.49	73.57	101.39	50.28	74.02	101.27	41.4	105.60	91.32
Averaged MC (%)	112.38	103.93	112.47	105.65	108.29	111.34	143.91	124.78	148.71	115.67
Variance $(\%)^2$	281.83	611.01	1184.78	22.79	806.39	1821.17	5902.24	916.48	2662.78	418.99

As there is no statistically significant difference in MC between foliage species types in all stands, different foliage species types were combined to check their FMC difference in different stands. The daily averaged maximum and minimum MC of foliage in different stands in all locations, as well as their observation number, are presented in Table 8. Open stands have the highest maximum MC (233.9%) and minimum MC (41.4%). When comparing the averaged MC of foliage with their daily averaged data, mature forests have -2.85% MC lower than juvenile stands (112.34%), however, the difference is not statistically significant with ($p > 0.05$). Open stands have 12.62% MC higher than juvenile forests, and the difference is statistically significant, with $p < 0.05$.

Table 8: The maximum, minimum of daily averaged MC, and averaged of daily averaged MC for foliage from different stands in 2021 and 2022.

Forest Stand	Juvenile	Mature	Open
Total Number	115	116	120
Maximum MC (%)	152.68	194.83	233.85
Minimum MC (%)	74.88	75.71	41.40
Averaged MC (%)	112.34	109.49	124.96
Variance ($\%^2$)	694.40	1066.87	1197.82

The time series of daily averaged FMC (consisting of three individual measurements averaged in each stand and study location) observed in duff, woody debris, and foliage for the summers of 2021 and 2022 are presented in Appendix 9 and Figure 13. In both 2021 and 2022, daily averaged MC in the duff layer is significant higher in mature forest stands, followed by juvenile and open stands. Fine woody debris at the mature and juvenile sites have a similar MC, with no statistically significant difference ($p > 0.05$). However, daily averaged fine woody debris MC at open stands are lower than mature and juvenile stands, with statistically significant difference ($p < 0.05$).

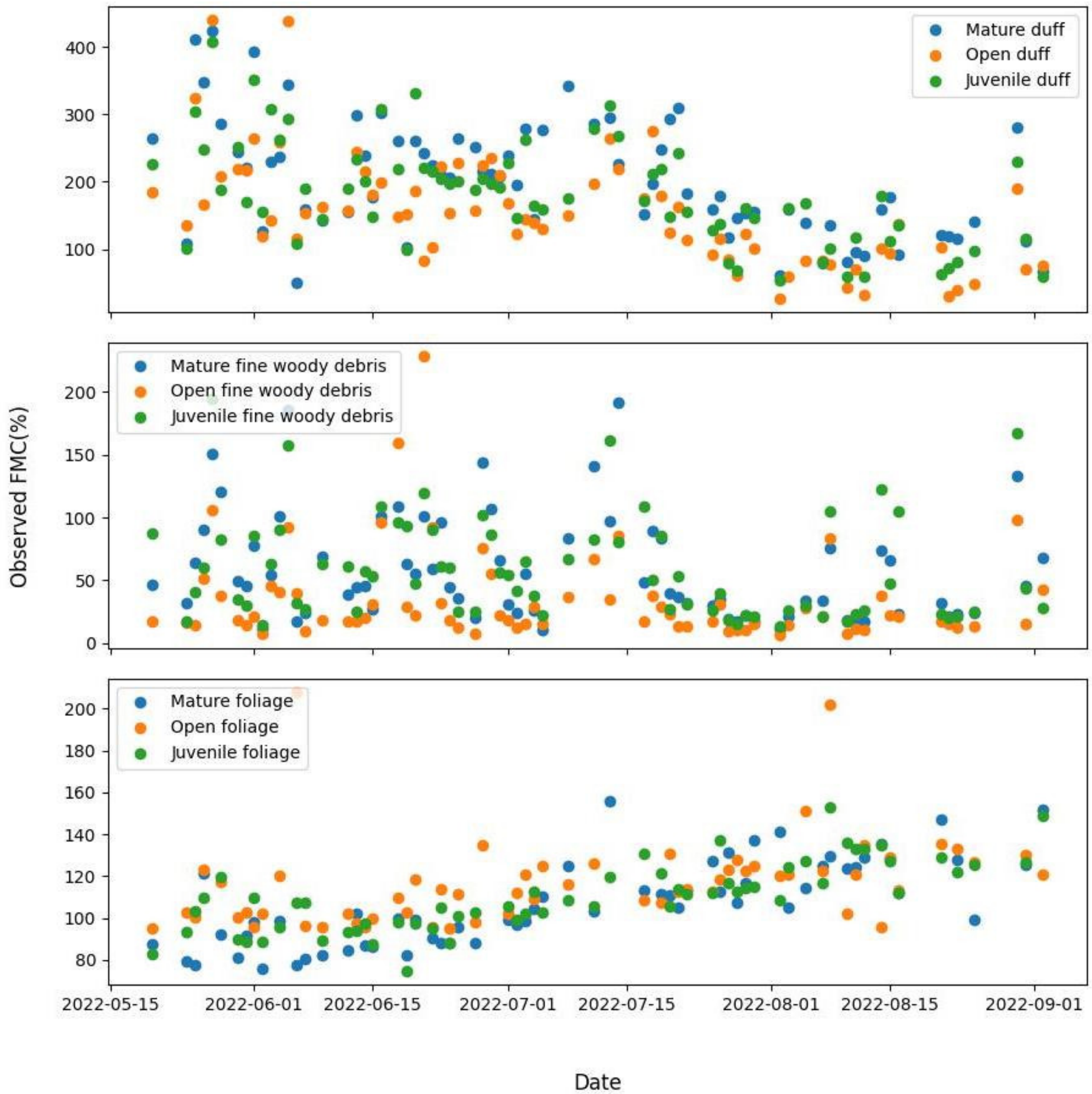

Figure 13: Daily average FMC in 2022 for different stands and fuel types at the Prince George and Smithers study locations. The number of observations averaged to create each point varies between 3 and 15, depending on the number of sites visited.

When comparing different fuel types and stands at each location, similar statistical results were found in Figure 14 to 16. To compare the FMC difference in different stands at each location, as the data is not normal distributed, Kruskal-Wallis test were also applied.

For foliage MC, open stands have higher MC compared to juvenile stands, and the difference is statistically significant at Barren, Tamarac, Chapman, and McDonnell sites ($p < 0.05$). The difference between juvenile and mature stands is generally not statistically significant, except at Chapman, where the mature stands have significantly higher MC ($p < 0.05$), and at McDonnell/Stone Creek, where the juvenile stands have significantly lower MC ($p < 0.05$).

For duff MC at different stands at each location, juvenile stands have significantly higher MC than open stands at most locations (Barren, Dennis, North Fraser, and Stone Creek, with $p < 0.05$), significantly lower MC at Chapman and McDonnell, and no statistically significant difference at Tamarac ($p > 0.05$). When comparing juvenile and open stands, most locations show no significant difference (Tamarac, Dennis, North Fraser, and Stone Creek with $p > 0.05$). However, at Barren and Dennis, juvenile stands have significantly higher averaged MC than open stands ($p < 0.05$), while at Chapman, they have significantly lower averaged MC than open stands ($p < 0.05$).

When comparing fine woody debris, juvenile stands have higher daily averaged MC than open stands at each location, and the difference is also statistically significant ($p < 0.05$). However, the difference is only significant at Barren and North Fraser sites when comparing mature and juvenile stands.

In summary, this study finds that location and stand differences play a crucial role in daily averaged FMC values for different fuel types. In the next sections, daily FMC values at each fuel types, location, and stand types were tested and compared with different methods.

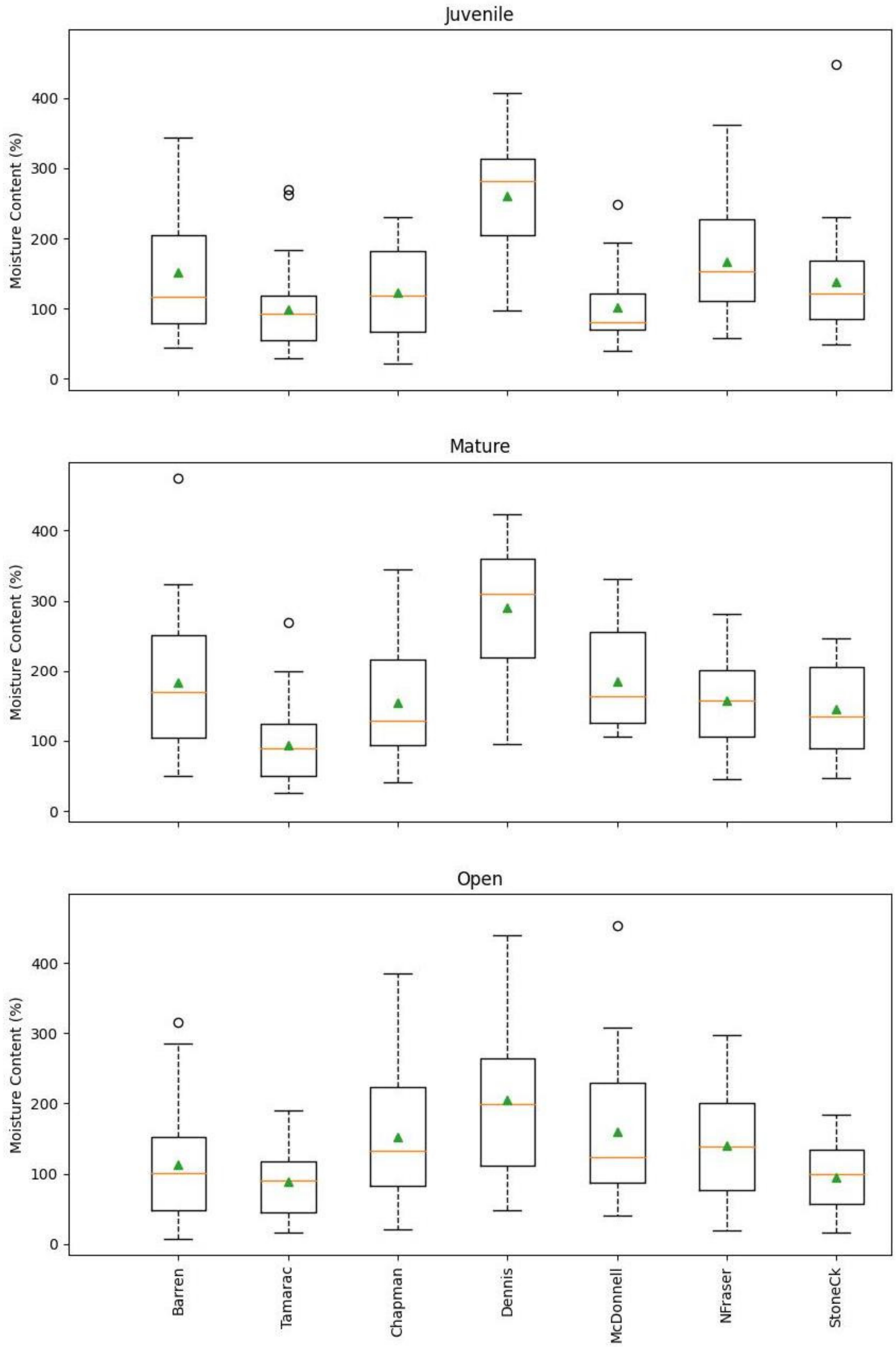

*Figure 14: Boxplots of daily averaged duff MC at different stands and locations in 2021 and 2022 around Prince George and Smithers. Lower box limits (first quartile -1.5 * IQR (Interquartile range), upper box limits (third quartile +1.5 * IQR), outliers (circles), mean values (green triangles), and median values (yellow horizontal lines) are shown.*

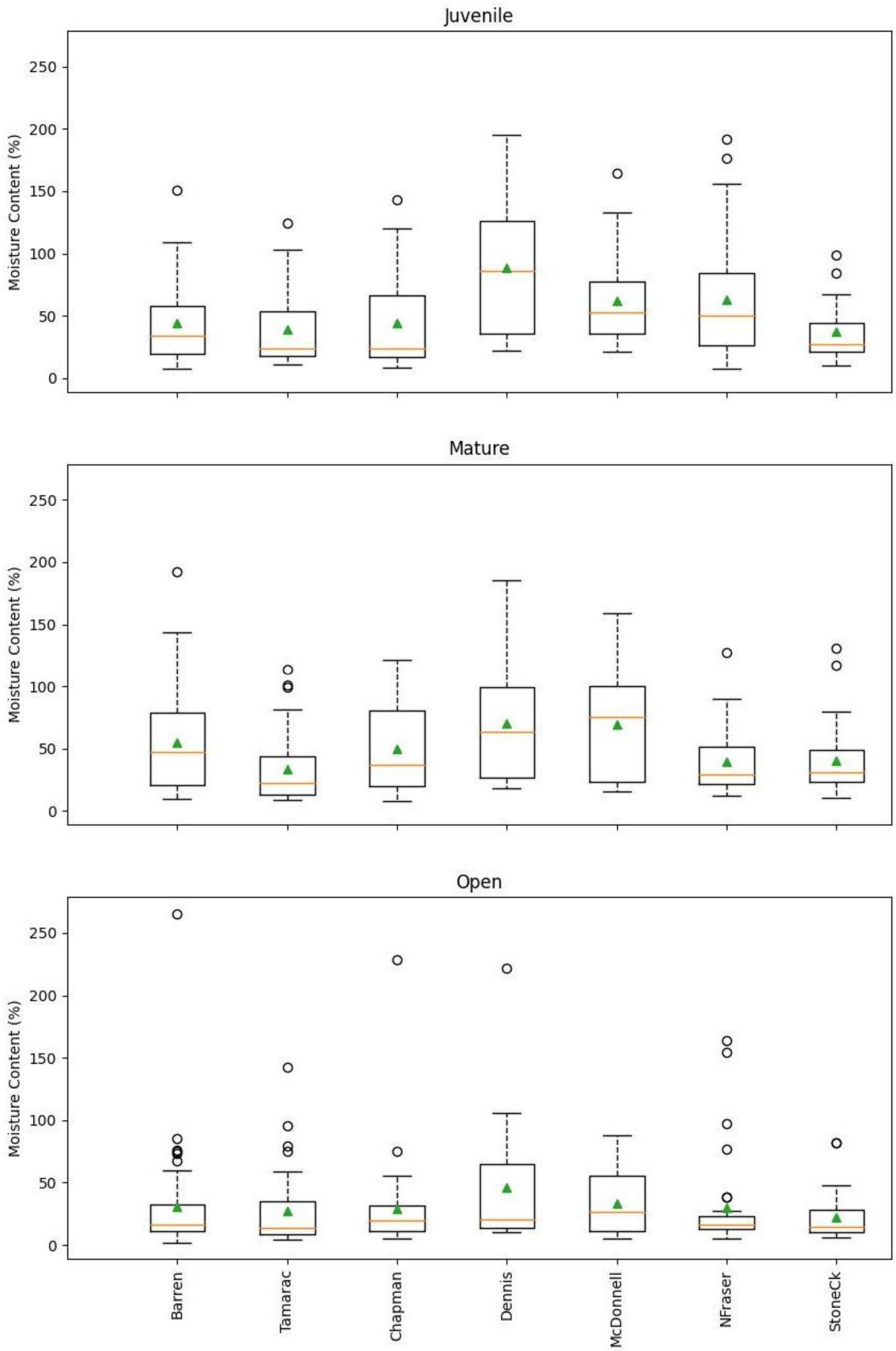

Figure 15: Boxplots of woody debris MC at different stands and sample collection sites in 2021 and 2022 around Prince George and Smithers.

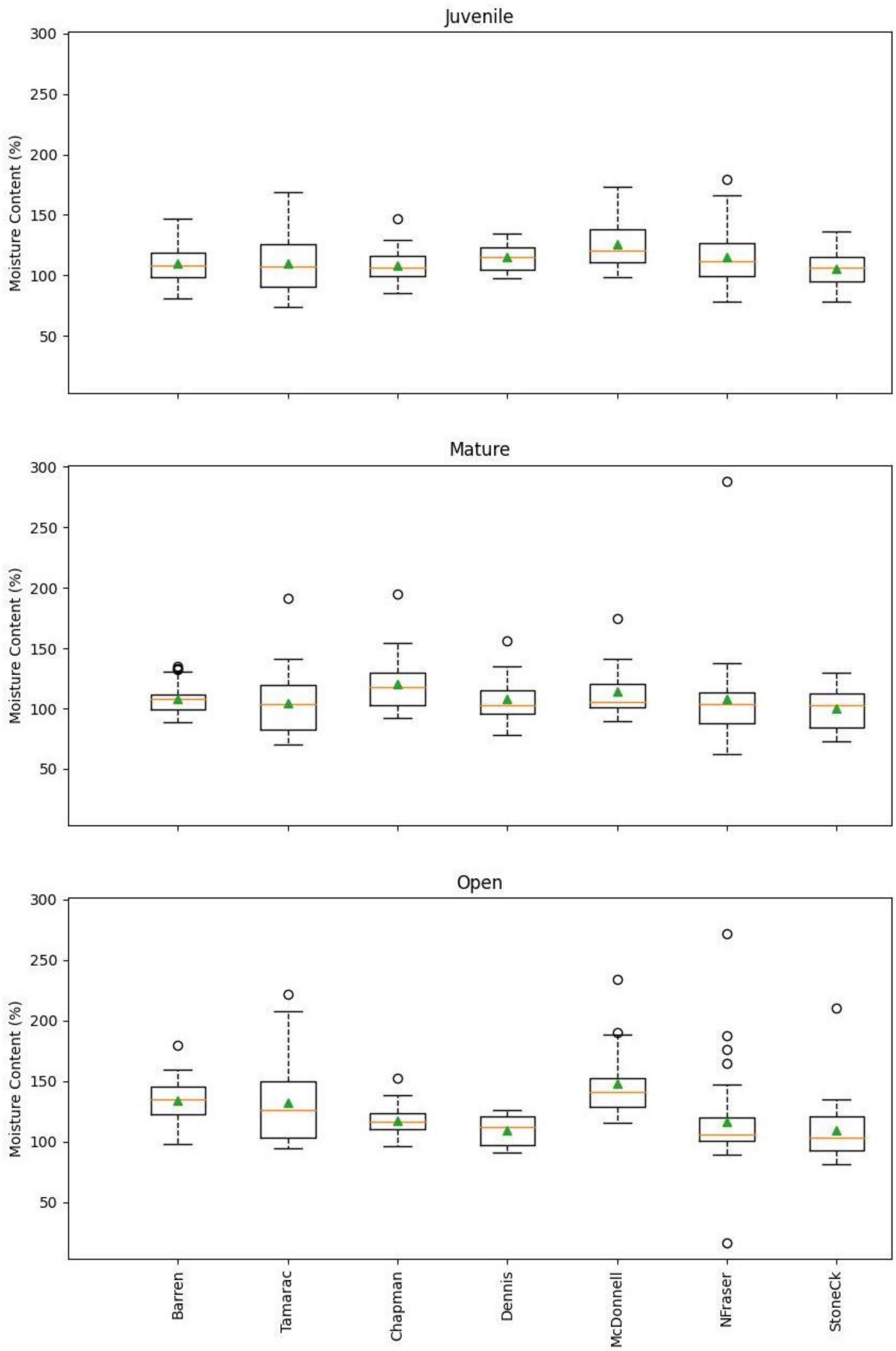

Figure 16: Boxplots of foliage MC at different stands and sample collection sites in 2021 and 2022 around Prince George and Smithers.

5.2 Meteorological Data

As the distance between fire weather stations and sample collecting sites ranges between XX and XX km, weather conditions may vary between fire weather stations and in-stand locations. Figure 17 shown an example of daily weather conditions plots between the open weather station at Barren site and the Houston fire weather station in the summer of 2022. The difference of relative humidity and precipitation between Barren open site and Houston fire weather station is not significant ($p>0.05$), however, there is a significant difference ($p<0.05$) for temperature and relative humidity.

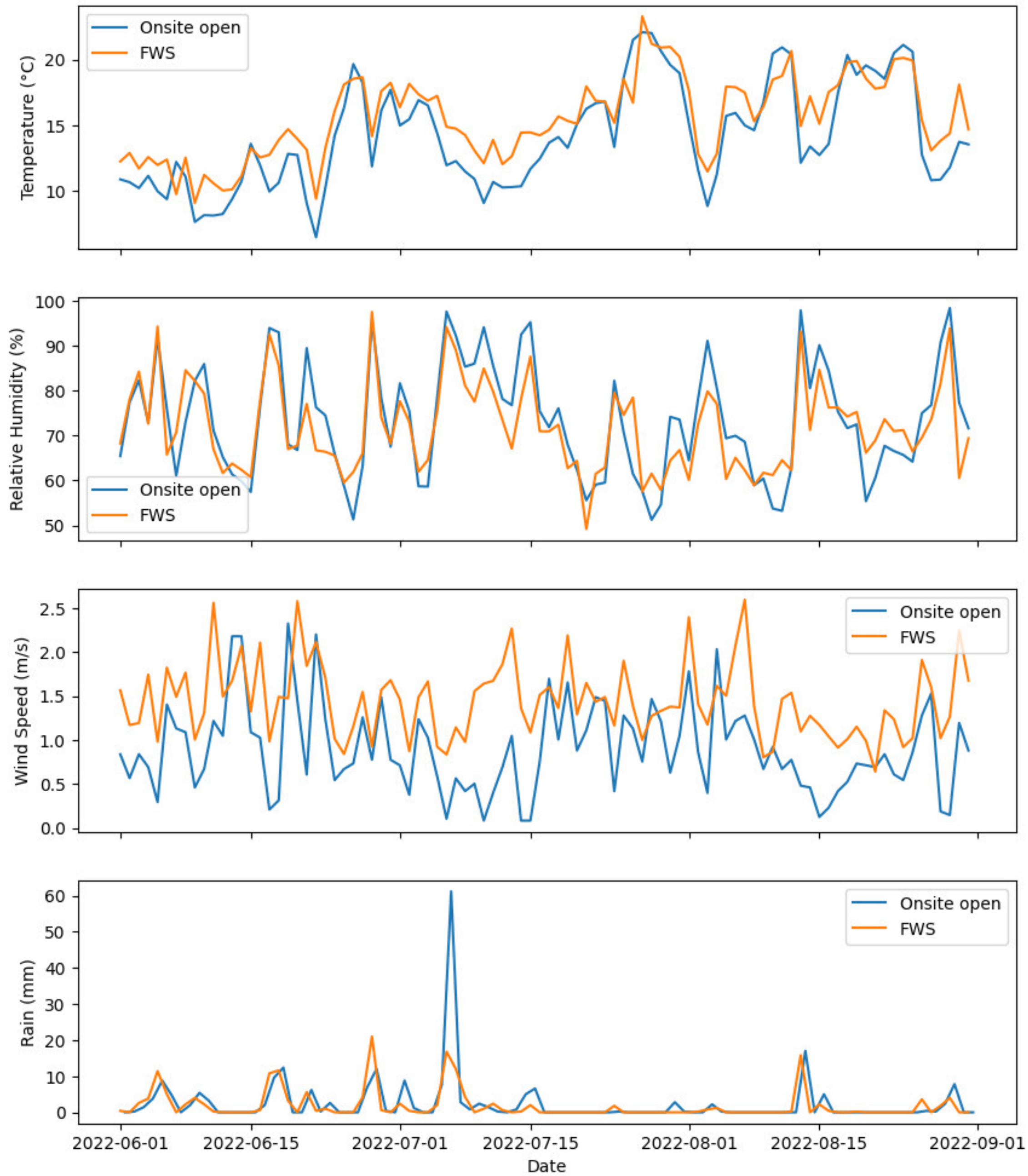

Figure 17: Weather condition comparison between the BC fire weather station (FWS, Houston) and onsite weather station in 2022 at Barren, BC.

Figure 18 demonstrates the differences in daily weather conditions at the Barren site in 2022, and summaries of the measured meteorological data are given in Appendix 4.

Comparisons of measured meteorological data from the six different locations and various stands to determine if significant differences exist between stands (Appendix 4).

Mature, juvenile, and open stands had average temperatures of 13.95°C, 14.17°C, and 15.29°C. The mean temperatures were not significantly different between mature and juvenile stands ($p>0.05$, the null hypothesis cannot be rejected), but the open stand had significantly higher temperatures.

The mature stand had an average relative humidity of 79.64%, while the juvenile stand had a significantly lower average of 72.71%. In open stands, the average relative humidity was 72.62%. The difference between open stands and both the mature and juvenile stands was also statistically significant ($p < 0.05$).

The daily averaged wind speed for the six locations in 2022 was also analyzed using the Kruskal-Wallis test due to the non-normal distribution of the data. The mature stand had an average wind speed of 0.10 m/s. In the juvenile stands, the average wind speed was 0.03 m/s. The difference between the mature and juvenile stands was not statistically significant ($p > 0.05$). However, the open stand had an average wind speed of 0.79 m/s, and the difference between the open stand and the juvenile stands was found to be significant ($p < 0.05$).

Finally, the daily accumulated precipitation was compared among the stands using the Kruskal-Wallis test. The mature stand had an average daily accumulated precipitation of 1.27 mm. The juvenile stands had an average of 1.54 mm of accumulated precipitation. The difference between the mature and juvenile stands was statistically significant ($p < 0.05$). In the open stands, the daily accumulated precipitation was 1.57 mm, slightly higher than the juvenile stands, but the difference was not statistically significant ($p > 0.05$).

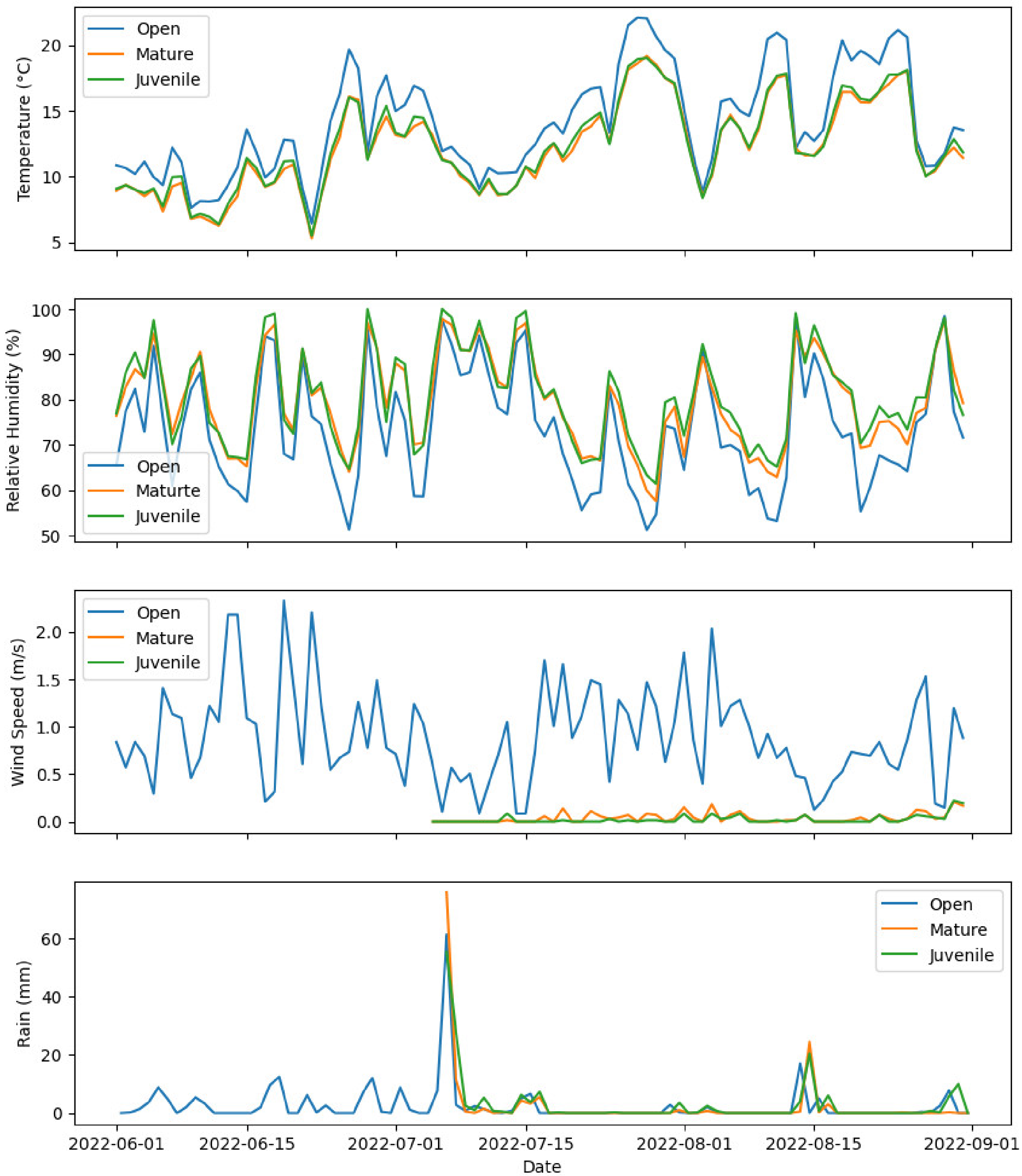

Figure 18: Weather condition comparison between on-site weather stations at different sites in 2022 at Barren, BC.

5.3 Estimates of FMC from FWI

5.3.1 Model 1: Original model with fire weather stations and empirical coefficients

Based on the methods in section 4.2, FMC for fine woody debris and duff were estimated from the fire weather station using the coefficients described in the empirical DMC and FFMC models. Modelled and observed FMC were compared for the different stands and years (Figure 19) using goodness-of-fit statistics. In 2021, the estimated duff MC was generally lower than the observed MC, with a large discrepancy between the best-fitting and one-to-one lines. However, in 2022, the estimated duff MC was generally like the observed MC, with plots closely surrounding the one-to-one line. The estimated and observed values for fine woody debris were generally close. However, in 2022 estimate fine woody debris MC in juvenile and mature stands was lower than observed in general.

Model performance (Table 9) varies among different stand types (open, mature, juvenile) and fuel types (duff and woody debris). Mean Bias Error (MBE) values for duff and woody debris range from -58.24 to 31.87 %, with the lowest MBE of -0.95 % observed in the open stand type with woody debris in 2021. RMSE values range from 26.78 to 85.35 %, with the lowest RMSE of 26.78 % observed in the juvenile stands with woody debris in 2021. The R^2 values for the duff multiple regression tests of observed and predicted values range from 0.17 to 0.44, depending on the stand type and year, with highest R^2 observed in the open stands in 2021. For fine woody debris, the R^2 values for multiple regression tests of observed and predicted values range from 0.17 to 0.65, with highest R^2 observed in the open stands in 2021. All p-values are less than 0.001, which suggests that the relationships between the predictor variable and the outcome variable are statistically significant for all combinations of stand and fuel type.

It can be observed that the ranges of RMSE and MBE are substantial for duff and fine woody debris. However, fine woody debris exhibits better statistical agreement than duff, particularly in open stands. The agreement between estimated and observed duff FMC improved in 2022 compared to 2021, while the statistical agreement for fine woody debris in 2021 was superior to that in 2022. Across years and fuel types, the RMSE and MBE in open sites are generally better than those in juvenile and mature sites.

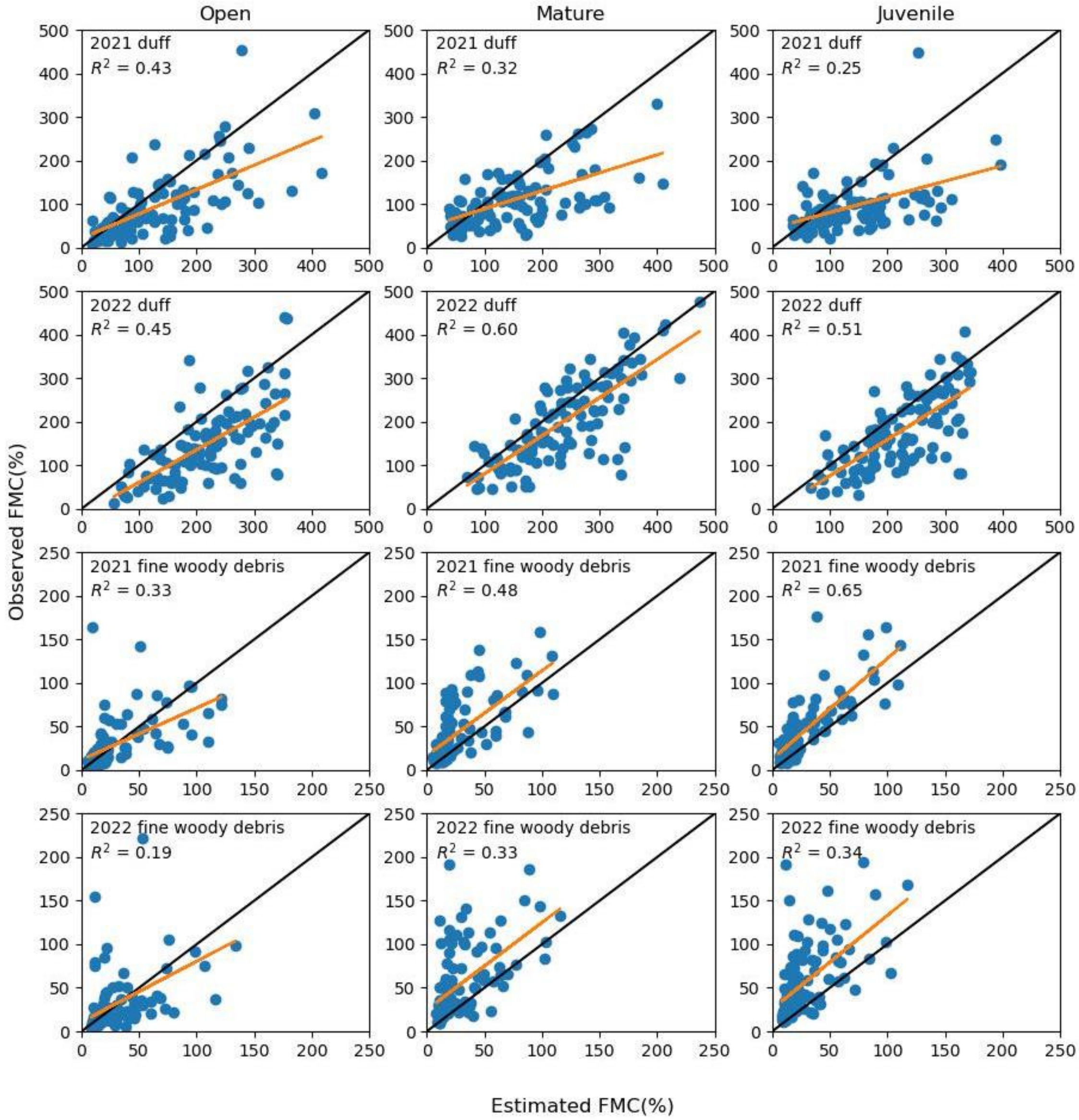

Figure 19: Estimated vs observed FMC from as-is weather empirical model at different stands, where black line indicates the one-to-one lines, orange line indicates the best fitting line.

Table 9: Errors in estimated MC for different stand and fuel types for the 'as-is' empirical model (FFMC/DMC) in 2021 and 2022. Mean Bias Error (MBE), Root Mean Squared Error (RMSE), R^2, p, and sample size (N) are given. "FWD" means fine woody debris, "x" is estimated FMC and "y" is observed FMC.

Model 1								
Year	Stand Type	Fuel Type	MBE (%)	RMSE (%)	R^2	p	Equation	N
2021	Open	duff	-56.22	83.94	0.44	<0.001	y = 0.71*x – 14.7	94
2021	Mature	duff	-39.25	78.08	0.22	<0.001	y = 0.41* x +49.08	93
2021	Juvenile	duff	-58.24	85.35	0.17	<0.001	y = 0.36*x + 41.63	94
2022	Open	duff	-30.82	68.93	0.42	<0.001	y = 1.02*x -40.79	106
2022	Mature	duff	17.16	82.99	0.35	<0.001	y = 1.07*x + 2.59	106
2022	Juvenile	duff	-6.49	59.95	0.39	<0.001	y = 0.99*x – 4.03	106
2021	Open	FWD	-0.95	27.72	0.32	<0.001	y = 0.56*x + 12.28	93
2021	Mature	FWD	13.77	30.26	0.48	<0.001	y = 0.81*x + 19.17	93
2021	Juvenile	FWD	15.37	26.78	0.65	<0.001	y = 0.98*x + 15.68	93
2022	Open	FWD	8.94	36.20	0.17	<0.001	y = 0.64*x + 12.13	128
2022	Mature	FWD	31.13	44.90	0.31	<0.001	y = 0.90*x + 27.59	128
2022	Juvenile	FWD	31.87	47.42	0.34	<0.001	y = 0.97*x + 27.8	128

5.3.2 Model 2: FFMC and DMC correction for local MC

Errors may increase when using the empirical weather model based on boreal and eastern Canada to estimate FMC in central BC. To mitigate this issue, the default maximum and minimum duff and fine woody debris MC (Table 6) was modified in the FFMC and DMC equations to minimum and maximum daily averaged values from all locations in 2021 and 2022 to reduce errors caused by varying fuel conditions across different stands. Furthermore, instead of using a default starting value of FFMC and DMC, the average MC of duff and fine woody debris on the first day of data collection was used to estimate the following day's MC in both 2021 and 2022 (Figure 20). However, the estimated MC for fine woody debris in juvenile and mature stands in 2022 is smaller than the levels observed.

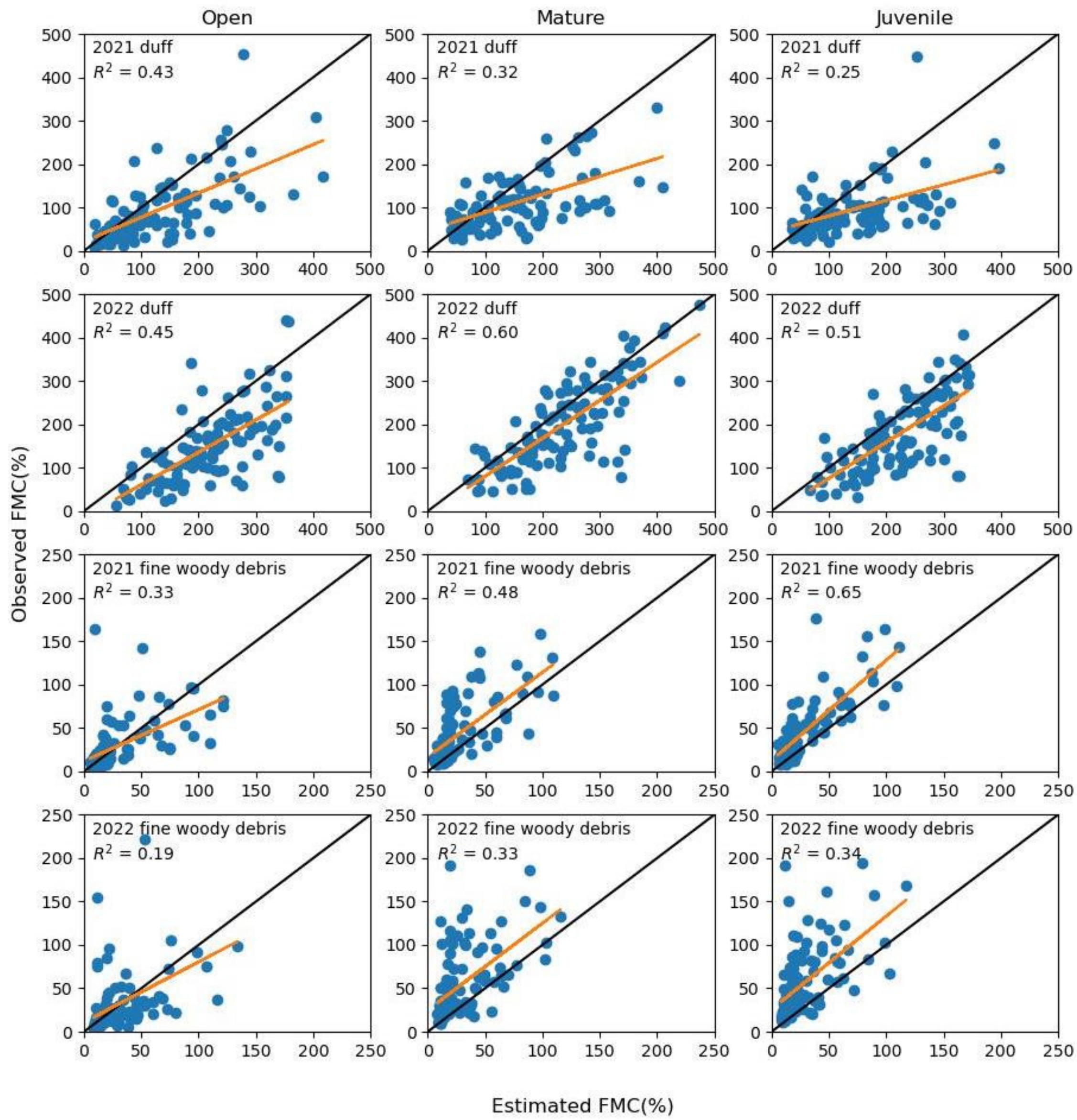

Figure 20: Estimated versus observed FMC from FWI (original model corrected by local MC), where black line indicates the one-to-one lines, orange line indicates the best fitting line.

MBE for estimated MC in fine woody debris and duff in 2021 and 2022 range from -68.19% to 27.75%, with the lowest MBE value (-0.17) occurring in the open stand type with woody debris in 2022. RMSE values range from 27.22 to 94.33%, with the lowest (27.20%) occurring in the juvenile stand type with woody debris in 2022. In terms of R^2, duff has highest R^2 (0.60) at mature stands in 2022, while fine woody debris has highest R^2 (0.65) at juvenile stands in 2021. All p-values presented in the Table 10 are less than 0.001, indicating the relationships between the predictor variable and the outcome variable are statistically significant for all combinations of stand and fuel type.

With Model 2 (local MC correction), fine woody debris MC generally exhibits better statistical agreement with predicted values across all stands and years than duff. In 2021-2022, the estimated errors for fine woody debris MC in Table 10 are similar or slightly lower than those in Table 9, whereas the MBE and RMSE for duff in Table 10 were slightly greater than in Table 9.

An improvement for fine woody debris MC prediction demonstrates the potential for more accurate results using local MC observations. However, large values for MBE and RMSE indicate that there is still room for improvement.

Table 10: Errors in estimated MC for different stand and fuel types for weather empirical model (FFMC/DMC) at different stands in 2021 and 2022, corrected by local MC. Mean Bias Error (MBE), Root Mean Squared Error (RMSE), R^2, p, and sample size (N) are given. "FWD" means fine woody debris, "x" is estimated FMC and "y" is observed FMC.

Model 2								
Year	Stand Type	Fuel Type	MBE	RMSE	R^2	p	Equation	N
2021	Open	duff	-38.01	78.96	0.43	<0.001	y = 0.6*x +21.35	93
2021	Mature	duff	-45.89	84.80	0.32	<0.001	y = 0.41*x +47.4	94
2021	Juvenile	duff	-48.47	87.51	0.25	<0.001	y = 0.36*x + 44.44	94
2022	Open	duff	-36.82	94.33	0.45	<0.001	y = 0.74*x – 13.90	106
2022	Mature	duff	-68.19	72.20	0.60	<0.001	y = 0.88*x – 7.45	106
2022	Juvenile	duff	-45.12	75.68	0.51	<0.001	y = 0.83*x – 7.70	106
2021	Open	FWD	-0.17	27.20	0.33	<0.001	y = 0.59*x + 11.81	94

2021	Mature	FWD	15.97	30.20	0.48	<0.001	y = 0.97*x + 16.74	93
2021	Juvenile	FWD	16.97	36.13	0.65	<0.001	y =1.12*x + 12.49	93
2022	Open	FWD	24.99	41.87	0.19	<0.001	y = 0.69*x + 10.93	106
2022	Mature	FWD	2.26	43.85	0.33	<0.001	y = 1.00*x + 25.00	106
2022	Juvenile	FWD	37.75	47.42	0.34	<0.001	y = 1.07*x + 25.68	106

5.3.3 Model 3: FFMC and DMC with local temperature and relative humidity

The previous section found that the use of FFMC and DMC models resulted in errors due to differences in weather conditions between the closest fire weather station and the sample observation sites. To address this issue, local weather data (temperature, relative humidity, precipitation, and wind speed) from sensors or weather stations were incorporated to determine if this could improve the accuracy of estimating FMC. Meanwhile, the use of initial MC of duff and woody debris, as well as FMC limits applied in Model 2 was continued in the model with local weather conditions.

In 2021 and 2022, HOBO sensors were installed at all sample collection sites and recorded temperature and relative humidity every 15 minutes at 30 cm above the ground. To estimate FMC, wind speed and precipitation data from the nearest fire weather station were combined with the in-stand HOBO sensors' temperature and relative humidity data, as not all sites had installed wind and precipitation sensors in 2021.

The estimated and observed FMC values in 2021 and 2022 are compared in Figure 21. The black line represents the most accurate estimation, and the orange line represents the best-fitting line. Unlike Figure 20, data from the in-stand HOBO sensors was used to replace the temperature and relative humidity inputs into the DMC and FFMC models.

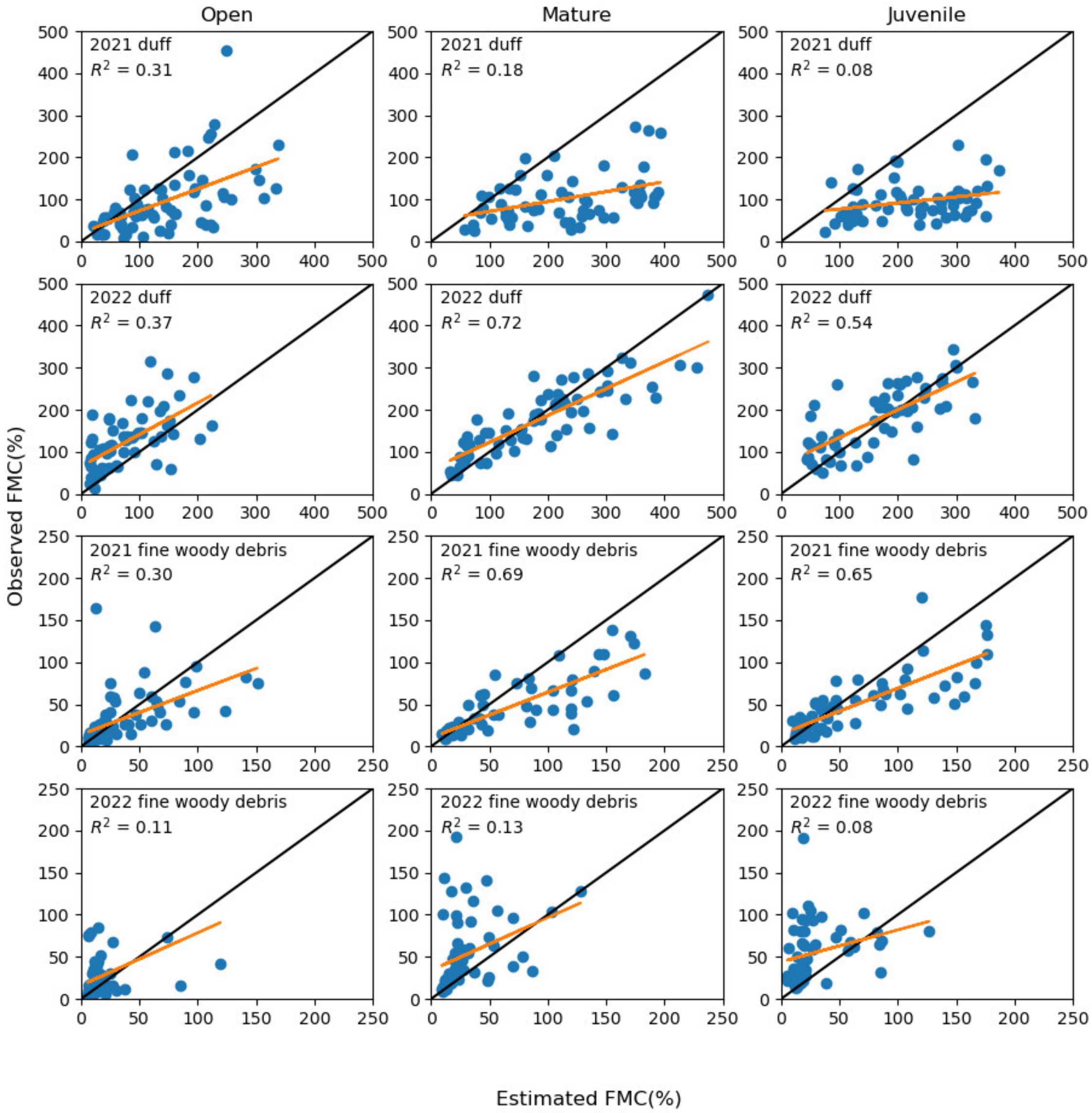

Figure 21: Estimated versus observed FMC with local in-stand temperature and relative humidity, where orange line indicates the best fitting line.

Table 11 presents MBE, RMSE, R², p values and their linear regression equations for Model 3 in 2021 and 2022. The MBE ranges from -130.23 to 47.31% (Table 11), with the lowest MBE at -9.13% when estimating duff MC at mature forests in 2022. The RMSE values range from 59.95 to 158.09%, where the lowest error is for estimating duff MC at mature stands in 2022 as well (Table 11). For fine woody debris, MBE ranges from -18.45 to 26.63%, with lowest MBE at 1.54 at open stands in 2021. In terms of RMSE, it ranges from 30.20 to 44.93%, with lowest RMSE at open stand in 2021 when estimating fine woody debris MC.

The R^2 ranges for duff and fine woody debris are 0.08-0.72 and 0.08-0.69, respectively. The p-values for most the stands are less than 0.001, indicating that the relationships between the predictor and response variables are statistically significant, except estimating duff MC in 2021 at mature juvenile stands and fine woody debris in 2022 at all stands. The highest R^2 for estimating duff MC is the mature stand type in 2022 with an R^2 of 0.72. For fine woody debris, the highest R^2 is at mature stand type in 2021 with an R^2 of 0.69.

After updating the local temperature and relative humidity data, the statistical results for some stands improved, such as estimating duff MC at mature stands in 2022, indicating that the method improved accuracy in some aspects. However, due to significant differences in wind and precipitation between open and juvenile/mature stands, combining the local in-stand data with data from nearby fire weather stations could result in errors.

Table 11: Errors in estimated MC for different stand and fuel types for the weather empirical model (FFMC/DMC) calibrated with local temperature and relative humidity, as well as local fuel correction. Mean Bias Error (MBE), Root Mean Squared Error (RMSE), and sample size (N) are given. "FWD" means fine woody debris, "x" is estimated FMC and "y" is observed FMC.

Model 3								
Year	Stand Type	Fuel Type	MBE	RMSE	R^2	p	Equation	N
2021	Open	duff	-44.84	86.99	0.31	<0.001	y = 0.52*x + 20.7	71
2021	Mature	duff	-127.86	158.09	0.18	<0.001	y = 0.23*x + 48.05	60
2021	Juvenile	duff	-130.23	153.63	0.08	0.021	y = 0.14*x + 62.56	64
2022	Open	duff	47.31	71.59	0.38	<0.001	y = 0.75*x + 65.82	62
2022	Mature	duff	-9.13	59.95	0.72	<0.001	y = 0.64*x + 58.85	64
2022	Juvenile	duff	11.44	60.30	0.54	<0.001	y = 0.66*x + 68.34	56
2021	Open	FWD	-1.54	30.20	0.30	<0.001	y = 0.52*x + 14.14	70

2021	Mature	FWD	-18.45	35.46	0.69	<0.001	y = 0.54*x + 10.25	61
2021	Juvenile	FWD	-13.23	34.07	0.65	<0.001	y = 0.54*x + 14.68	64
2022	Open	FWD	9.39	36.59	0.11	0.009	y = 0.62*x + 16.14	62
2022	Mature	FWD	23.09	44.93	0.13	0.003	y = 0.63*x + 33.92	64
2022	Juvenile	FWD	26.63	44.87	0.08	0.033	y = 0.38*x + 43.99	56

5.3.4: Model 4: FFMC and DMC with local weather conditions

In 2022, all sample collection locations were equipped with tipping bucket rain gauges and wind speed sensors, in addition to HOBO sensors that recorded temperature and relative humidity. The data collected from these devices were utilised to calculate the MC of duff and fine woody debris. Integrating data from multiple sources allowed for a more comprehensive assessment of fuel conditions, as it considered precipitation, wind speed, temperature, and relative humidity (Figure 22). In juvenile and mature stands, tipping buckets were only installed during in the middle of the sample collection season, and sample numbers were reduced in Model 4 compared to the other three models.

When comparing the RMSE and MBE values in Model 4 (Table 12) to those of Models 1, 2, and 3, it can be seen that for both duff and fine woody debris fuel types, the agreement between predicted and observed values are generally better. For duff, the smallest RMSE value in Table 15 was 66.11% for duff in mature stands. For fine woody debris, the lowest RMSE is 21.13 when estimating woody debris MC at juvenile stands. In terms of the of MBE (Table 12), the range was from -60.71 to -35.84 (duff), with a lowest MBE at mature stands. The MBE range for fine woody debris was lower (-1.32 to 6.20%) than for duff, where the lowest values (best agreement) as found for open stands (-1.32%). The highest R^2 was the mature stand with an R^2 of 0.71 when estimating duff MC. For fine woody debris, the highest R^2 was the juvenile stand type with an R^2 of 0.76. All the stands have statistically significant relationships between the predictor and response variables of the linear regression at the p-value limit of 0.001.

This suggests that Model 4 produces better predictions regarding the spread of residuals (errors) compared to Models 1, 2, and 3.

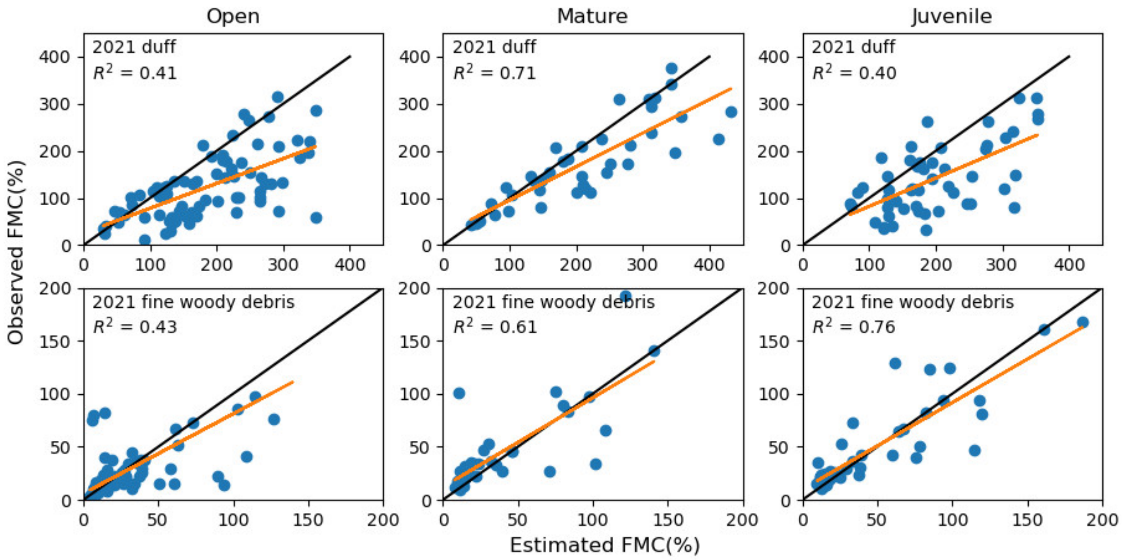

Figure 22: Estimate vs observation FMC with local weather conditions, where black line indicates the one-to-one lines, orange line indicates the best fitting line.

Table 12: Errors in estimated MC for different stand and fuel types for weather empirical model (FFMC/DMC) with local temperature, relative humidity, wind speed, and accumulated precipitation, as well as local fuel correction. Mean Bias Error (MBE), Root Mean Squared Error (RMSE), and sample size (N) are given. "FWD" means fine woody debris, "x" is estimated FMC and "y" is observed FMC.

Model 4								
Year	Stand Type	Fuel Type	MBE	RMSE	R^2	p	Equation	N
2022	Open	duff	-60.71	89.40	0.41	<0.001	y = 0.53*x + 25.67	71
2022	Mature	duff	-35.84	66.11	0.71	<0.001	y = 0.71*x + 24.54	60
2022	Juvenile	duff	-56.23	85.53	0.40	<0.001	y = 0.60*x + 22.40	64
2022	Open	FWD	-1.32	27.20	0.43	<0.001	y = 0.75*x + 5.92	70
2022	Mature	FWD	6.20	25.26	0.61	<0.001	y = 0.84*x + 12.09	61
2022	Juvenile	FWD	1.65	21.13	0.76	<0.001	y = 0.82*x + 9.99	64

5.4 Estimates of FMC from Remote Sensing

5.4.1 Estimating FMC with Sentinel 2 data in 2021

In 2021, Sentinel 2 was used as the source of remote sensing data compared with field observation data, while in 2022, both Landsat 8 & 9 and Sentinel 2 data were used (Table 13). When extracting remote sensing indices from GEE, the time series was set between May 1st to September 30th in 2021 and May 1st to September 3rd in 2022 to cover and match the sample collection period. Due to the smoke created by the wildfires, valid images available in 2021 (11.48 - 32.79 %) were fewer than in 2022 (50 - 65.38 %) when using Sentinel 2 data (Table 13). Landsat 8 & 9 data have fewer total image numbers (31 - 62 images), and the valid percent was generally low (12.77% - 17.65%).

Table 13: Study area's cloud/shadow free images in the summer of 2021 and 2022 from Smithers and Prince George

Year	Satellite	Site name	Valid	Total	Valid Percent (%)
2021	Sentinel 2	Tamarac	15	62	24.19
2021	Sentinel 2	North Fraser	18	61	29.51
2021	Sentinel 2	Stone Creek	20	61	32.79
2021	Sentinel 2	Chapman	8	61	13.11
2021	Sentinel 2	McDonnell	7	61	11.48
2021	Sentinel 2	Houston	8	61	13.11
2022	Sentinel 2	Tamarac	27	53	50.94
2022	Sentinel 2	North Fraser	31	50	62.00
2022	Sentinel 2	Stone Creek	26	51	50.98
2022	Sentinel 2	Chapman	33	52	63.46

2022	Sentinel 2	Dennis	27	54	50.00
2022	Sentinel 2	Houston	34	52	65.38
2022	Landsat 8&9	Tamarac	6	62	9.68
2022	Landsat 8&9	North Fraser	5	31	16.13
2022	Landsat 8&9	Stone Creek	6	47	12.77
2022	Landsat 8&9	Chapman	6	34	17.65
2022	Landsat 8&9	Dennis	5	32	15.63
2022	Landsat 8&9	Houston	5	32	15.63

Example maps for the five indices used in this research are shown in Figure 23. For NDMI and NMDI, juvenile and mature forests generally have higher index values than open stands, while VARI and GNDVI have lower index values instead (Figure 23). However, the situation might change from other days' satellite imagery and another location.

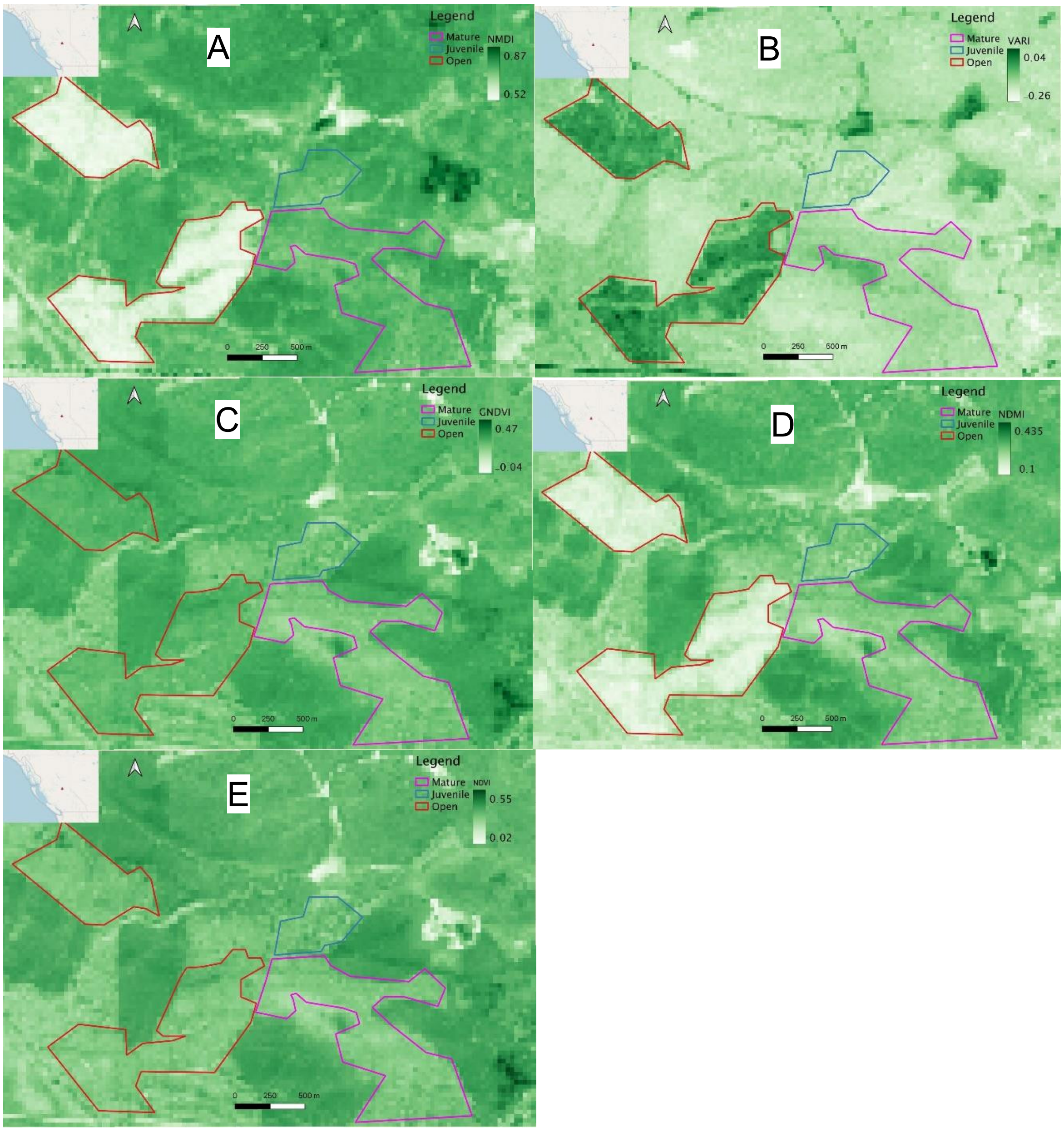

Figure 23: Example of remote sensing indices. A) NMDI, B) VARI, C) GNDVI, D) NDMI, E) NDVI at North Fraser sites on June 2nd , 2022, where red polygons indicate the open stand, purple polygons indicate juvenile stands, and blue polygons indicate mature stands. Darker green colours indicate higher indices values (denser and healthy forest, opposite with VARI), and whiter colour indicating lower indices values (bare vegetation cover, opposite with VARI).

Figures 24 - 27, blue points are the training data, and the green line is their best fitting line, while orange points are the test points.

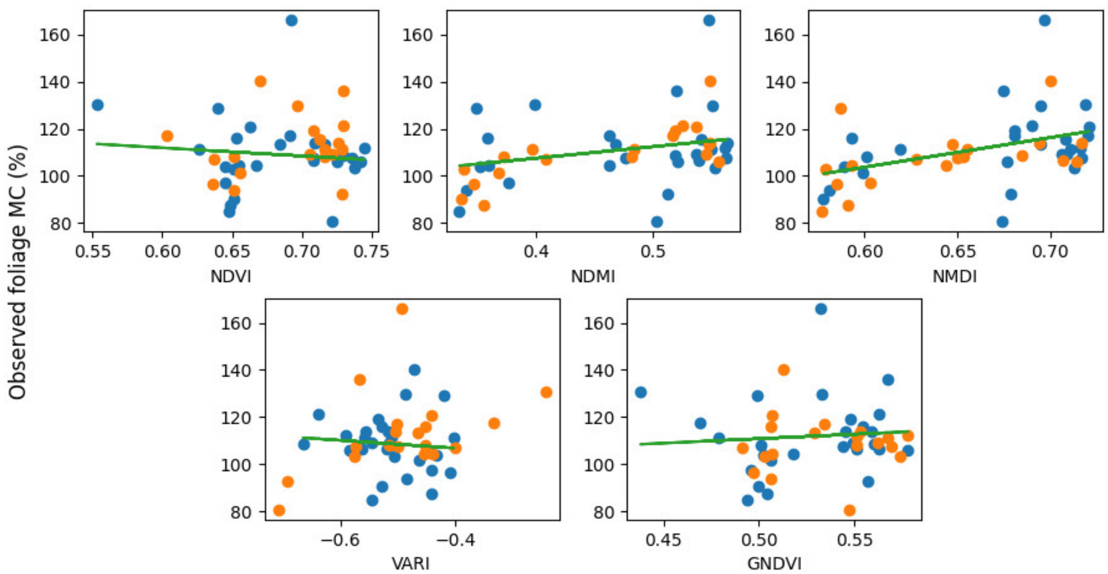

Figure 24: Foliage MC compared with five remote sensing indices at juvenile stands with Sentinel 2 data in 2021, where blue points are train data, green lines are the linear regression based on blue points, and orange points are test data.

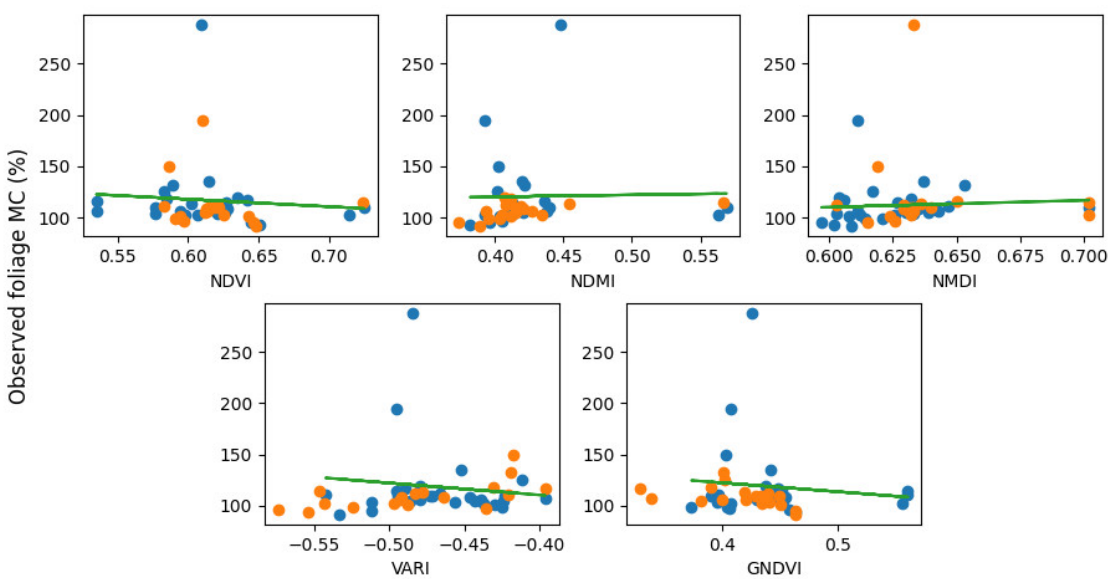

Figure 25: Foliage MC compared with five remote sensing indices at mature stands with Sentinel 2 data in 2021, where blue points are train data, green lines are the linear regression based on blue points, and orange points are test data.

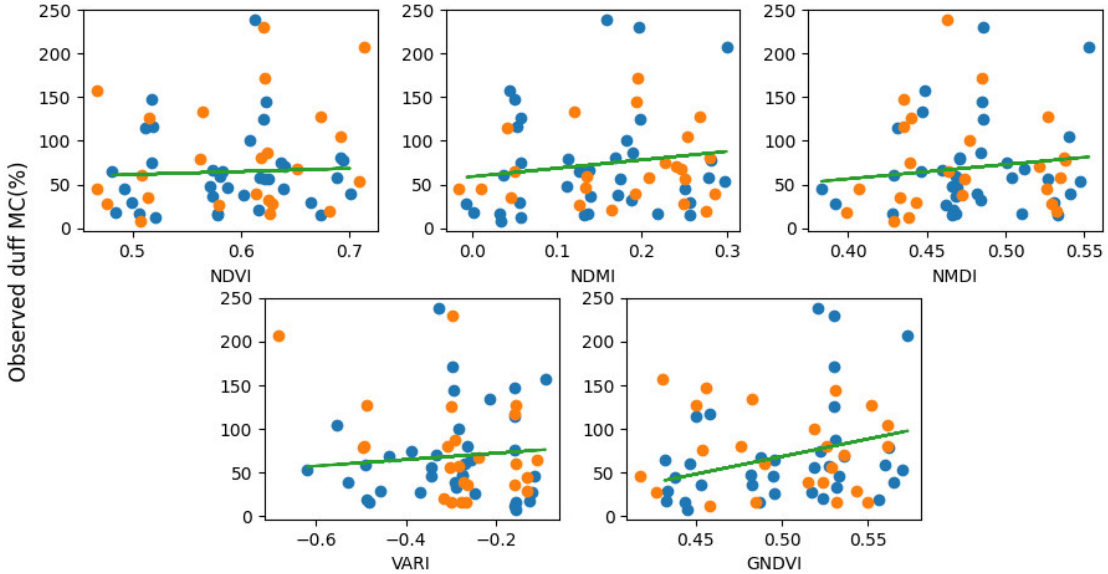

Figure 26: Duff MC compared with five remote sensing indices at open stands with Sentinel 2 data in 2021, where blue points are train data, green lines are the linear regression based on blue points, and orange points are test data.

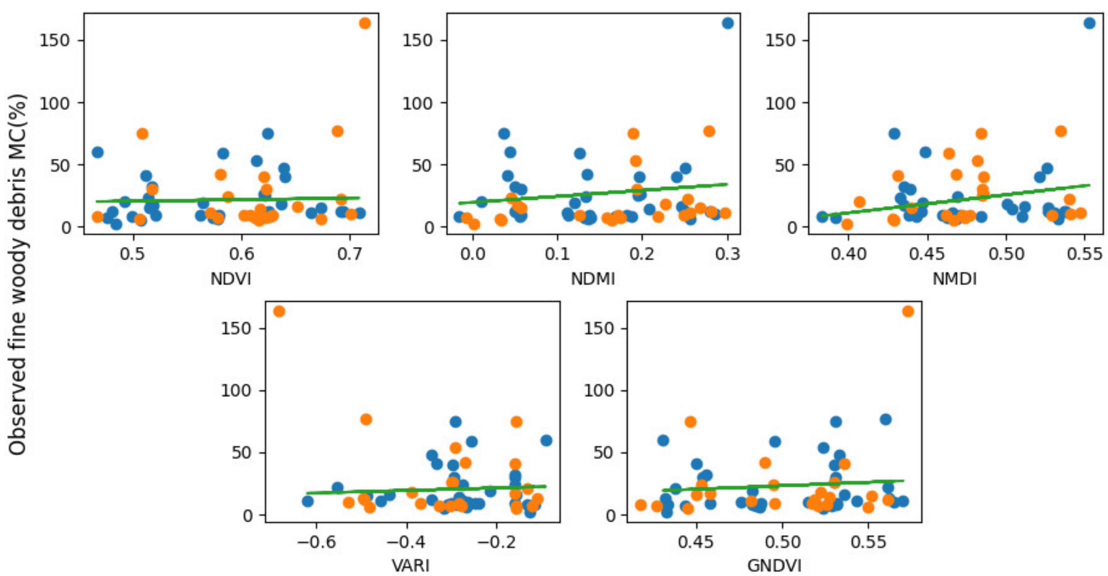

Figure 27: Fine woody debris MC compared with five remote sensing indices at open stands with Sentinel 2 data in 2021, where blue points are train data, green lines are the linear regression based on blue points, and orange points are test data.

Regression models for estimating MC from remote sensing indices using the 2021 data are mostly poor (Table 14). Only one relationship (NMDI versus foliage MC in juvenile stand) appears to be statistically significant, with ($R^2 = 0.334$ and $p < 0.05$).

Other than NDMI for juvenile stands, all the other indices R^2 values are less than 0.10, and/or p-values are greater than 0.05. In general, RSME calculated from independent observations and the regression model are lower in juvenile stands than in mature stands. VARI-predicted foliage MC in juvenile stands had the lowest RMSE (12.76), while GNDVI at the mature site had the lowest RMSE at 14.61 (Table 14).

Table 14: Statistical results of remote sensing indices with second year foliage MC at juvenile and mature stands (2021 Sentinel 2), where "y" is the observed foliage MC. Significant relations ($p < 0.05$) shown in bold.

Index	Stand Type	R^2	p	RMSE	Equation (train)	N train	N test
NDVI	Juvenile	0.009	0.2198	13.58	y = -32.23*NDVI + 134.96	27	19
NDMI	Juvenile	0.128	0.0671	13.97	y = 64.82*NDMI + 80.73	27	19
NMDI	**Juvenile**	**0.334**	**0.0016**	**17.86**	**y = 141.40*NMDI + 13.53**	**27**	**19**
VARI	**Juvenile**	**0.087**	**0.0500**	**12.76**	**y = 55.05*VARI + 138.83**	**27**	**19**
GNDVI	Juvenile	0.040	0.3170	18.88	y = 76.34*GNDVI + 67.51	27	19
NDVI	Mature	0.007	0.6720	23.50	y = -72.51*NDVI + 161.45	27	19
NDMI	Mature	0.000	0.9710	15.92	y = 18.95*NDMI + 112.71	27	19
NMDI	Mature	0.005	0.7170	43.00	y = 66.62*NMDI + 70.22	27	19
VARI	Mature	0.013	0.3178	20.35	y = -116.98*VARI + 63.75	27	19
GNDVI	Mature	0.012	0.5930	14.61	y = -87.54*GNDVI + 157.48	27	19

Statistical results for duff and woody debris MC models in open stands are shown in Table 15. No significant relations ($p < 0.05$) could be identified. At open sites, NMDI had a stronger correlation (R^2 at 0.046, p at 0.22) with fine woody debris. In comparison, GNDVI had a slightly stronger correlation when estimating duff MC than other indices, as indicated by their relatively higher R^2 value (0.092) and lower p-value

(0.07). Duff predictions had generally much higher RMSE (around 41.64 – 63.29) than for fine woody debris (20.90 - 36.43) with all indices. However, all indices in Table 15 were not good enough to estimate duff and woody debris MC, with their lower R^2 (less than 0.1) and higher p-values.

Table 15: Statistical results of remote sensing indices with fine woody debris/ duff MC at open stands (2021 Sentinel 2), where FWD means fine woody debris, y is observed FMC. No significant relations were identified.

Index	Fuel Type	R^2	p	RMSE	Equation (train)	N train	N test
NDVI	duff	0.002	0.0800	63.29	y = 35.22*NDVI +43.78	36	24
NDMI	duff	0.020	0.6803	41.64	y = 95.98*NDMI +59.00	36	24
NMDI	duff	0.016	0.5537	55.82	y = 164.38*NMDI – 9.27	36	24
VARI	duff	0.009	0.3133	57.84	y = 36.71*VARI + 79.70	36	24
GNDVI	duff	0.092	0.0728	50.83	y = 402.45*GNDVI-132.72	36	24
NDVI	FWD	0.002	0.0661	34.86	y = 11.66*NDVI + 14.76	35	24
NDMI	FWD	0.020	0.6574	20.90	y = 48.33*NDMI + 19.52	35	24
NMDI	FWD	0.046	0.2150	21.68	y = 145.27*NMDI - 46.97	35	24
VARI	FWD	0.005	0.1599	36.43	y = 10.16*VARI + 23.41	35	24
GNDVI	FWD	0.014	0.4761	32.34	y = 55.75*GNDVI – 4.73	35	24

5.4.2 Estimating FMC with Landsat 8 & 9 data in 2022.

With the launch of Landsat 9 in 2022, image frequency increased, and indices could be combined for both Landsat 8 & 9, which have the same spectral bands. Cloud- and shadow-free images of Landsat 8 and 9 data were extracted from GEE, then compared with field observation data at different stands. Similar to section 5.3.1, daily averaged foliage MC data at juvenile and mature stands were compared with remote sensing indices (Figures 28 and 29), and duff and fine woody debris MC were compared with remote sensing indices in open stands (Figures 30 and 31).

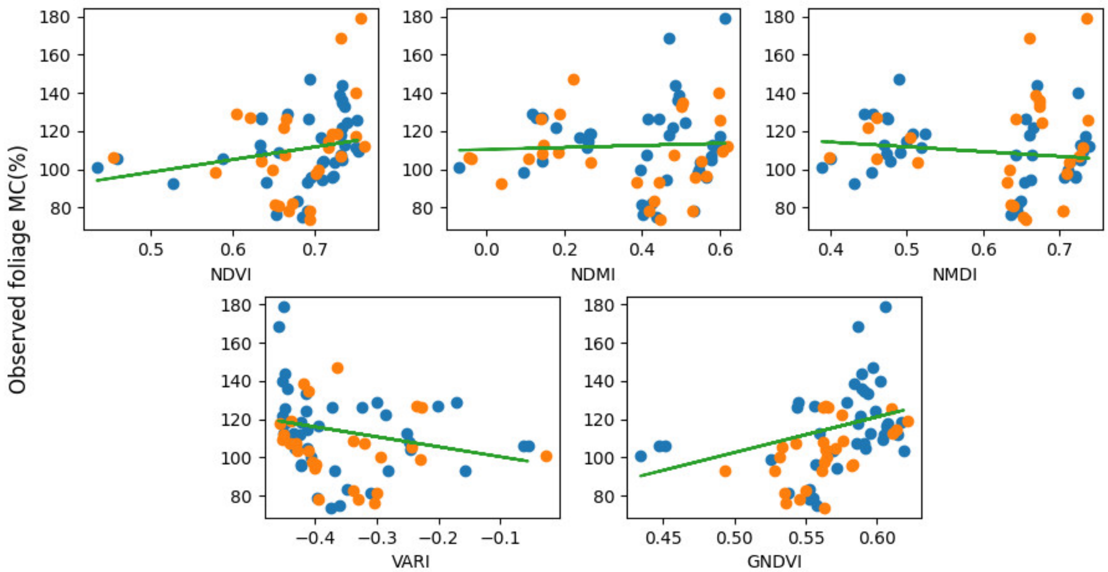

Figure 28: Foliage MC compared with five remote sensing indices at juvenile stands with Landsat 8 & 9 data in 2022, where blue points are training data, green lines are the linear regression based on blue points, and orange points are test data.

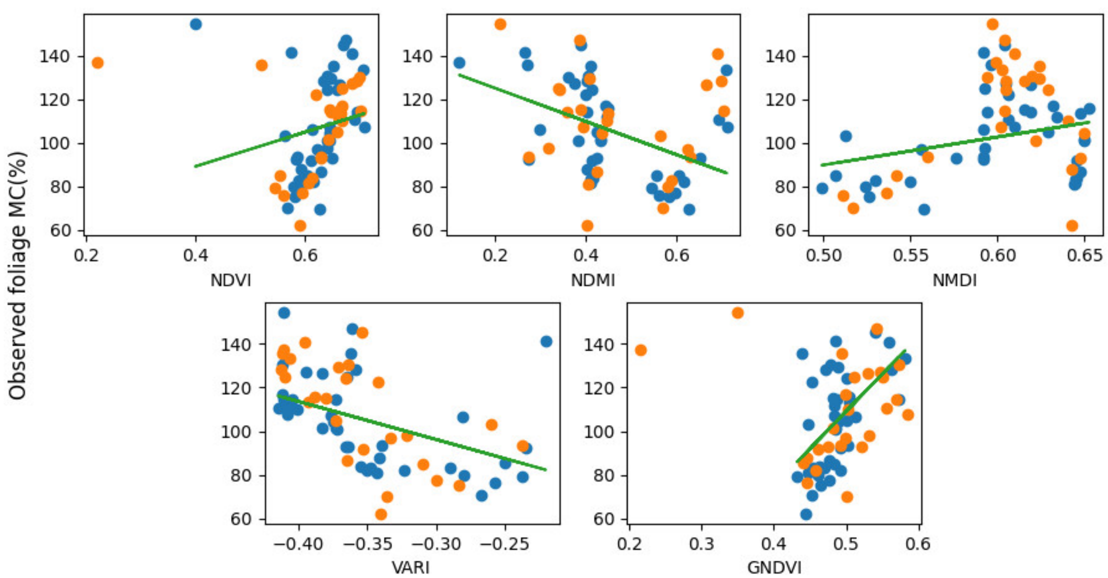

Figure 29: Foliage MC compared with five remote sensing indices at mature stands with Landsat 8 & 9 data in 2022, where blue points are training data, green lines are the linear regression based on blue points, and orange points are test data.

Model summaries and error statistics for remote sensing of foliage MC in juvenile and mature forests are shown in Table 16. R^2 values range from 0.002 to 0.126 for juvenile stands and from 0.032 to 0.297 for mature stands, while p values range from

0.0247 to 0.2890 for juvenile stands and from 0.0003 to 0.2740 for mature stands, which indicates weak relationships. When analysing the results for each stand individually, it can be observed that the GNDVI index had the highest R^2 value of 0.297 for the mature stands, and the GNDVI index had the highest R^2 value of 0.126 for the juvenile stands. For the test data, the RMSE range for juvenile stands was between 18.01 and 26.89, with the lowest RMSE observed using GNDVI. In contrast, for mature stands, the RMSE range was between 19.60 and 34.98, and the lowest RMSE was observed using VARI.

Table 16: Statistical results of remote sensing indices with foliage MC at juvenile and mature stands (2022 Landsat 8 & 9) where y is observed FMC.

Index	Stand Type	R^2	p	RMSE	Equation (train)	N train	N test
NDVI	Juvenile	0.070	0.0999	24.01	y = 66.4*NDVI + 65.23	40	27
NDMI	Juvenile	0.002	0.0623	19.47	y = 5.32*NDMI + 110.34	40	27
NMDI	Juvenile	0.030	0.2890	26.89	y = -24.92*NMDI + 124.21	40	27
VARI	Juvenile	0.062	0.1200	19.61	y = -52.18*VARI + 95.09	40	27
GNDVI	**Juvenile**	**0.126**	**0.0247**	**18.01**	**y = 186.36*GNDVI + 9.33**	**40**	**27**
NDVI	Mature	0.032	0.2740	21.56	y = 78.39*NDVI + 57.80	39	26
NDMI	**Mature**	**0.212**	**0.0032**	**24.31**	**y = -79.70*NDMI + 140.56**	**39**	**26**
NMDI	Mature	0.090	0.0632	25.67	y = 128.12*NMDI + 25.79	39	26
VARI	**Mature**	**0.216**	**0.0029**	**19.60**	**y = -174.08*VARI + 49.98**	**39**	**26**
GNDVI	**Mature**	**0.297**	**0.0003**	**34.98**	**y = 341.56*GNDVI – 61.71**	**39**	**26**

Model summaries and error statistics for linear models were developed between remote sensing indices and duff and fine woody debris MC at open stands (Figures 30 and 31) and are presented in Table 17. Similar to the findings in Section 5.3.1, the relationship between the indices and duff and fine woody debris MC is relatively weak compared to their relationship to foliage MC, indicating that these indices may not be suitable for estimating woody debris MC. However, when using indices to estimate fine woody debris MC, it has lower RMSE (17.57 – 44.40) compared to duff (59.10 – 69.32).

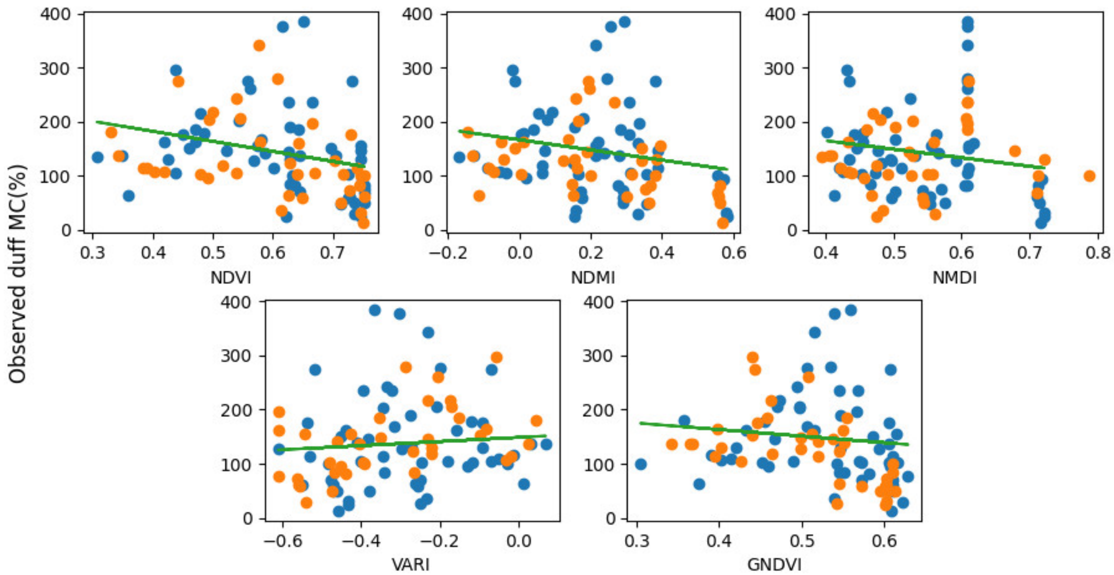

Figure 30: Duff MC compared with five remote sensing indices at open stands with Landsat 8 & 9 data in 2022, where blue points are training data, green lines are the linear regression based on blue points, and orange points are test data.

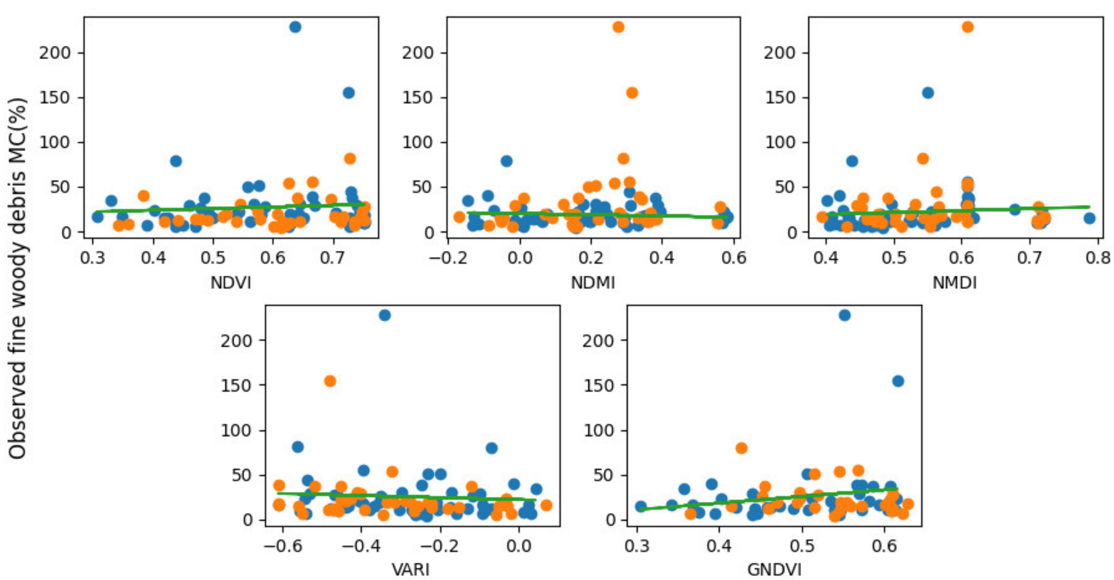

Figure 31: Fine woody debris MC compared with five remote sensing indices at open stands with Landsat 8 & 9 data in 2022, where blue points are training data, green lines are the linear regression based on blue points, and orange points are test data.

Table 17: Statistical results of remote sensing indices with duff and fine woody debris MC at open stands, where FWD means fine woody debris, y is observed FMC (2022 Landsat 8 & 9).

Index	Fuel Type	R^2	P	RMSE	Equation (train)	N train	N test
NDVI	**duff**	**0.079**	**0.0374**	**69.32**	**y = -185.32*NDVI + 256.41**	**55**	**38**
NDMI	duff	0.036	0.1650	59.93	y = -93.98*NDMI + 166.56	55	38
NMDI	duff	0.027	0.2290	64.59	y = -157.4*NMDI + 227.79	55	38
VARI	duff	0.006	0.5900	59.10	y = 37.99*VARI + 148.66	55	38
GNDVI	duff	0.013	0.4130	65.48	y = -120.98*GDNVI + 211.58	55	38
NDVI	FWD	0.004	0.6390	17.57	y = 17.87*NDVI + 16.66	55	38
NDMI	FWD	0.012	0.4250	44.40	y = -6.70*NDMI + 19.96	55	38
NMDI	FWD	0.008	0.5240	36.63	y = 21.19*NMDI + 10.56	55	38
VARI	FWD	0.004	0.6590	23.99	y = -11.25*VARI + 22.09	55	38
GNDVI	FWD	0.029	0.2640	18.90	y = 74.00*GNDVI – 11.41	45	31

When comparing the results between sections 5.3.1 (Sentinel 2, 2021) and 5.3.2 (Landsat 8 & 9, 2022), it can be seen that the R^2 values are generally higher, p-values are generally lower in Table 16 and 17 than in Table 14 and 15. This suggests that the relationship between the indices and foliage/duff MC is stronger and more statistically significant when using Landsat 8 & 9 data in 2022 than Sentinel 2 in 2021.

As previously discussed in the Methods chapter, the occurrence of multiple wildfires in central BC during 2021 resulted in significant smoke that may have impacted the remote sensing data collected during that year. Additionally, the sample collection dates in 2021 were only sometimes closely aligned with satellite collection dates, which may have further contributed to potential errors in the data. To determine which method is more reliable, the remote sensing index derived from Sentinel 2 data was compared to the observed FMC data collected in 2022.

5.4.3 Estimating FMC with Sentinel 2 data in 2022.

As stated in section 4.4.1, after January 25, 2022, the Sentinel 2 harmonized collection shifted data in new scenes to match the range of previous scenes. While using the harmonized collection, the QA bands were ineffective in removing cloudy pixels, so an NDVI filter was used instead. In 2022, sample collections around Smithers and Prince George were timed to coincide with Sentinel 2 overpasses, resulting in higher sample numbers than in 2021. Relationships between different remote sensing indices and observed MC are shown in Figures 32 and 33, with the orange lines indicating their best-fitting lines. Although there were more samples compared to data from 2021 using Sentinel 2 and Landsat 8 and 9 data in 2022, it created more noise and errors.

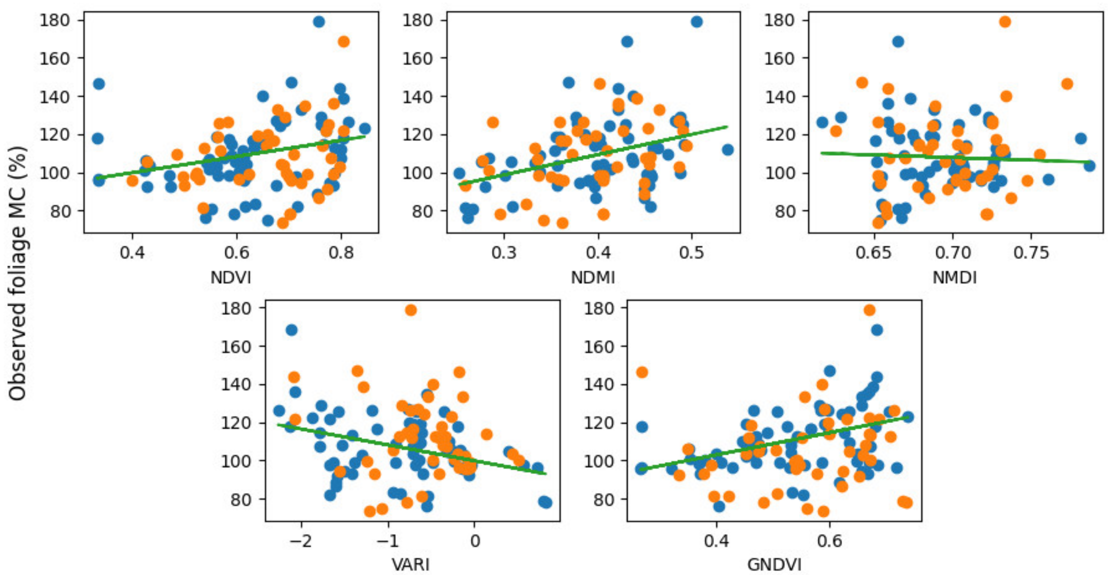

Figure 32: Remote sensing indices compared with foliage MC for juvenile stands with Sentinel 2 data in 2022, where blue points are training data, green lines are the linear regression based on blue points, and orange points are test data.

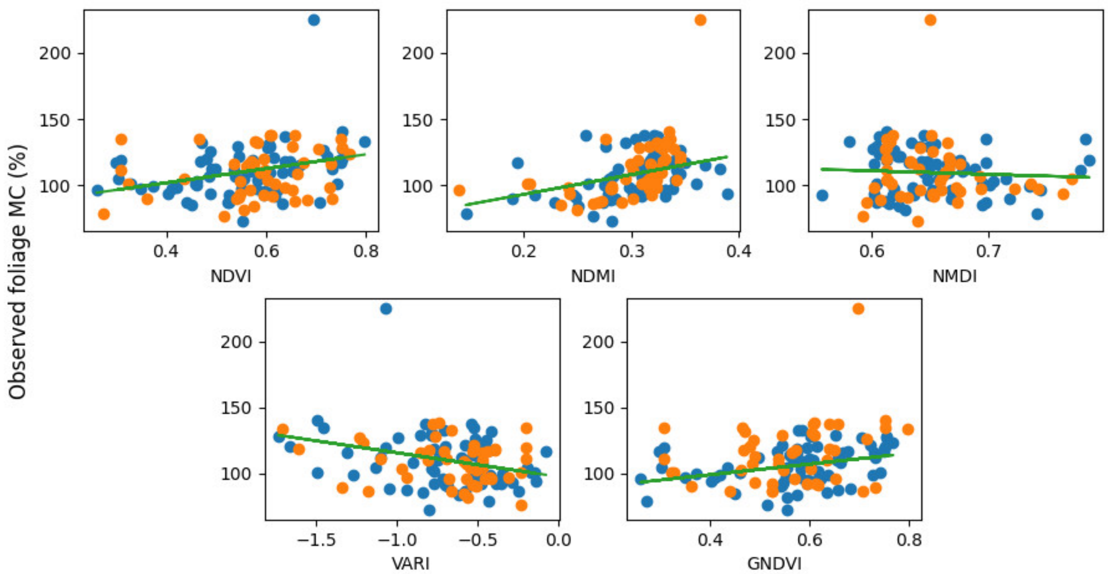

Figure 33: Remote sensing indices compared with foliage MC for mature stands with Sentinel 2 data in 2022, where blue points are training data, green lines are the linear regression based on blue points, and orange points are test data.

Statistical results from the 2022 Sentinel 2 MC models are given in Table 18. At juvenile stands, GNDVI had the highest R^2 value (0.175) and the lowest p value (0.0004) among all the indices, followed by VARI (R^2 = 0.139 and p = 0.0019) and NDMI (R^2 = 0.137 and p = 0.0021. For mature stands, NMDI had higher R^2 value (0.160) among all the indices, followed by GNDVI (R^2 at 0.124), NDVI (R^2 at 0.110). Linear regression models showed stronger relationships for juvenile stands than mature stands when estimating foliage MC. The RMSE range for juvenile stands is between 16.97 – 22.87, which is close to mature forests (15.50 to 24.94).

Table 18: Statistical results of remote sensing indices relationships with foliage MC at juvenile and mature stands (Sentinel 2, 2022), where y is observed foliage MC.

Index	Stand Type	R^2	P	RMSE	Equation (train)	N train	N test
NDVI	**Juvenile**	**0.083**	**0.0181**	**17.56**	**y = 42.31*NDVI + 82.85**	**67**	**45**
NDMI	**Juvenile**	**0.137**	**0.0021**	**16.97**	**y = 105.56*NDMI + 66.97**	**67**	**45**
NMDI	Juvenile	0.003	0.1858	21.22	y = -27.35*NMDI + 126.85	67	45

VARI	**Juvenile**	**0.139**	**0.0019**	**21.82**	**y = -8.31*VARI + 99.8**	**67**	**45**
GNDVI	**Juvenile**	**0.175**	**0.0004**	**22.87**	**y = 58.23*GNDVI + 79.51**	**72**	**45**
NDVI	**Mature**	**0.110**	**0.0058**	**17.88**	**y = 53.63*NDVI + 80.34**	**68**	**46**
NDMI	**Mature**	**0.160**	**0.0006**	**20.81**	**y = 149.52*NDMI + 63.17**	**69**	**46**
NMDI	Mature	0.006	0.4144	23.41	y = -26.37*NMDI + 126.7	69	46
VARI	Mature	0.092	0.0119	15.50	y = -18.03*VARI + 97.73	68	46
GNDVI	**Mature**	**0.124**	**0.0033**	**24.94**	**y = 40.42*GNDVI + 82.97**	**68**	**46**

Relationships between duff and fine woody debris moisture contents in open stands were examined with Sentinel 2 indices in 2022 (Figures 34 and 35). Similar to the results from Sentinel 2 data in 2021 and Landsat 8/9 data in 2022, the relationship between the indices and fine woody debris MC is generally weak (Table 19). However, there is some promise in estimating duff MC with NDVI and GNDVI indices, which have relatively higher R^2 values (0.210 and 0.157) and lower p-values (<0.05) (Table 19). Although there are no clear relationships between woody debris MC and remote sensing indices, RMSE values for fine woody debris models (21.36 to 56.56) are lower than for duff (69.26 to 85.88) (Table 19).

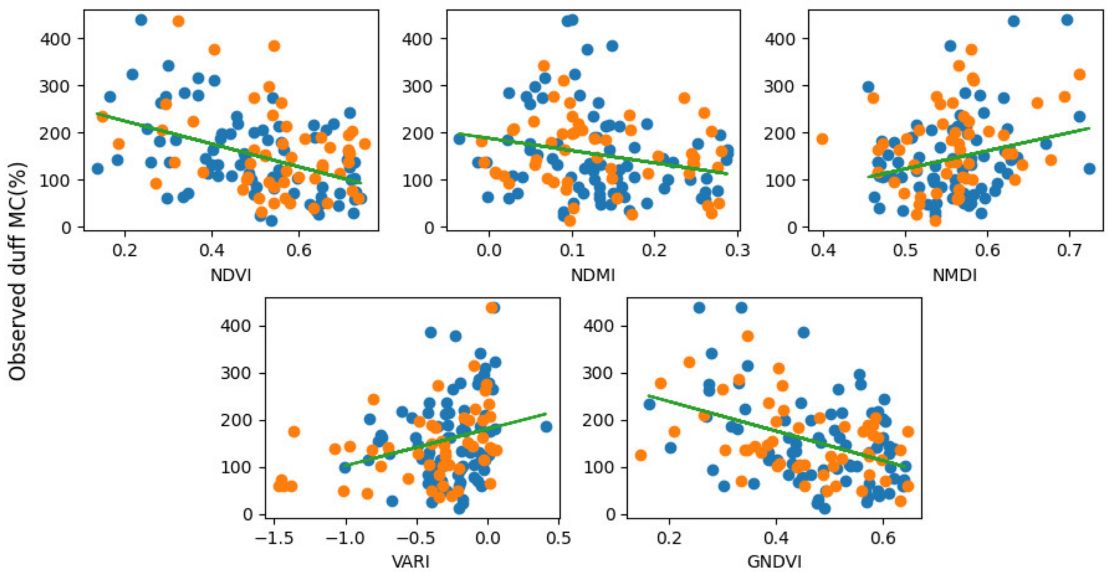

Figure 34: Remote sensing indices compared with duff MC at open stands with Sentinel 2 data in 2022, where blue points are training data, green lines are the linear regression based on blue points, and orange points are test data.

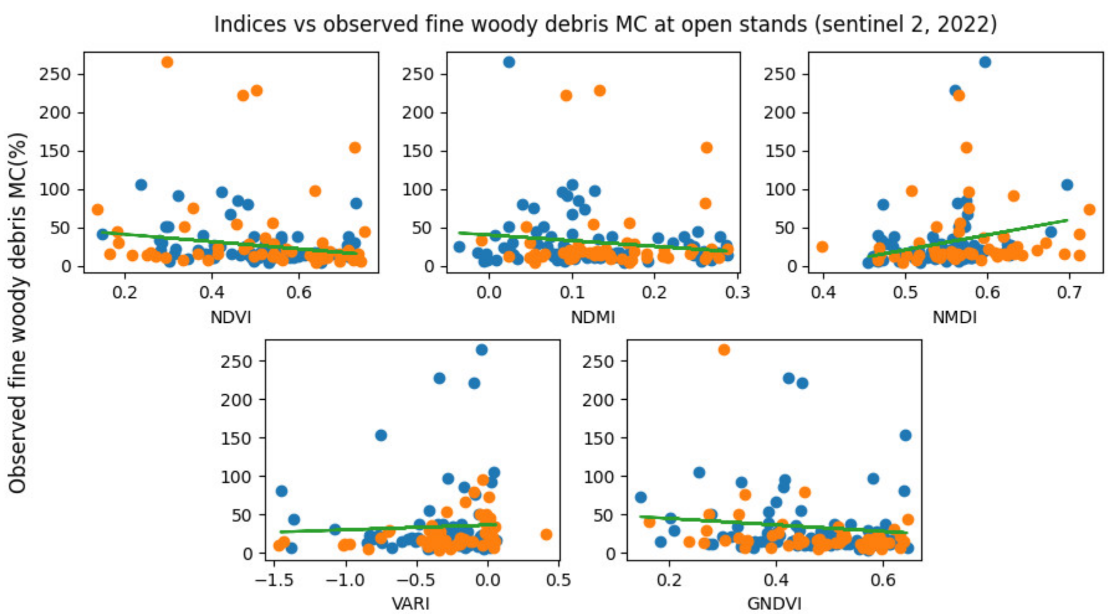

Figure 35: Remote sensing indices compared with woody debris MC at open stands with Sentinel 2 data in 2022, where blue points are training data, green lines are the linear regression based on blue points, and orange points are test data.

Table 19: Statistical results of remote sensing index relationships with fine woody debris and duff MC at open stands (2022 Sentinel 2), where FWD means fine woody debris, and y is observed FMC.

Index	Fuel Types	R^2	P	RMSE	Equation (train)	N Train	N Test
NDVI	**duff**	**0.210**	**<0.0001**	**85.22**	**y = -243.00*NDVI + 272.87**	**78**	**52**
NDMI	duff	0.048	0.0549	73.49	y = -260.71*NDMI +187.38	78	52
NMDI	**duff**	**0.072**	**0.0174**	**85.88**	**y = 383.11*NMDI – 69.23**	**78**	**52**
VARI	duff	0.045	0.0629	72.80	y = 77.74*VARI + 180.20	78	52
GNDVI	**duff**	**0.157**	**0.0003**	**69.26**	**y = -313.80*GNDVI + 301.72**	**78**	**52**
NDVI	FWD	0.094	0.0064	56.56	y = -47.42*NDVI +50.36	78	52
NDMI	FWD	0.031	0.1250	45.36	y = -73.29*NDMI + 39.98	78	52
NMDI	**FWD**	**0.060**	**0.0303**	**39.92**	**y = 194.32*NMDI – 76.61**	**78**	**52**
VARI	FWD	0.002	0.1336	21.36	y = 6.23*VARI + 36.50	78	52
GNDVI	FWD	0.015	0.2810	36.41	y = -42.25*GNDVI + 53.55	78	52

Taken as a whole, these results indicate that in 2021 and 2022, for juvenile stands, the GNDVI, NDVI, and NMDI had a stronger correlation with field observations and Sentinel 2 data, as evidenced by its higher R^2 values and lower p-values. NMDI had stronger relationships and correlations in 2021, although its low R^2 and high p-value in 2022 may make it unreliable. No solid relationships were found between observed MC and remote sensing indices in the 2021 data for mature stands. However, in 2022, NDMI, GNDVI, and NDVI both had relatively high R^2 values and lower p-values. Furthermore, at open stands, the correlation between remote sensing indices with duff and fine woody debris MC is relatively weak in 2021 and 2022 with Sentinel 2 data.

However, NDVI and GNDVI showed stronger relationships and correlations in 2022 when estimating duff at open stands.

For Landsat 8 & 9 data in 2022 for juvenile stands, only GNDVI had a higher R^2 value and a lower p-value, while at mature stands, GNDVI, NDVI and GNDVI show statistically significant relationships. All indices had poor statistical results when using Landsat 8 & 9 data to estimate duff and fine woody debris MC.

In conclusion, GNDVI appears to work best to estimate foliage MC in juvenile and mature stands, followed by NDVI and NMDI. In open stands, GNDVI and NDVI have better statistical results than other indices when estimating duff MC, and no index worked well with estimating woody debris MC. In the following sections, the use of GNDVI as an index of pre-fire FMC and comparing it with estimates of the burn severity will be discussed and explored.

5.5 Burn severity, moisture, indices, and FMC

Distributions of dNBR and RBR burn severities for open, juvenile, and mature stands in the Plateau Complex Fire are shown in Figures 36 and 37. Results indicate that juvenile stands had lowest fire intensities/severities, followed by mature forests, and open stands (high intensity/severity) (Figures 36 and 37)

The juvenile blocks (blue polygons) had lower burn severity than mature and open stands, as measured by dNBR and RBR (Figures 36 and 37). It is reasonable to find some low burn severity patches not related to underlying indices/fuel differences, as they may have burned under cooler conditions (e.g., at night), or the fire has stopped or changed its direction while spreading. For example, in Figures 36 and 37, most open forests (recent clearcuts) have experienced high severity fire, but the open patches surrounded by juvenile forests only had low burn severity. Before comparing the indices and burn severities, it is essential to understand the fire behaviour and test the accuracy of using remote sensing to estimate burn severity.

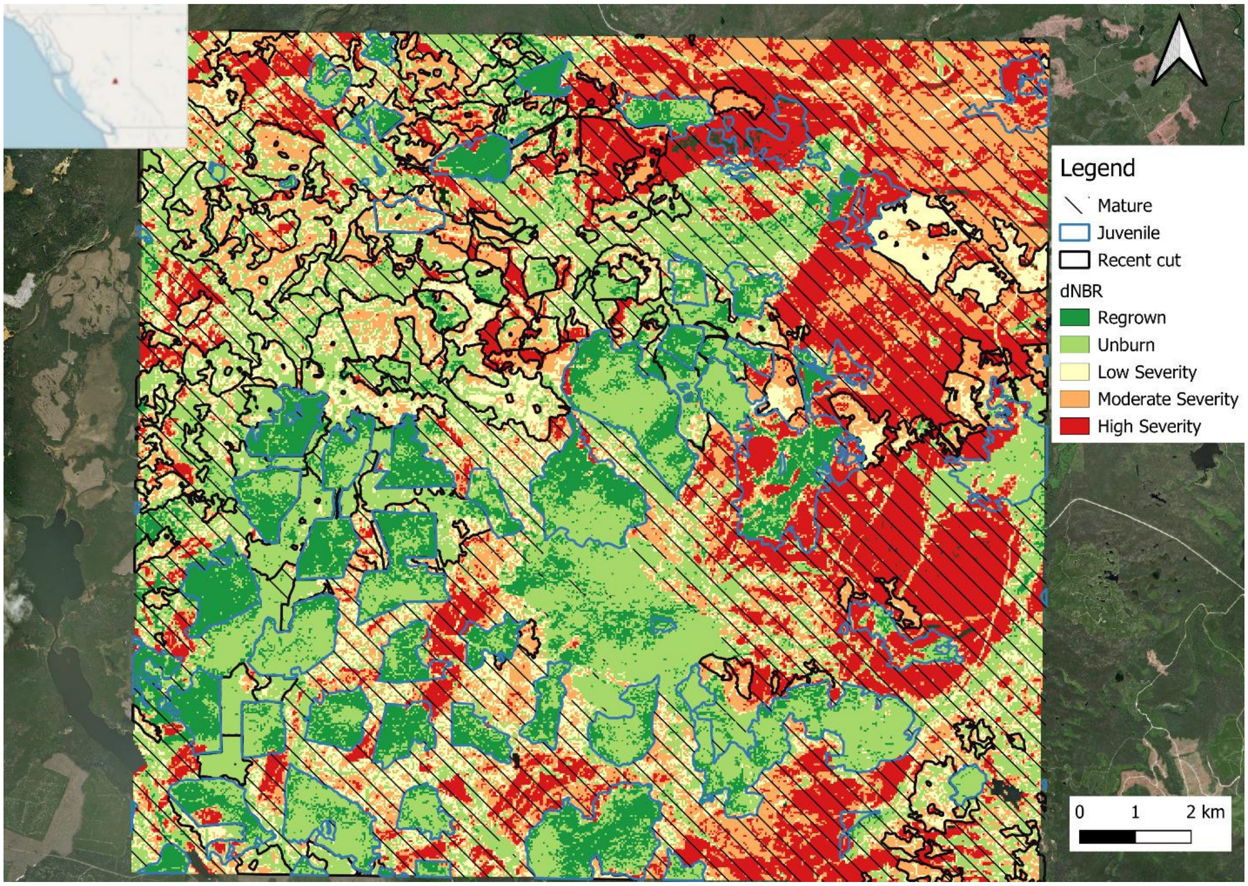

Figure 36: dNBR for different stands on 6th July 2017 at Plateau Complex, centred on 52.94105 N, -124.01571 W.

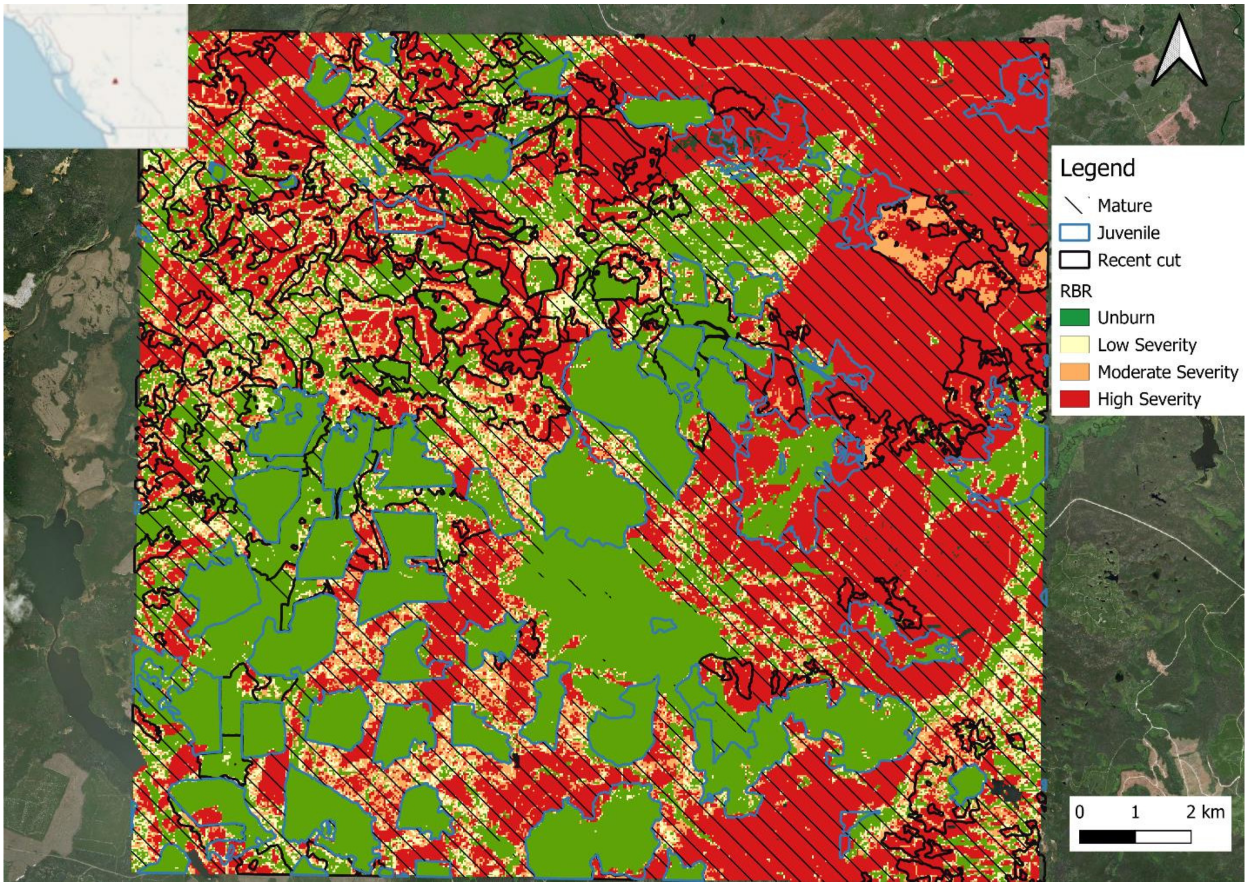

Figure 37: RBR value for different stands on 6th July 2017 at Plateau Complex, centred on 52.94105 N, -124.01571 W.

Regardless of using dNBR and RBR, juvenile stands are mainly unburned (majority of dNBR <100 and RBR <35, Figures 38- 39). At the same time, mature forests showed a wide distribution of unburned to higher burn severity (higher than 660 for dNBR and 298 for RBR, Figures 38- 39) values. Open stands had higher dNBR and RBR in general, which indicates the majority of the recently logged open forest has burned (Figures 38- 39).

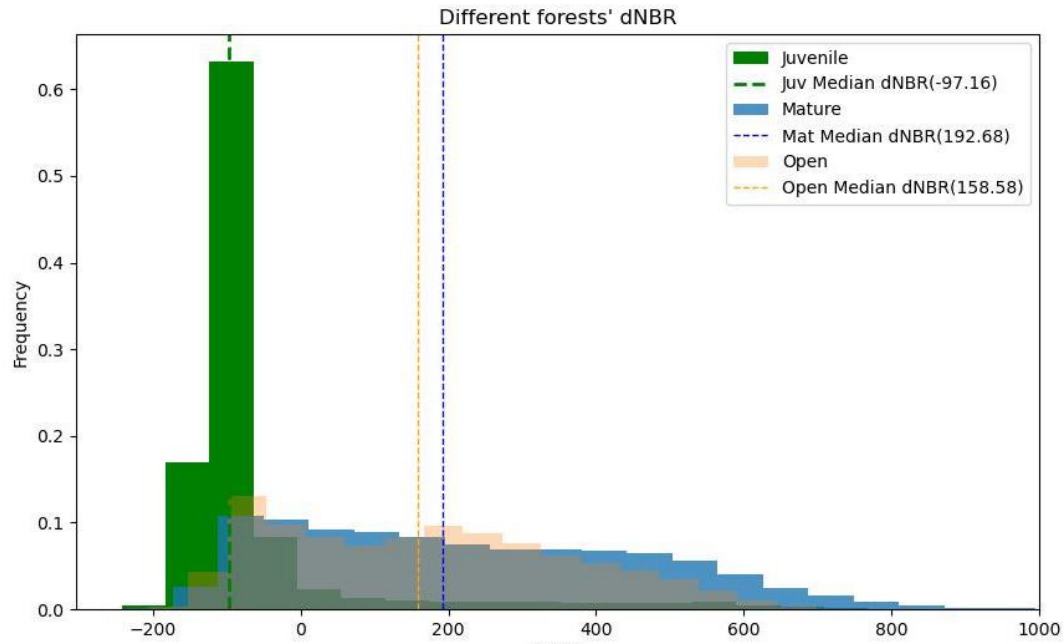

Figure 38: Histogram of dNBR for different stand types, where dashed lines represent median dNBR.

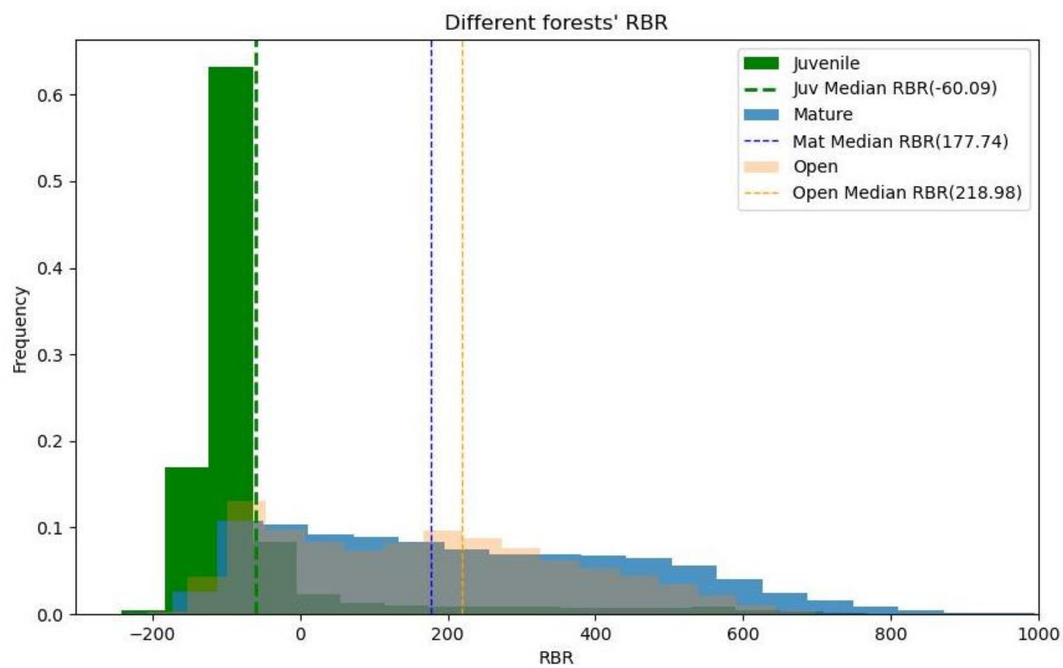

Figure 39: RBR histogram in different stands, where dashed lines represent median RBR.

Pre-fire NDMI, NMDI, NDVI, VARI and GNDVI at different stands were used to compare with dNBR and RBR, as their relationships to the FMC had been determined in the previous section. The relationships between remote sensing indices and dNBR/RBR in different stands are shown in Figures 40 to 45. As there are more than 49,000 data points, hexbin plots were used to visually investigate their relationships, where darker colour means more dense points/points overlay. There is a wide range of weak relationship when comparing burn severities and indices, as the study area is a mix of burned and unburned forests.

Most open forests within the scene selected in the Plateau Complex Wildfire have been burned, as shown by relatively high dNBR/RBR. Mature forests have moderate burn severity values compared to the other two stand types. For juvenile forests, within the scene selected, the majority of juvenile forests was unburned. The relationship between indices and burn severities is unclear in juvenile and open forests. However, despite the noise, all indices except VARI in mature stands have an inverse relationship to burn severities (Figures 40 and 43): as the indices decreased, the burn severity increased.

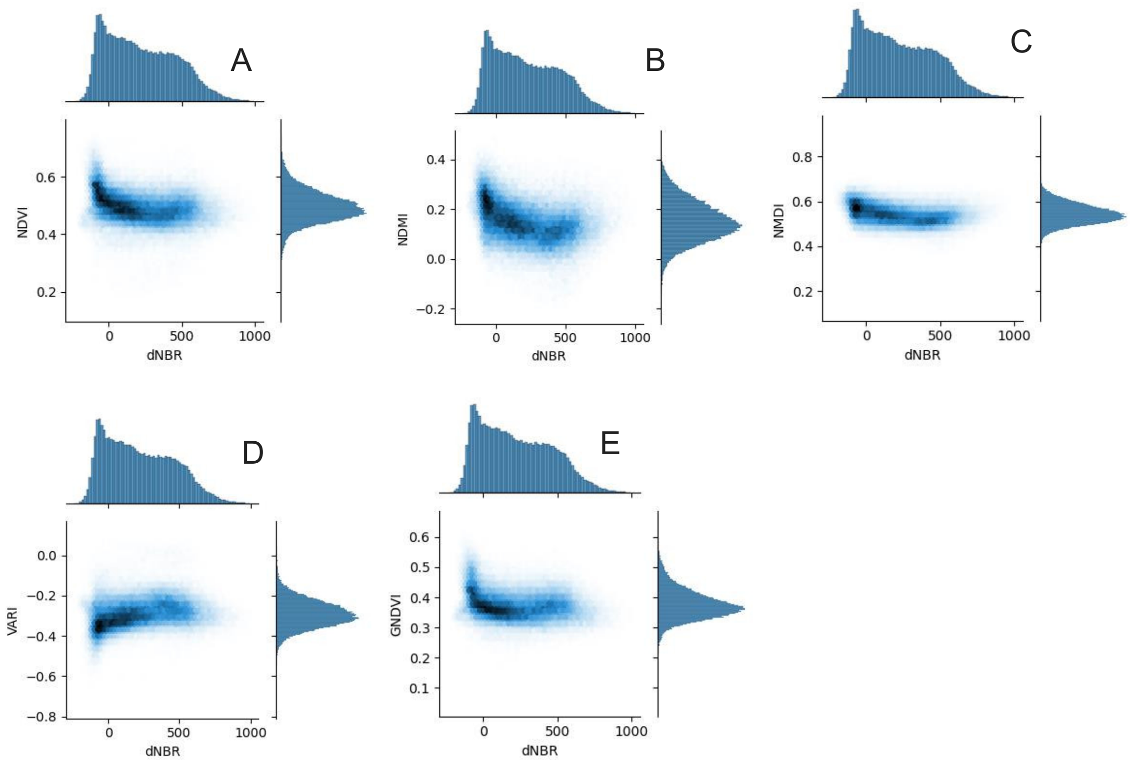

Figure 40: A) NDVI, B) NDMI, C) NMDI, D) VARI and E) GNDVI vs dNBR for mature forests, with their frequency distributions

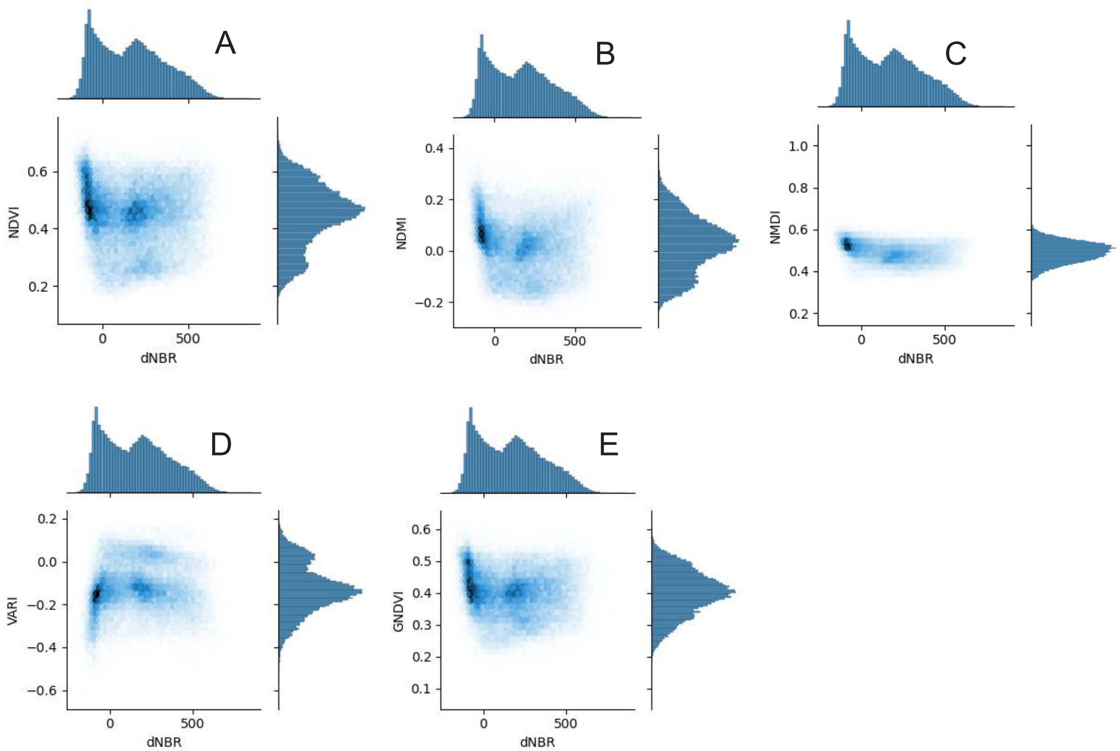

Figure 41: A) NDVI, B) NDMI, C) NMDI, D) VARI and E) GNDVI vs dNBR for open forests, with their frequency distributions

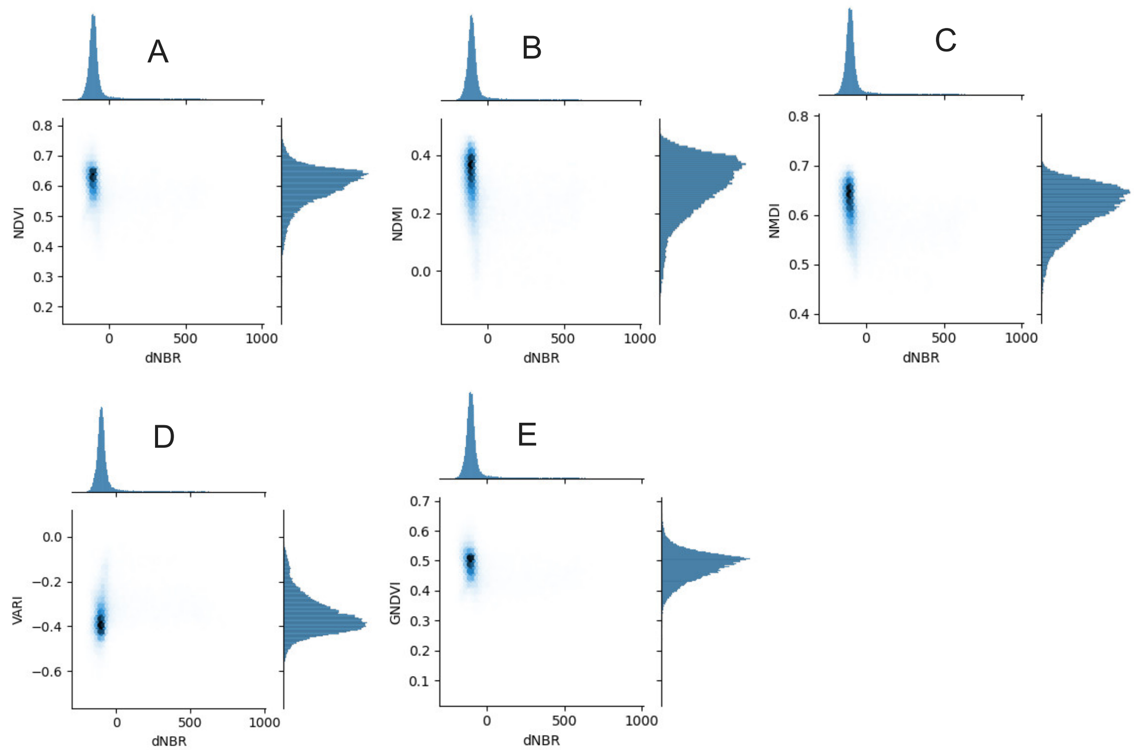

Figure 42: A) NDVI, B) NDMI, C) NMDI, D) VARI and E) GNDVI vs dNBR for juvenile forests, with their frequency distributions.

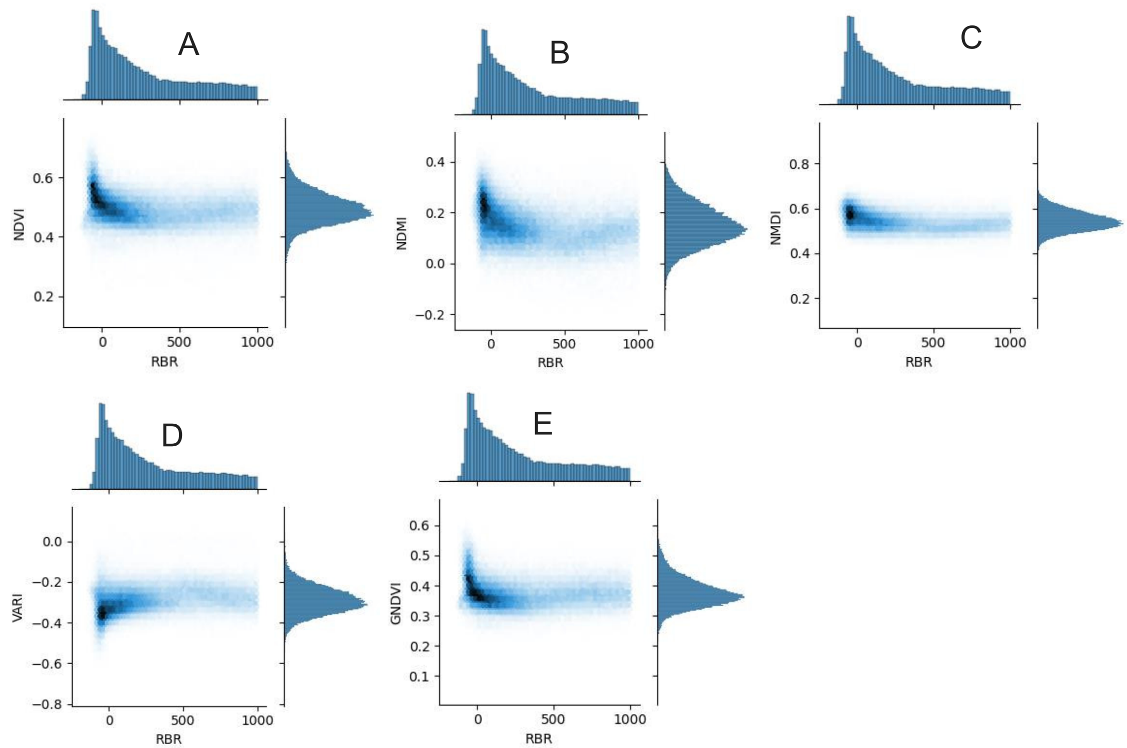

Figure 43: A) NDVI, B) NDMI, C) NMDI, D) VARI and E) GNDVI vs RBR for mature forests, with their frequency distributions.

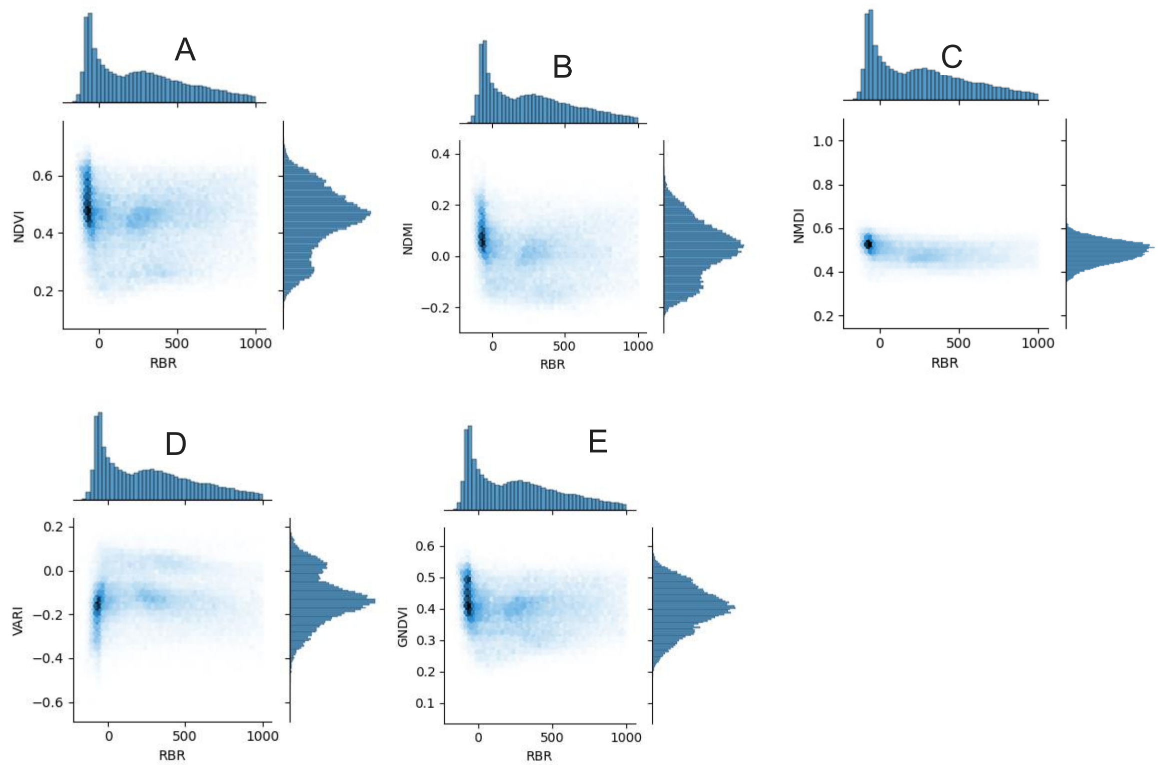

Figure 44: A) NDVI, B) NDMI, C) NMDI, D) VARI and E) GNDVI vs RBR for open forests, with their frequency distributions.

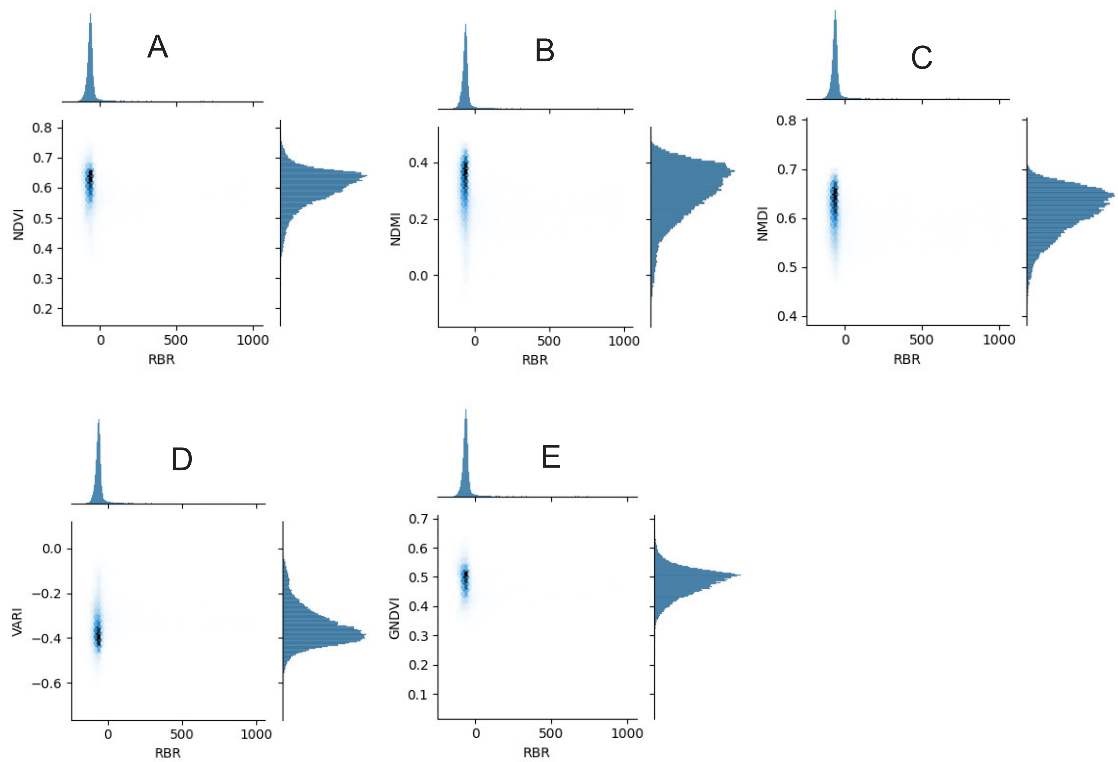

Figure 45: A) NDVI, B) NDMI, C) NMDI, D) VARI and E) GNDVI vs RBR for juvenile forests, with their frequency distributions.

The relationship between remote sensing indices, such as NDMI and FMC, was investigated for different stand types in previous sections. Results indicate a relationship between the two in various stands; however, the remote sensing indices in different stands do not relate to subsequent burning severity in general.

Both NDMI and GNDVI have relatively higher R^2 and lower p values when used to estimate foliage MC at juvenile and mature forests (Table 19). These relationships were used in juvenile and mature stands to estimate their FMC in different stands. Figures 46 and 47 shows estimated FMC at mature and juvenile forest computed by equations from Table 19. Juvenile forest has higher FMC in general than mature forest, regardless of using NDMI or GNDVI equations. For FMC calculated by NDMI (Figure 46), most of the juvenile forest have FMC 100-120 % as well, however, at mature forest, FMC is between 60-100%, which is generally lower than juvenile. In Figure 47 (computed by GNDVI), most of the juvenile forest have FMC between 100-120%, while most of mature forest have FMC between 80-100 %.

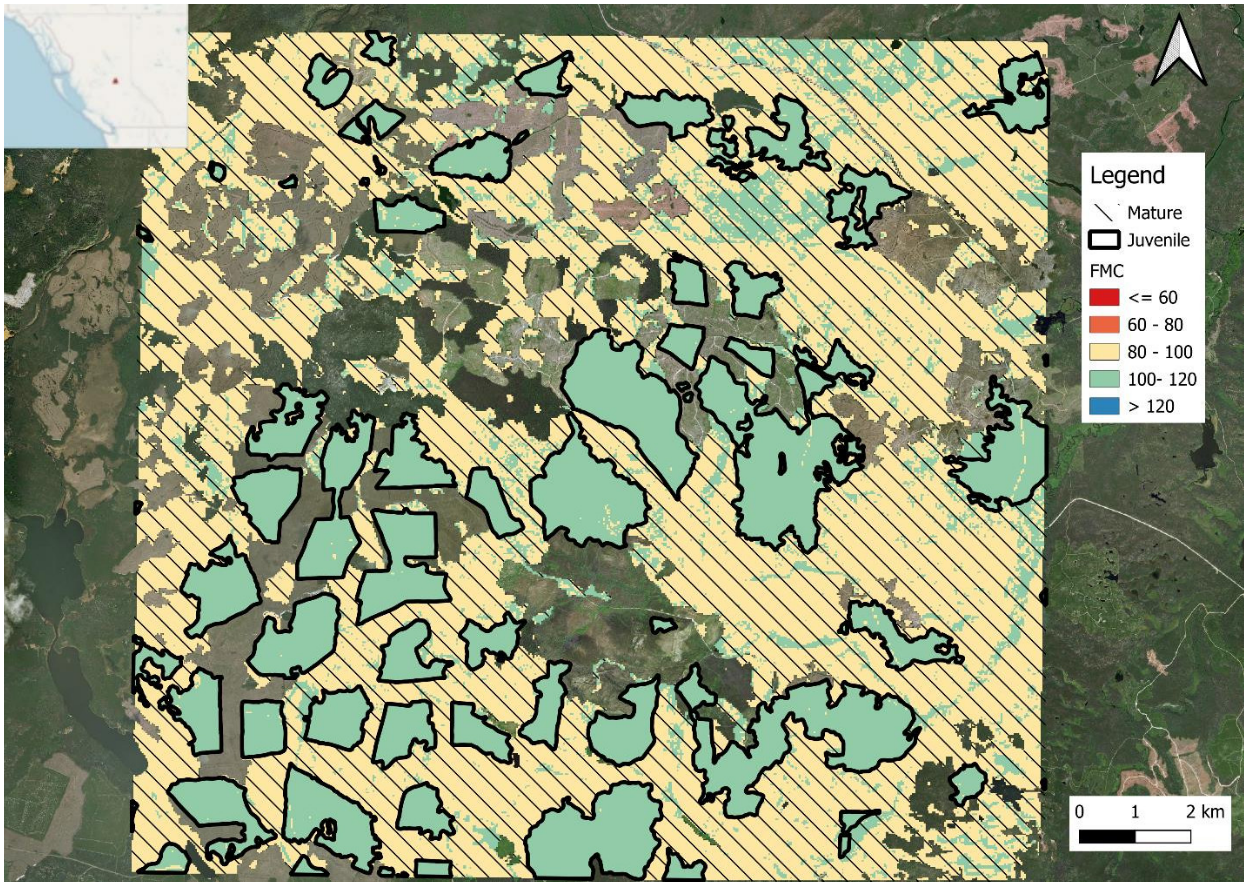

Figure 46: FMC calculated by NDMI for juvenile and mature stand on 6th July 2017 at Plateau Complex, centred on 52.94105 N, -124.01571 W.

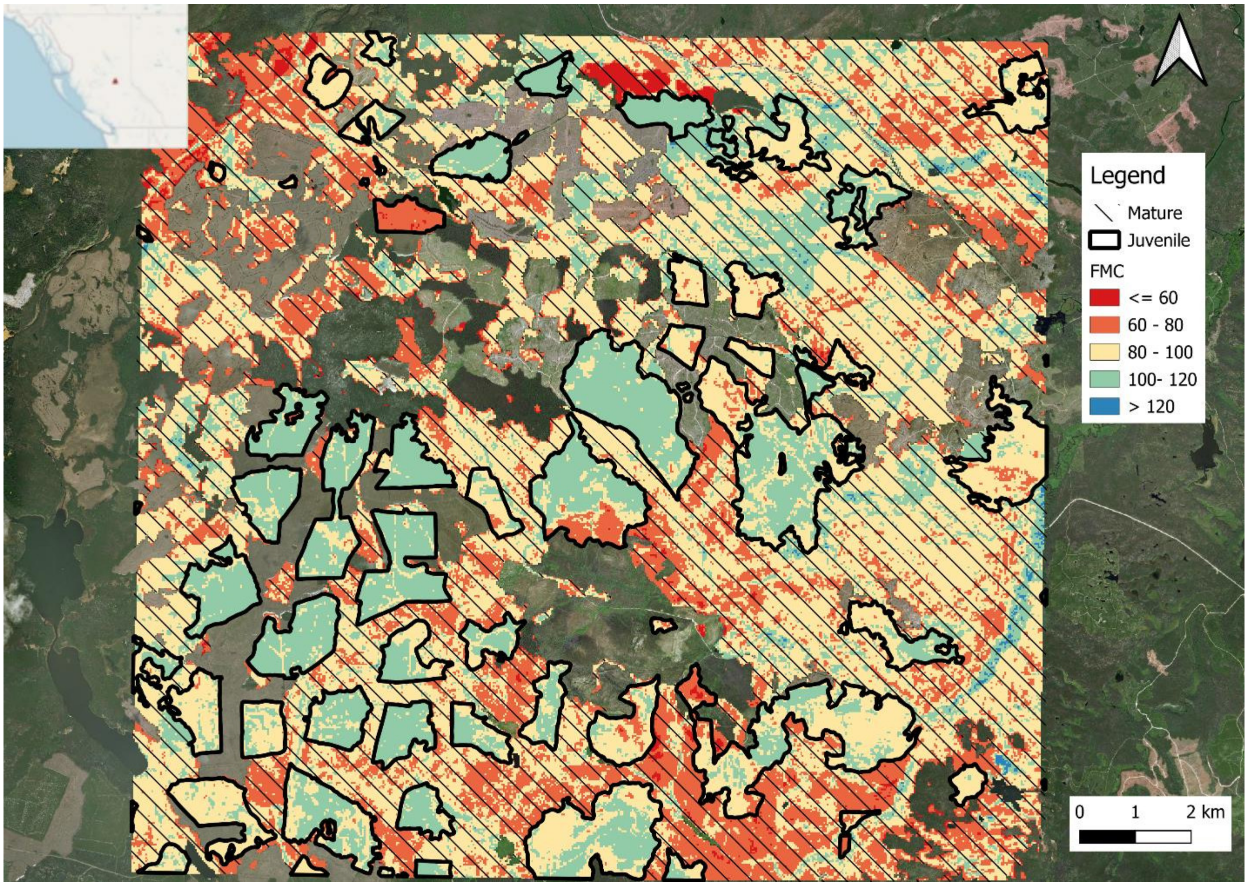

Figure 47: FMC calculated by GNDVI at juvenile and mature stand on 6th July 2017 at Plateau Complex, centred on 52.94105 N, -124.01571 W.

In Figure 48 and 49, FMC estimated from NDMI and GNDVI at juvenile and mature strands were compared with the burn severities. Similar to NDMI/ GNDVI and burn severity in Figure 40 and 43, despite the noise, FMC calculated by NDMI and GNDVI at mature stands have an inverse relationship to burn severities; as the FMC decreased, the burn severity increased. There is no clear relation between FMC at juvenile stands and burn severities, as most of juvenile stands were unburned.

Different stands with similar remote sensing indices and FMC values tend to have a wide range of burn severity (Figures 40 to 45, Figures 48 and 49), which suggests that remote sensing indices and FMC alone is not determining whether a stand has been burned.

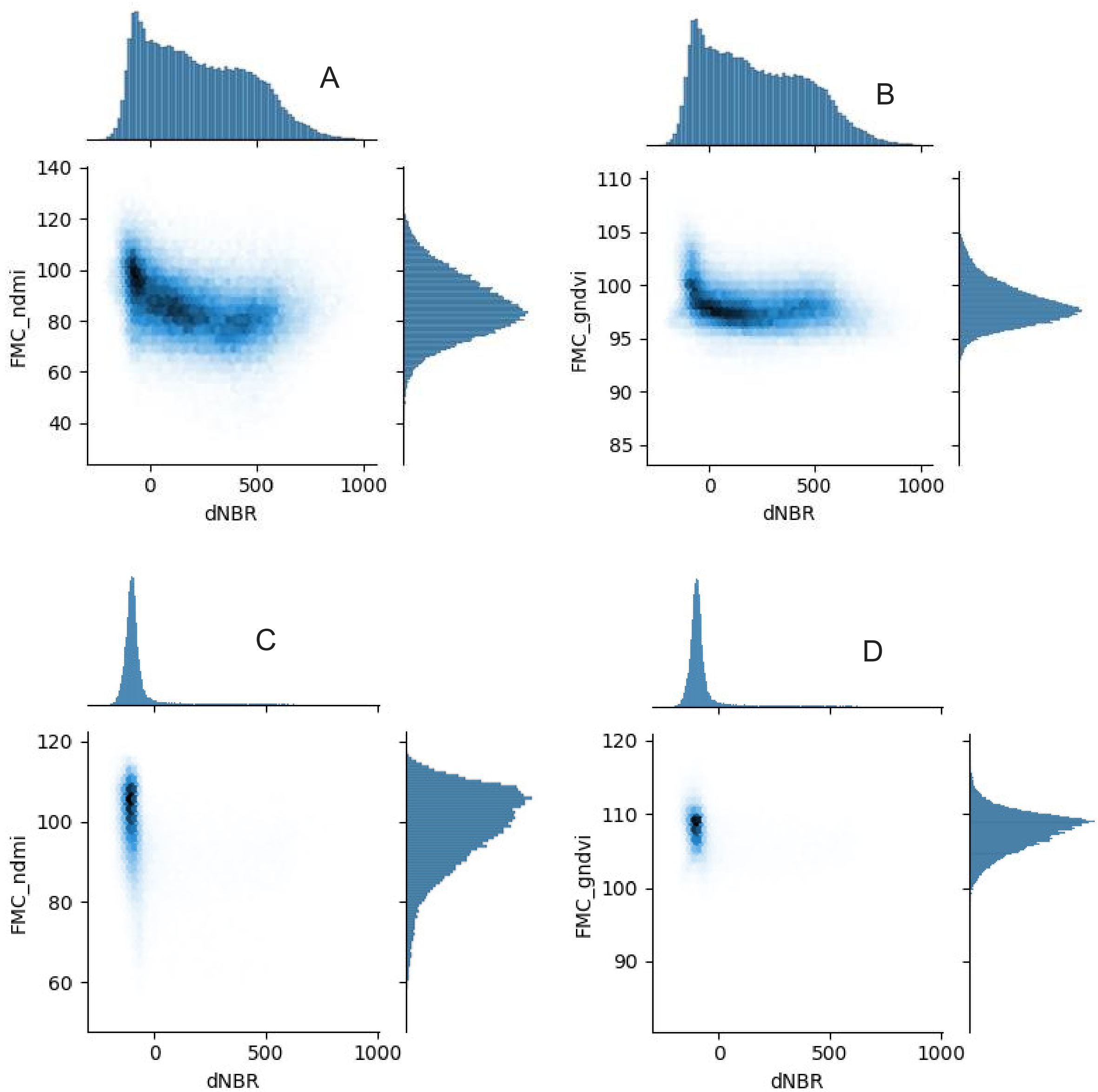

Figure 48: A). FMC calculated by NDMI at mature stands, B). FMC calculated by GNDVI at mature stands, C). FMC calculated by NDMI at juvenile stands, D). FMC calculated by GNDVI at juvenile stands compared with dNBR.

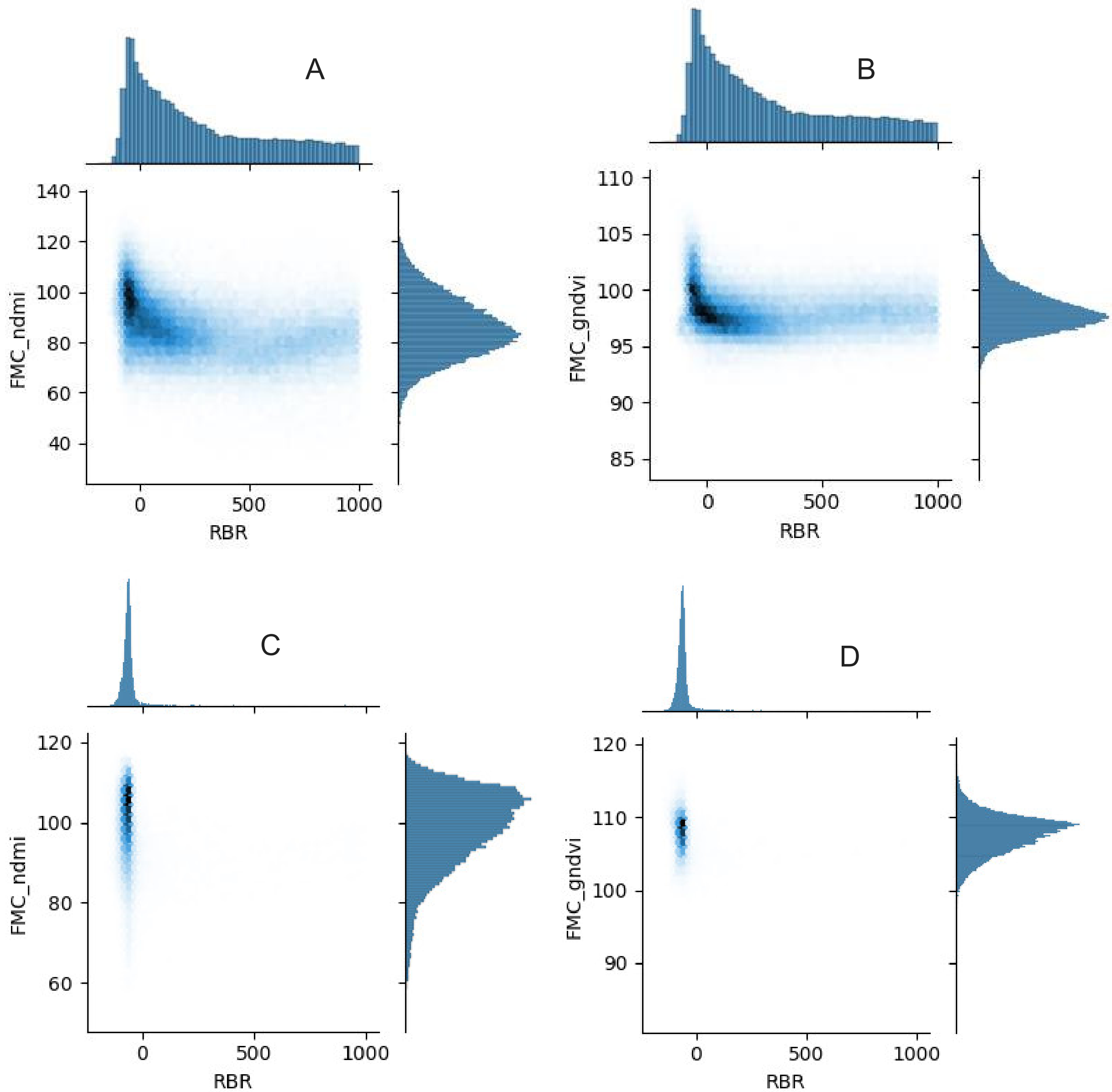

Figure 49: A). FMC calculated by NDMI at mature stands, B). FMC calculated by GNDVI at mature stands, C). FMC calculated by NDMI at juvenile stands, D). FMC calculated by GNDVI at juvenile stands compared with RBR.

6. Discussion

6.1 Field observations

As mentioned in section 5.1, the moisture content (MC) of duff, fine woody debris, and foliage were compared in different stand types. In 2021 and 2022, duff had a significantly higher daily averaged MC in mature stands, followed by juvenile and open stands. For fine woody debris, the daily averaged MC was similar in mature and juvenile stands, with no significant difference (p=0.851). However, open stands had a significantly lower daily averaged MC than juvenile stands. When looking at foliage MC, open forests had a significantly higher daily averaged MC, while mature and juvenile forests had similar daily averaged MC without significant differences.

Mature forests shed more needles/foliage, creating a thicker layer of litter that can trap moisture and slow down evaporation, resulting in higher MC in the duff layer (Harmon et al., 1986). Fine woody debris in mature conifer forests may have undergone more decomposition than in juvenile conifer forests, resulting in a higher overall moisture content, however, this can be offset by the accumulation of new fine woody debris in mature forests (Brown, 2003; Harmon et al., 1996). The major reason why open stands have lower duff and fine woody debris MC could be the lack of canopy cover. Mature and juvenile forests have denser canopy cover that shades the forest floor and reduces the rate of evaporation, helping to maintain moisture levels in the fine woody debris and duff layer (Wotton et al., 2005).

At open stands, foliage was collected from actively growing trees younger than 10 years old. Active growth in younger trees might result in higher moisture content as they require a high level of water intake (Lambers et al., 1998).

Although field observations of FMC yield direct estimates of moisture levels in forest fuels, it is time-consuming and costly (Caccamo et al., 2011). Collecting samples on the day of satellite image acquisition is desirable to correlate field measurements directly with satellite data; however, collecting samples from all six locations used in this study in one day was not possible. Specific errors and outliers occurred throughout the summer collection, such as negative values of FMC caused by recording errors. Several reasons might have contributed to the defects and inconsistencies, including.

1. Transportation: In the beginning, the team in Prince George used sealed sandwich bags to retain the samples, with water frequently left on the bottom before measurement (lower moisture content than expected).
2. Need for more experience and canopy access for sample collection: Failure to correctly label tree foliage species may have led to data analysis errors. Samples collected primarily from lower tree branches in juvenile and mature stands are also controversial to compare with remote sensing data as their exposed canopies were too high to reach.
3. Calculation/ measurement errors: The loss of samples happened several times while measuring and transferring in and out of the oven. Collecting samples while raining, or immediately following a rain event, may also have caused measurement errors if not properly labelled to allow exclusion.

An improved sample collection procedure could provide a more reliable observation database to compare with both empirical models and remote sensing indices. Future sample collection should use different methods such as drones or shotguns to collect higher foliage exposed to sunlight (Charron et al. 2020).

6.2 Empirical Models to Estimate Fuel Moisture Content

Weather conditions can vary across geographic regions and forest types, and the current fire weather stations can only accurately represent a limited range of forest areas. Results presented in section 5.2 suggest that the installation of in-stand sensors may yield a more accurate estimate of FMC, but a full revision of the FWI model, or the development of new empirical models to estimate FMC that considers in-stand data may be required. The operation of in-stand sensors can be costly and labour-intensive: sensors installed in remote forest areas require maintenance and regular visits to prevent data loss from wildlife and extreme weather. Alternatives to in-stand meteorological observations include interpolation of weather conditions from multiple nearby fire weather stations, weather satellites and high-resolution dynamically downscaled meteorological fields (Mandel et al., 2011). Weather satellites have the potential to be used to monitor fuel moisture content remotely. However, their finest resolution is from the United States Department of Defense's Meteorological Satellite (DMSP) (2.7 km), Advanced Baseline Imager (ABI) (500m), JAXA Himawari Monitor (500 m), and which is too low to monitor different forest stands (Mohsin Butt, 2013; National Oceanic and Atmospheric Administration, 2021; Japan Aerospace Exploration Agency, 2015).

Over the course of the fieldwork conducted for this research, some sensors were damaged by animals, causing data loss and equipment damage. Methods such as spraying anti-chew spray and surrounding sensors with metal/ plastic chicken wire have been used to protect the equipment.

Due to the lack of equipment and the challenge of setting them up in dense forests, most of the weather sensors used in this research are quite different from the standard fire weather station. At all open sites around Smithers and Prince George, although temperature and relative humidity were measured at a screen level (1.5 metres), wind speed was collected at a height of approximately 2 metres instead of 10 metres. In juvenile and mature stands, the wind speed sensor was installed at a height of approximately 2 metres, and temperature and relative humidity were collected around 0.30 m above the ground. These measurement heights may be more relevant to surface fuel conditions but make comparisons with standard weather and FWI data difficult.

The comparison of different FMC models in section 5.2 revealed that while updating local weather and fuel conditions improved the models' performance, they could have worked more consistently. The updated models performed better for open sites than for mature and juvenile forest stands. The weather data for calculating and converting drying and wetting rates in the DMC and FFMC models were based on empirical relationships derived for pine forests in boreal and eastern Canada. Differences in forest types and weather conditions can result in differing empirical drying and wetting rates, leading to potential errors when using these rates in central BC. Given that the FWI model was developed and completed in the 1960 to 1970s (Van Wagner, 1987), it is necessary to update the empirical model to include fuel collection data from different forests and regions. As research and operational experience progress, fire management challenges change, and technology advances, along with the expansion of data on the fire environment, the Canadian Forest Service Fire Danger Rating System (CFFDRS) must continue to update and evolve, despite previous updates (Canadian Forest Service Fire Danger Group, 2021).

Empirical models had greater skill and reduced errors in the estimation of fine woody debris MC than for duff MC. This is likely due to the high variability of observed duff MC. One of the critical reasons for the high variability in the MC of duff is its high porosity, which allows for rapid absorption and release of moisture in response to environmental conditions (Stocks et al., 2004). Factors such as temperature, humidity, wind, and solar radiation influence the moisture absorption and loss rate and can lead to significant variability in duff MC over short periods and short distances (Deeming et al., 1997). Additional reasons behind this variability could be the difficulty of collecting duff in open and juvenile stands or improper identification of the duff layer, as mentioned in section 6.1.

6.3 Remote Sensing of FMC

In section 5.3, none of the remote sensing indices tested showed a strong relationship with the FMC, which can be attributed to several reasons. Firstly, the time series of remote sensing data were interpolated using lowess interpolation methods, but the accuracy of this approach depends on the frequency and quality of data. During the wildfires in central BC in the summer of 2021, clouds and smoke significantly decreased the number of usable image capture days. Figure 50 shows the number of useable images from Sentinel 2 at the different sample sites in 2021. The significant gaps in image capture likely led to inaccuracies in the remote sensing index values extracted from the lowess function. Fortunately, in 2022, there were fewer wildfires, providing more frequent data than in 2021. However, the harmonised 2022 data resulted in the QA bands not working when filtering out clouds and cirrus clouds. This study used a NDVI threshold to remove cloud and shadow pixels, however, using NDVI to remove cloud/shadow pixels may introduce errors. Although matching sample collection days and satellite visit days can minimise the errors caused by the lowess function, due to labour limitations, MC samples could not be collected for all clear satellite visit days, which made it still necessary to use the lowess function for the 2022 data. Running a smoothing function through the remote sensing index time series could also introduce errors, as it may not reflect the actual indices at the sample collection dates accurately. Further research could test the parameters of the lowess smoothing functions, but without more field observations and greater image frequency it will be a challenge to accurately compare field and remote sensing data.

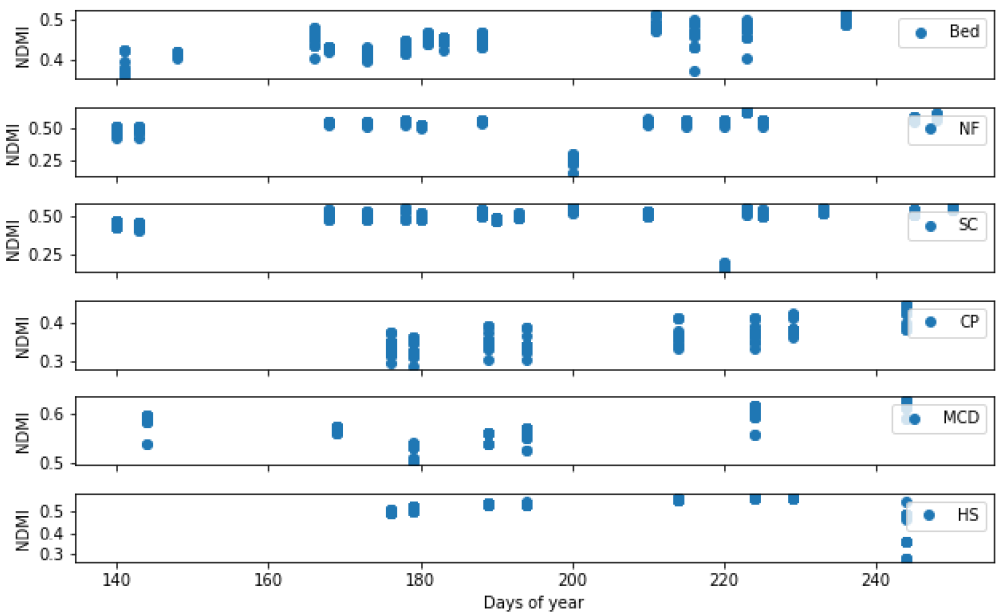

Figure 50: Usable NDMI indices in 6 sample collection sites in 2021 summer (late May to September)

The relationship between FMC and remote sensing indices should also consider factors such as the type of foliage (pine, spruce, or fir), sun or shade exposure, and the foliage's height. However, in this study, only three samples were taken per stand per visit, and the challenge of keeping the foliage type and exposure consistent was not considered. Although the daily averaged foliage MC for different foliage types also don't have significant different as well as the same stand, it might still be better to keep using the same foliage type at same stands. As a result, the comparison between remote sensing indices and FMC is not fully representative. In future studies, using exposed fuel data/ foliage from the canopy top could provide more representative results. Satellites such as Sentinel 2 and Landsat 8 & 9, with a resolution of 30 metres, can introduce inaccuracies in comparing remote sensing indices and FMC as each pixel includes non-foliage components such as trails, trees, and ground (as shown in Figure 3). Additionally, the frequency and timing of satellite visits can also impact the accuracy of results. For example, Landsat 8/9 visited the sample collection sites around Prince George and Smithers at around 10 a.m., but many samples were taken at 2 - 3 pm due to transportation and labour constraints. To obtain more accurate results, future studies could use drone-based remote sensing data, which has a higher resolution, is less impacted by clouds, and is closer to the sample collection time.

Additionally, the regression models used to estimate FMC from remote sensing indices are sensitive to the subset of points used for model training. Further research into this sensitivity is required.

6.4 Burn Severity Case Study

A portion of the 2017 Plateau Complex Wildfire was explored as a case study to examine potential relationships between wildfire severity and remote sensing indices related to pre-fire fuel moisture content. While harvest data provides mapped areas of open stands, and VRI data defined most of the forest with their forest age, there were still some forests not defined. Clouds, shadows, and smoke can also decrease the chance of getting pre-fire imagery prior to the wildfire event, which may lead to false pre-fire forest conditions.

The results shown in section 5.4 indicated that there is no strong relation between remote sensing indices and burn severity ratios. In general, most open, recently logged stands had high burn severities, many juvenile forest stands remained unburned, while mature forests have an intermediate distribution of burn severity.

At the end of summer in 2021, ground-based severity assessments were conducted Plateau Complex wildfire sites (data not presented). To evaluate burn severity results between remote sensing and on-site observation, 15 of the unburned forests (fire island) and 17 burned forests were visited. When visiting unburned areas/fire islands, it was common to notice that their edges had a relatively higher burn severity than the centre of the juvenile forest stand. From burn severity assessments and fieldwork observation, wildfires are not just suddenly stopped when they meet the juvenile stands, they burn the edges of the stands, and their spreading slows as they go deeper into the forest. Evidence of low intensity fire close to the ground, such as scorched tree bases, less moss and recently established fireweed (*Epilobium angustifolium*), was found frequently within the fire refugia, even far from the edge of the forest. Open stands and very young juvenile stands, for example, can have a higher burn severity potential due to their high woody debris components after recent logging (Brown 2003, Lindenmayer et al. 2009).

Section 5.1 showed that FMC was similar in juvenile and mature forests in Prince George and Smithers in 2021 and 2022, and that weak relationships exist between remote sensing indices and FMC. GNDVI, NDMI, and NDVI indices showed potential in estimating future wildfire severity in mature stands (Figures 44 and 47). However, no strong relations were found between pre-fire FMC and burn severities, which suggests that FMC is not a decisive factor for forest survival during wildfires. Linear and non-linear models were not examined in this research due to the spread of the data. Future work should attempt to identify the form of the relation between burn severity and moisture/greenness indices.

The high forest density in juvenile forests may also play a role in reducing the spread of fire by decreasing wind speed. In section 4.3.3, wind speed was found to be significantly lower than mature and open stands, which may prevent fire spread and create fire refugia. This highlights the complex interplay between various factors that can influence the impact of wildfires on forests, and the importance of considering a range of factors when evaluating the resilience of forests to fire.

7. Conclusions

This research compares empirical models and remote sensing indices for predicting forest duff, fine woody debris, and foliage MC values measured in central BC. Burn severities and their relation to pre-fire remote sensing indices were also analysed in different stands from the wildfire case study to understand the fire behaviour in fire refugia.

The FWI and its locally modified versions were tested in this research. By comparing the different approaches in DMC and FFMC models, it was found that using local fuel limits and weather station data resulted in better estimates of duff and woody debris MC. However, the cost of weather stations and sensors and various wetting and drying rates in the model made it difficult for any of the models to work consistently well. When comparing the performance of FWI models in different stand types, open (recently logged) stands had lower errors than juvenile and mature conifer stands, as the model was designed to estimate MC with weather data collected in open stands in Eastern Canada. Although the model was designed to and intended to be representative of natural forests, the mature and juvenile forests in central BC are different than forests in Eestern Canada and US. In general, FFMC and its locally updated version worked better than DMC at predictive local MC of fine woody fuels and duff, possibly due to the greater variability of observed duff MC (14.38 – 439.27 % compared to fine woody debris 2.17 – 228.38 %).

After comparing observed MC and remote sensing indices at the different stands and sites, a few relationships can be highlighted. Firstly, Sentinel-2 data yielded stronger relationships between moisture content and remote sensing indices. GNDVI, NDMI, and NDVI had higher R^2 values (higher than 0.1) and lower p-values (less than or equal to 0.005) when estimating foliage MC in juvenile and mature stands, compared to NDVI and GNDVI. When estimating duff MC in open stands, NDVI and GNDVI had better statistical results (higher R^2 and lower p-value) than other remote sensing indices. In contrast, almost none of the remote sensing indices had a clear relationship with fine woody debris MC in open stands. In general, the results of using remote sensing indices to estimate FMC were not convincing and accurate, with the highest R^2 being 0.175 (GNDVI) for foliage in mature forests, 0.160 (NDMI) for juvenile forests, 0.210 (NDVI) for duff, 0.094 (NDVI) for fine woody debris in open stands. Due to the impact of satellite visit frequency, band resolution, weather, and the quality and quantity of observation data, it is unlikely that strong relationships between remote sensing indices and FMC can be obtained.

A case study of the 2017 Plateau Complex fire in central British Columbia was used to examine pre-and post-fire forest conditions through remote sensing. The results showed that juvenile stands in the Plateau complex fire had lowest burn severity in general, followed by mature forests and open stands. Remote sensing indices related to moisture or greenness could not be used to determine fire severity in juvenile stands but did provide information on the fire severity in mature stands. By using NDMI and GNDVI equations, juvenile forests tended to have a higher moisture content level than mature forests, however, the relations of FMC between FMC and dNBR/RBR is still undetermined. Thus, FMC might not be a conclusive factor in the observation that juvenile forests can function as fire refugia. The relationship between remote sensing indices and burn severity is still being determined when looking at a broader study area. Juvenile stands had significantly lower in-stand wind speeds than both mature and open stands (Figure 18), and this should be investigated further for understanding fire refugia and wildfire behaviour in central British Columbia.

8. References

Anderson, H. E. 1982. Aids to determining fuel models for estimating fire behavior. USDA Forest Service, Intermountain Forest and Range Experiment Station.

Bao, W., Yu, F., Chang, Y., Guo, M., Zhou, F., & Zhong, C. 2022. Estimation of fuel load using remote sensing data in Hulunbuir Grassland. Natural Hazards Research (pp. 375-383).

Blackmarr, W. H., & Flanner, W. B. 1968. Seasonal and diurnal variation in moisture content of six species of pocosin shrubs (GTR- 033). US Department of Agriculture, Forest Service, Southeastern Forest Experiment Station.

Brown, J. K. 2003. Coarse woody debris: managing benefits and fire hazard in the recovering forest. Gen.Tech. Rep. RMS-GTR-105, USDA Forest Service, Ogden, UT. 16 p.

Burton, P. 2022. understanding the effects of forest management and prior disturbances on forest fire risk and behavior, Natural Resources Canada year report, Victoria, B.C, 12p.

Burton, P., C. Mahood, A. Boxwell, S. Taylor, L. McCulloch, and M. Dale. 2019. Why have recent mega-fires in British Columbia left some established plantations unburned? North American Forest Ecology Workshop, 24 June 2019, Flagstaff, Arizona.

Butt, M. J. 2012. Estimation of light pollution using satellite remote sensing and geographic information system techniques. *GIScience & Remote Sensing*, *49*(4), 609-621.

Byram, G. M. 1959. Combustion of forest fuels. In Forest fire: control and use (pp. 61-89). McGraw-Hill

Caccamo, G., Chisholm, L. A., Bradstock, R. A., & Puotinen, M. L. 2011. Assessing the sensitivity of MODIS to monitor drought in high biomass ecosystems. Remote Sensing of Environment, *115*(10), 2626-2639.

Caccamo, G., Chisholm, L. A., Bradstock, R. A., Puotinen, M. L., & Pippen, B. G. 2011. Monitoring live fuel moisture content of heathland, shrubland and sclerophyll forest in south-eastern Australia using MODIS data. International Journal of Wildland Fire, 21(3), 257-269.

Camacho, J. 2014. Visualizing big data with compressed score plots: approach and research challenges. Chemometrics and Intelligent Laboratory Systems, 135, 110-125.

Canadian Forest Service Fire Danger Group. 2021. The Vision for the Next Generation of the Canadian Forest Fire Danger Rating System. Information Report GLC-X-26. Canadian Forest Service, Sault Ste. Marie, ON. 56 p

Ceccato, P., Flasse, S., & Gregoire, J. M. 2002. Designing a spectral index to estimate vegetation water content from remote sensing data: Part 2. Validation and applications. Remote sensing of Environment, *82*(2-3), 198-207.

Charron, G., Robichaud-Courteau, T., La Vigne, H., Weintraub, S., Hill, A., Justice, D., ... & Lussier Desbiens, A. 2020. The DeLeaves: a UAV device for efficient tree canopy sampling. *Journal of Unmanned Vehicle Systems*, *8*(3), 245-264.

Chuvieco, E. 2008. Satellite observation of biomass burning. In *Earth Observation of Global Change* (pp. 109-142). Springer, Dordrecht.

Chuvieco, E., Aguado, I., Cocero, D., & Riano, D. 2003. Design of an empirical index to estimate fuel moisture content from NOAA-AVHRR images in forest fire danger studies. International Journal of Remote Sensing, 24(8), 1621-1637.

Chuvieco, E., Aguado, I., Yebra, M., Nieto, H., Salas, J., Martín, M. P., ... & Zamora, R. 2010. Development of a framework for fire risk assessment using remote sensing and geographic information system technologies. Ecological modeling, 221(1), 46-58.

Chuvieco, E., González, I., Verdú, F., Aguado, I., & Yebra, M. 2009. Prediction of fire occurrence from live fuel moisture content measurements in a Mediterranean ecosystem. International Journal of Wildland Fire, 18(4), 430-441.

Cleveland, W. S. 1979. Robust locally weighted regression and smoothing scatterplots. Journal of the American Statistical Association, 74(368), 829-836.

Cohen, W. B., Spies, T. A., & Fiorella, M. 1995. Estimating the age and structure of forests in a multi-ownership landscape of western Oregon, USA. International Journal of Remote Sensing, 1*6*(4), 721-746.

Danson, F. M., & Bowyer, P. 2004. Estimating live fuel moisture content from remotely sensed reflectance. *Remote Sensing of Environment*, *92*(3), 309-321.

Data Catalogue. 2022. Retrieved January 28, 2023, from https://catalogue.data.gov.bc.ca/dataset/harvested-areas-of-bc-consolidated-cutblocks-

De Groot, W. J. 1998. Interpreting the Canadian forest fire weather index (FWI) system. In Proc. of the Fourth Central Region Fire Weather Committee Scientific and Technical Seminar.

Deeming, J. E., Burgan, R. E., & Cohen, J. D. 1997. The National Fire Danger Rating System - 1978. General Technical Report INT-GTR-341, USDA Forest Service, Intermountain Forest and Range Experiment Station.

Dennison, P. E., Moritz, M. A., & Taylor, R. S. 2008. Evaluating predictive models of critical live fuel moisture in the Santa Monica Mountains, California. International Journal of Wildland Fire, 17(1), 18-27.

Dunn, C. J., & Bailey, J. D. 2016. Tree mortality and structural change following mixed-severity fire in Pseudotsuga forests of Oregon's western Cascades, USA. Forest Ecology and Management, 365, 107-118.

Flannigan, M. D., Stocks, B. J., & Wotton, B. M. 2000. Climate change and forest fires. Science of the total environment, *262*(3), 221-229.

Fonseca, L., & Andrade, P. 2019. Cloud removal from Sentinel-2 imagery for land use classification using the NDVI threshold method. European Journal of Remote Sensing, 52(1), 357-368.

Fosberg, M. A. 1971. Fine herbaceous fuels in fire-danger rating (Vol. 185). Rocky Mountain Forest and Range Experiment Station, Forest Service, US Department of Agriculture.

Furlaud, J. M., Prior, L. D., Williamson, G. J., & Bowman, D. M. 2021. Fire risk and severity decline with stand development in Tasmanian giant Eucalyptus forest. Forest Ecology and Management, 502, 119724.

Gao, B. C. 1996. NDWI—A normalized difference water index for remote sensing of vegetation liquid water from space. *Remote sensing of environment*, *58*(3), 257-266.

Gao, J., Chen, S., & Wang, J. 2018. Assessment of soil moisture in a semi-arid region using remote sensing data. Remote Sensing, 10(1), 21.

Gitelson, A. A., Kaufman, Y. J., Stark, R., & Rundquist, D. 2002. Novel algorithms for remote estimation of vegetation fraction. *Remote sensing of Environment*, *80*(1), 76-87.

Google Earth Engine. (2022). Copernicus Sentinel-2 Surface Reflectance Harmonized [Data set]. Retrieved from https://developers.google.com/earth-engine/datasets/catalog/COPERNICUS_S2_SR_HARMONIZED

Government of Canada, Canadian Forest Service. (n.d.). Fire Weather Index (FWI). Retrieved from https://cwfis.cfs.nrcan.gc.ca/background/summary/fwi

Government of British Columbia. (n.d.). Harvested Areas of BC: Consolidated Cutblocks. Retrieved from https://catalogue.data.gov.bc.ca/dataset/harvested-areas-of-bc-consolidated-cutblocks

Government of British Columbia. (Year). Vegetation Resources Inventory (VRI) Spatial Datasets .Open Government of Canada. Retrieved from https://open.canada.ca/data/en/dataset/02dba161-fdb7-48ae-a4bb-bd6ef017c36d?wbdisable=true

Hartford, R. A., & Frandsen, W. H. 1992. When it's hot, it's hot... or maybe it's not!(Surface flaming may not portend extensive soil heating). International Journal of Wildland Fire, 2(3), 139-144.

Japan Aerospace Exploration Agency. 2015 PTree User's Guide. Earth Observation Research Center. Retrieved from https://www.eorc.jaxa.jp/ptree/userguide.html.

Jin, S., Tian, L., & Chen, Y. 2021. Monitoring vegetation growth and its response to climate change in the Yellow River Basin, China. Environmental Science and Pollution Research, 28(1), 19-30.

Jolly, W. M., Cochrane, M. A., Freeborn, P. H., Holden, Z. A., Brown, T. J., Williamson, G. J., & Bowman, D. M. 2015. Climate-induced variations in global wildfire danger from 1979 to 2013. Nature Communications, 6(1), 1-11

Kane, V. R., Cansler, C. A., Povak, N. A., Kane, J. T., McGaughey, R. J., Lutz, J. A., ... & North, M. P. 2015. Mixed severity fire effects within the Rim fire: relative importance of local climate, fire weather, topography, and forest structure. Forest Ecology and Management, 358, 62-79.

Karki, S., & Chaudhary, R. P. 2018. The Impact of Forests on Local Climate: A Study of Temperature and Precipitation in Nepal. Forests, 9(8), 481

Key, C., & Center, G. F. S. 2006. Evaluate sensitivities of burn-severity mapping algorithms for different ecosystems and fire histories in the United States. Final Report to the Joint Fire Science Program.

Key, C. H., & Benson, N. C. 2006. Landscape assessment (LA). FIREMON: Fire effects monitoring and inventory system, 164, LA-1.

Klinka, K., Krajina, V. J., CESIS Forestry Sciences, UBC, Vancouver, B. C., & Carter, R. E. 1999. Indicator plants of coastal British Columbia. University of British Columbia Press.

Krawchuk, M. A., Haire, S. L., Coop, J., Parisien, M. A., Whitman, E., Chong, G., & Miller, C. 2016. Topographic and fire weather controls of fire refugia in forested ecosystems of northwestern North America. Ecosphere, *7*(12), e01632.

Krawchuk, M. A., Moritz, M. A., Parisien, M. A., Van Dorn, J., & Hayhoe, K.. 2009. Global pyrogeography: the current and future distribution of wildfire. *PloS one*, *4*(4), e5102.

Landsat NASA. 2021. *Landsat 9 Bands | Landsat Science*. Landsat Science | a Joint NASA/USGS Earth Observation Program. Retrieved from https://landsat.gsfc.nasa.gov/satellites/landsat-9/landsat-9-bands/

Lawson, B. D., & Armitage, O. B. 2008. Weather guide for the Canadian forest fire danger rating system.

Lindenmayer, D. B., Hunter, M. L., Burton, P. J., & Gibbons, P. 2009. Effects of logging on fire regimes in moist forests. Conservation Letters, 2(6), 271-277.

Mandel, J., Beezley, J. D., Coen, J. L., & Kim, M. 2011. WRF-Fire: Coupled weather–wildland fire modeling with the Weather Research and Forecasting Model. Journal of Applied Meteorology and Climatology, 50(2), 344-367.

Masek, J. G., Wulder, M. A., Markham, B., McCorkel, J., Crawford, C. J., Storey, J., & Jenstrom, D. T. 2020. Landsat 9: Empowering open science and applications through continuity. Remote Sensing of Environment, 248, 111968.

McGee, Tara, Bonita McFarlane, and Cordy Tymstra 2015. "Wildfire: a Canadian perspective." Wildfire hazards, risks and disasters. Elsevier,. 35-58.

Meigs, G. W., Dunn, C. J., Parks, S. A., & Krawchuk, M. A. 2020. Influence of topography and fuels on fire refugia probability under varying fire weather conditions in forests of the Pacific Northwest, USA. Canadian Journal of Forest Research, 50(7), 636-647.

Miller, B. W., Lutz, J. A., Holden, Z. A., & Morgan, P. 2019. Mapping burn severity using Landsat and Sentinel-2 data: A comparison of dNBR and RdNBR. Remote Sensing, 11(11), 1307.

Miller, J. D., Knapp, E. E., Key, C. H., Skinner, C. N., Isbell, C. J., Creasy, R. M., & Sherlock, J. W. 2009. Calibration and validation of the relative differenced Normalized Burn Ratio (RdNBR) to three measures of fire severity in the Sierra Nevada and Klamath Mountains, California, USA. Remote Sensing of Environment, *113*(3), 645-656.

Ministry of Forests, Lands, Natural Resource Operations and Rural Development. 2014. Biogeoclimatic zones of British Columbia. Government of British Columbia.

Moreno, Á., García-Haro, F. J., Martínez, B., & Gilabert, M. A. 2014. Noise reduction and gap filling of fAPAR time series using an adapted local regression filter. *Remote Sensing*, *6*(9), 8238-8260.

Munoz-Salinas, E., Rodriguez-Gonzalez, P. M., Casal-Roscón, L. M., & Ramirez-Suarez, A. 2018. Post-fire vegetation recovery assessment using multi-temporal Landsat imagery in northwestern Mexico. Journal of Applied Remote Sensing, 12(2), 155-171.

Natural Resources Canada. 2017. Canada's Ecozones and Ecoregions. https://www.nrcan.gc.ca/maps-tools-publications/maps/canadas-ecozones-ecoregions/17050

Natural Resources Canada. (n.d.). Fire Weather Index (FWI). Canadian Wildland Fire Information System (CWFIS). Retrieved from https://cwfis.cfs.nrcan.gc.ca/background/summary/fwiNational Oceanic and Atmospheric Administration. 2021. ABI. GOES-R Series. Retrieved from https://www.goes-r.gov/spacesegment/abi.html

Nelson Jr, R. M. 2001. Water relations of forest fuels. In Forest fires (pp. 79-149). Academic Press.

Nolan, R. H., Boer, M. M., Resco de Dios, V., Caccamo, G., & Bradstock, R. A. 2016. Large-scale, dynamic transformations in fuel moisture drive wildfire activity across southeastern Australia. Geophysical Research Letters, 43(9), 4229-4238.

Norum, R. A. 1984. Measuring fuel moisture content in Alaska: standard methods and procedures (Vol. 171). US Department of Agriculture, Forest Service, Pacific Northwest Forest and Range Experiment Station.

Paltridge, G. W., & Barber, J. 1988. Monitoring grassland dryness and fire potential in Australia with NOAA/AVHRR data. Remote sensing of Environment, 25(3), 381-394.

Parks, S.A., Dillon, G.K. and Miller, C., 2014. A new metric for quantifying burn severity: the relativized burn ratio. Remote Sensing, 6(3), pp.1827-1844.

Pompe, A., & Vines, R. G. 1966. The influence of moisture on the combustion of leaves. Australian Forestry, 30(3), 231-241.

Qi, Y., Dennison, P. E., Jolly, W. M., Kropp, R. C., & Brewer, S. C. 2014. Spectroscopic analysis of seasonal changes in live fuel moisture content and leaf dry mass. Remote Sensing of Environment, 150, 198-206.

Quintano, C., Fernández-Manso, A., & Fernández-Manso, O. 2018. Combination of Landsat and Sentinel-2 MSI data for initial assessment of burn severity. International journal of applied earth observation and geoinformation, *64*, 221-225.

Rao, K., Williams, A. P., Flefil, J. F., & Konings, A. G. 2020. SAR-enhanced mapping of live fuel moisture content. Remote Sensing of Environment, 245, 111797.

Ryan, K. C. 2002. Dynamic interactions between forest structure and fire behavior in boreal ecosystems. Silva Fennica, 36(1), 13-39.

Schneider, P., Roberts, D.A. and Kyriakidis, P.C., 2008. A VARI-based relative greenness from MODIS data for computing the Fire Potential Index. Remote Sensing of Environment, 112(3), pp.1151-1167.
Scott, J. H., & Burgan, R. E. 2005. Standard fire behavior fuel models: A comprehensive set for use with Rothermel's surface fire spread model. USDA Forest Service, Rocky Mountain Research Station, General Technical Report RMRS-GTR-153

Service, B. C. W. 2022. Wildfire season summary. Province of British Columbia. Retrieved January 27, 2023, from https://www2.gov.bc.ca/gov/content/safety/wildfire-status/about-bcws/wildfire-history/wildfire-season-summary

Stocks, B. J., Fosberg, M. A., Lynham, T. J., Mearns, L., Wotton, B. M., & Yang, Q. 2004. Climate change and forest fire potential in Russian and Canadian boreal forests. Climatic Change, 67(3), 233-249.

Trowbridge, R., & Feller, M. C. 1988. Relationships between the moisture content of fine woody fuels in lodgepole pine slash and the Fine Fuel Moisture Code of the Canadian Forest Fire Weather Index System. Canadian Journal of Forest Research, 18(1), 128-131.

Tucker, C. J. 1979. Red and photographic infrared linear combinations for monitoring vegetation. Remote sensing of Environment, 8(2), 127-150.

Tymstra, C., Stocks, B. J., Cai, X., & Flannigan, M. D. 2020. Wildfire management in Canada: Review, challenges and opportunities. Progress in Disaster Science, 5, 100045.

USGS EROS Archive - Sentinel-2 - Comparison of Sentinel-2 and Landsat | U.S. Geological Survey. 2022. Retrieved from https://www.usgs.gov/centers/eros/science/usgs-eros-archive-sentinel-2

Van Wagner, C. E., & Forest, P. 1987. Development and structure of the Canadian forest fire weather index system. In Can. For. Serv., Forestry Tech. Rep.

Van Wagner, CE, and TL Pickett. 1085. Equations and FORTRAN program for the Canadian forest fire weather index system. Flight. 33. 1985.

Viegas, D. X., Viegas, M. T. S. P., & Ferreira, A. D. 1992. Moisture content of fine forest fuels and fire occurrence in central Portugal. International Journal of Wildland Fire, 2(2), 69-86.

Wang, L., & Qu, J. J. 2007. NMDI: A normalized multi-band drought index for monitoring soil and vegetation moisture with satellite remote sensing. Geophysical Research Letters, 34(20).

Wang, X., Wotton, B. M., Cantin, A. S., Parisien, M. A., Anderson, K., Moore, B., & Flannigan, M. D. 2017. cffdrs: an R package for the Canadian forest fire danger rating system. Ecological Processes, 6(1), 1-11.

Wang, Y., Wei, X., del Campo, A. D., Winkler, R., Wu, J., Li, Q., & Liu, W. 2019. Juvenile thinning can effectively mitigate the effects of drought on tree growth and water consumption in a young Pinus contorta stand in the interior of British Columbia, Canada. Forest Ecology and Management, 454, 117667.

White, J. D., Ryan, K. C., Key, C. C., & Running, S. W. 1996. Remote sensing of forest fire severity and vegetation recovery. International Journal of Wildland Fire, 6(3), 125-136

Williams Lake Community Forest. 2022. Retrieved January 27, 2023, from https://williamslakecommunityforest.com/operations/

Wilson, E. H., & Sader, S. A. 2002. Detection of forest harvest type using multiple dates of Landsat TM imagery. Remote Sensing of Environment, 80(3), 385-396.

Wotton, B. M. 2009. Interpreting and using outputs from the Canadian Forest Fire Danger Rating System in research applications. Environmental and Ecological Statistics, 16(2), 107-131.

Xiong, Q., Wang, Y., Liu, D., Ye, S., Du, Z., Liu, W., Huang, J., Su, W., Zhu, D., Yao, X. and Zhang, X., 2020. A cloud detection approach based on hybrid multispectral features with dynamic thresholds for GF-1 remote sensing images. Remote Sensing, 12(3), p.450.

Yang, Z., Dan, T., & Yang, Y. 2018. Multi-temporal remote sensing image registration using deep convolutional features. Ieee Access, *6*, 38544-38555.

Yebra, M., Dennison, P. E., Chuvieco, E., Riano, D., Zylstra, P., Hunt Jr, E. R., ... & Jurdao, S. 2013. A global review of remote sensing of live fuel moisture content for fire danger assessment: Moving towards operational products. Remote Sensing of Environment, 136, 455-468.

Yoder, B. J., Ryan, M. G., Waring, R. H., Schoettle, A. W., & Kaufmann, M. R. 1994. Evidence of reduced photosynthetic rates in old trees. Forest Science, 40(3), 513-5270.

Zald, H. S., & Dunn, C. J. 2018. Severe fire weather and intensive forest management increase fire severity in a multi-ownership landscape. Ecological Applications, *28*(4), 1068-1080.

Zhang, D., & Zhou, G. 2016. Estimation of soil moisture from optical and thermal remote sensing: A review. *Sensors*, *16*(8), 1308.

Zhu, X., Chen, J., & Gao, F. 2019. Combining Landsat and Sentinel-2 data to improve forest species classification in the northeastern United States. Remote Sensing of Environment, 231, 111228.

Zhou, X., Zhu, X., Dong, Z., & Guo, W. 2016. Estimation of biomass in wheat using random forest regression algorithm and remote sensing data. The Crop Journal, 4(3), 212-219.

Appendix

Appendix 1: Sample sites around Prince George and Smithers

Site Name	Elevation (m)	Latitude	Longitude
North Fraser Juvenile	710	54.24368	-122.48823
North Fraser Mature	698	54.242285	-122.48995
North Fraser Open	698	54.243852	-122.49074
Stone Creek Juvenile	860	53.6139	-122.53723
Stone Creek Mature	895	53.616179	-122.53591
Stone Creek Open	881	53.616222	-122.5379

Tamarac Juvenile	858	53.8701	-123.37023
Tamarac Mature	869	53.872643	-123.36881
Tamarac Open	865	53.871334	-123.37044
Barren Juvenile	1051	54.51044	-126.61434
Barren Mature	1043	54.511318	-126.61125
Barren Open	1059	54.50796	-126.61509
Chapman Juvenile	848	54.8839	-126.62353
Chapman Mature	854	54.882793	-126.6376
Chapman Open	809	54.88272	-126.62893
McDonnell Juvenile	990	54.780862	-127.52063
McDonnell Mature	981	54.781871	-127.50614
McDonnell Open	980	54.78217	-127.51434
Dennis Juvenile	883	54.761853	-127.46593
Dennis Mature	885	54.762177	-127.46537
Dennis Open	885	54.761427	-127.46753

Appendix 2: Sample sites around Prince George and Smithers

Fire Weather Station (FWS)	Elevation (m)	Latitude	Longitude	Sample site name	Distance (km)
Bear Lake	715	54.482	-122.683	North Fraser	27.3
Hixon	615	53.411	-122.596	Stone Creek	22.1
Bednesti	825	53.865	-123.323	Tamarac	3.21
Houston	608	54.394	-126.618	Barren	11
Upper Fulton	900	55.034	-126.8	Chapman	20.1
Pine Creek	1320	54.684	-127.326	McDonnell/Dennis	18.5/12.5

Appendix 3: List of weather stations installed and used in this research in 2021-2022, where Temp=Air temperature (°C), RH= Relative humidity (%), WS=Wind speed (Kph), P=precipitation (mm), NF =North Fraser, SC= Stone Creek, TM=Tamarac, MD=McDonnell, DS=Dennis, Br= Barren, and CP=Chapman. Notice all the tipping buckets and wind sensors at juvenile and mature stands were only installed after mid-summer of 2022. The recoding interval for 30 cm HOBO loggers were set at 15 mins and one hour for open weather stations.

Site Name	Sensor Installed	Parameters measured	Latitude	Longitude	Elevation(m)	Date of data collection
NF Juvenile	Hobo, wind sensor, tipping bucket	TEMP, RH, WS, P	54.243689	-122.48823	710	2021-06-08 to 2022-10-18
NF Mature	Hobo, wind sensor, tipping bucket	TEMP, RH, WS, P	54.242285	-122.48995	698	2021-06-08 to 2022-10-18
NF Open	Hobo, weather station, tipping bucket	TEMP, RH, WS, P	54.243852	-122.49074	698	2021-06-08 to 2022-10-18
SC Juvenile	Hobo, wind sensor, tipping bucket	TEMP, RH, WS, P	53.613937	-122.53723	860	2021-06-09 to 2022-10-18
SC Mature	Hobo, wind sensor, tipping bucket	TEMP, RH, WS, P	53.616179	-122.53591	895	2021-06-09 to 2022-10-18
SC Open	Hobo, weather station, tipping bucket	TEMP, RH, WS, P	53.616222	-122.53790	881	2021-06-09 to 2022-10-18
TM Juvenile	Hobo, wind sensor, tipping bucket	TEMP, RH, WS, P	53.870100	-122.37023	858	2021-06-09 to 2022-10-18
TM Mature	Hobo, wind sensor, tipping bucket	TEMP, RH, WS, P	53.872643	-123.36881	869	2021-06-09 to 2022-10-18
TM Open	Hobo, weather station	TEMP, RH, WS, P	53.871334	-123.37044	865	2021-06-09 to 2022-10-18
MD Juvenile	Hobo	TEMP, RH	54.780862	-127.52063	990	2021-07-08 to 09-03
MD Mature	Hobo	TEMP, RH	54.781871	-127.50614	981	2021-07-08 to 09-03

MD Open	Hobo, weather station	TEMP, RH, WS, P	54.782170	-127.51434	980	2021-07-08 to 09-03
DS Juvenile	Hobo, wind sensor, tipping bucket	TEMP, RH, WS, P	54.761853	-127.46593	883	2022-07-06 to 10-27
DS Mature	Hobo, wind sensor, tipping bucket	TEMP, RH, WS, P	54.762177	-127.46537	885	2022-07-06 to 10-27
DS Open	Hobo, weather station	TEMP, RH, WS, P	54.761427	-127.46753	885	2022-07-06 to 10-27
BR Juvenile	Hobo, wind sensor, tipping bucket	TEMP, RH, WS, P	54.510444	-126.61434	1051	2021-07-09 to 2022-10-27
BR Mature	Hobo, wind sensor, tipping bucket	TEMP, RH, WS, P	54.511318	-126.61125	1043	2021-07-09 to 2022-10-27
BR Open	Hobo, weather station	TEMP, RH, WS, P	54.507960	-126.61509	1059	2021-07-09 to 2022-10-27
CP Juvenile	Hobo, wind sensor, tipping bucket	TEMP, RH, WS, P	54.883900	-126.62353	848	2021-07-09 to 2022-10-27
CP Mature	Hobo, wind sensor, tipping bucket	TEMP, RH, WS, P	54.882793	-126.63760	854	2021-07-09 to 2022-10-27
CP Open	Hobo, weather station	TEMP, RH, WS, P	54.882720	-126.62893	809	2021-07-09 to 2022-10-27

Appendix 4: List of weather stations installed and used in this research in 2021-2022, where T=Air temperature (°C), RH= Relative humidity (%), Wind=Wind speed (Kph), Pre=precipitation (mm), for data precision, the number means precision after 0.

Sensor Name	Data measured	Sampling Frequency	Data precision	Data measured height (m)
Open weather station	T, RH, Wind, Pre	Hourly	T (0.001°C), RH/Pre (0.1%/0.1mm), Wind (0.01kph)	2
Hobo U23 sensors	T, RH	15 mins	T (0.001°C), RH(0.001%)	0.3
Tipping bucket	Pre	hourly	Pre (0.01%)	0.3
Wind speed sensor	wind	15 mins	Wind (0.01mm)	2

Appendix 5: Average and variance of temperature (T, °C), relative humidity (RH, %), wind speed (ws, kph) as well as Precipitation (P, mm) in different stands from data collected in summer of 2022.

Stand	Avg T	Var T	Avg RH	Var RH	Avg ws	Var ws	Avg P	Var P
Juvenile	14.17	10.49	72.71	615.64	0.1	0.03	1.57	18.23
Mature	13.95	11.94	79.64	157.15	0.03	0	1.27	36.62
Open	15.29	14.2	72.61	130.32	0.79	0.4	1.54	22.89

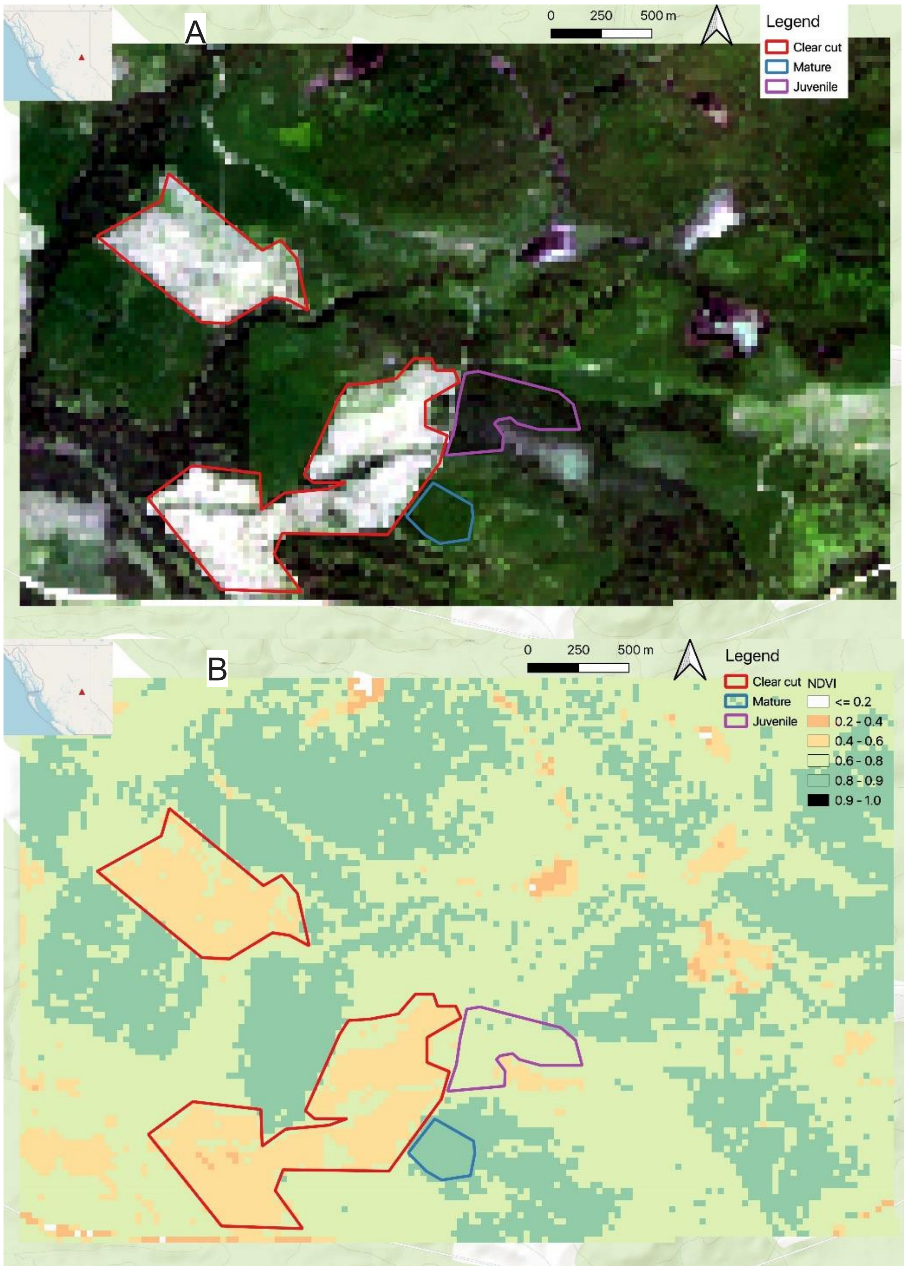

Appendix 6: A) Cloud and shadow-free true colour image, and B) NDVI for the North Fraser site, image captured on June 2nd, 2022, centred at 54.252924 N, 122.499171 W.

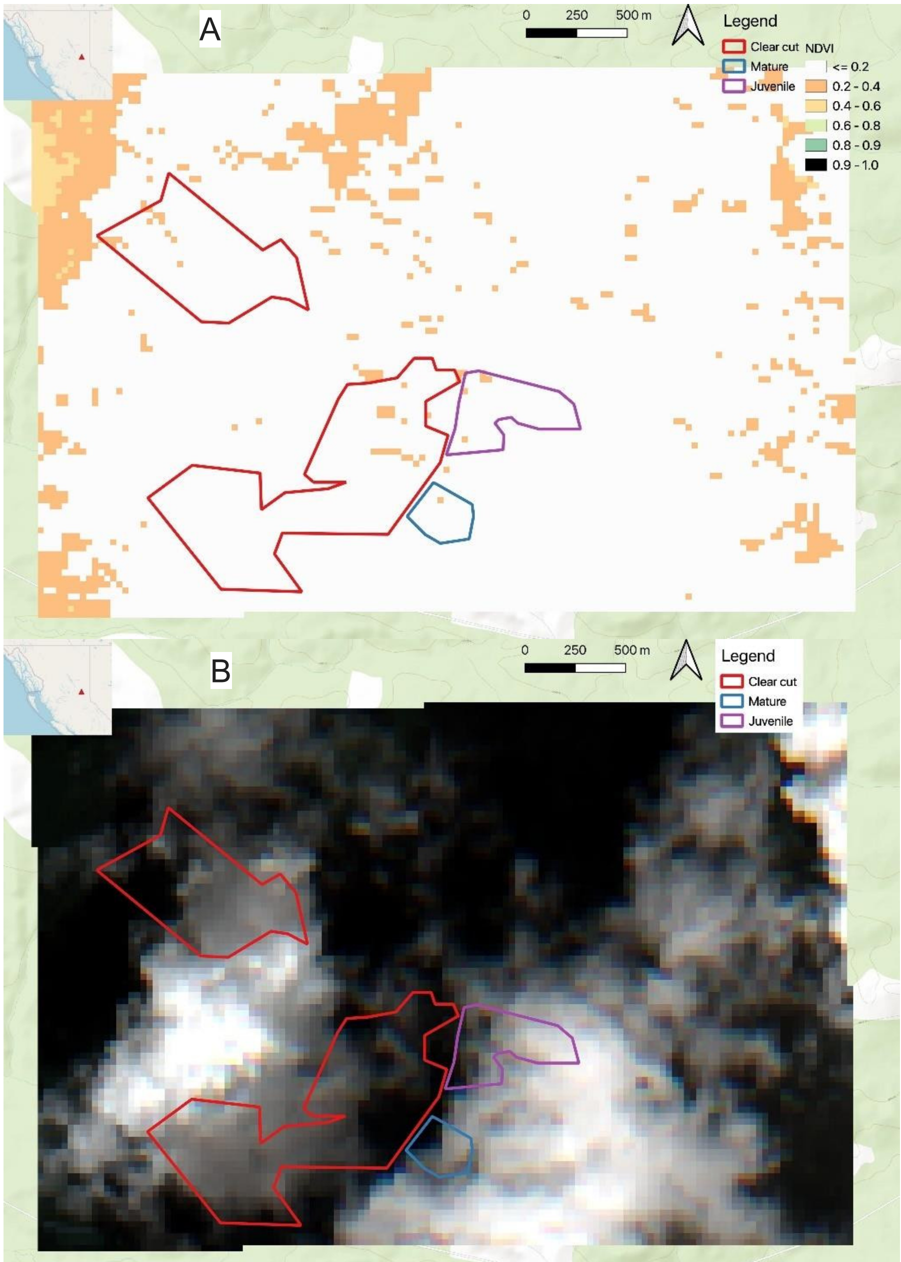

Appendix 7: -A Cloudy and cloud-shadowed true colour image, and B) NDVI for the North Fraser site, image captured on June 4th, 2022, centred at 54.252924 N, 122.499171 W.

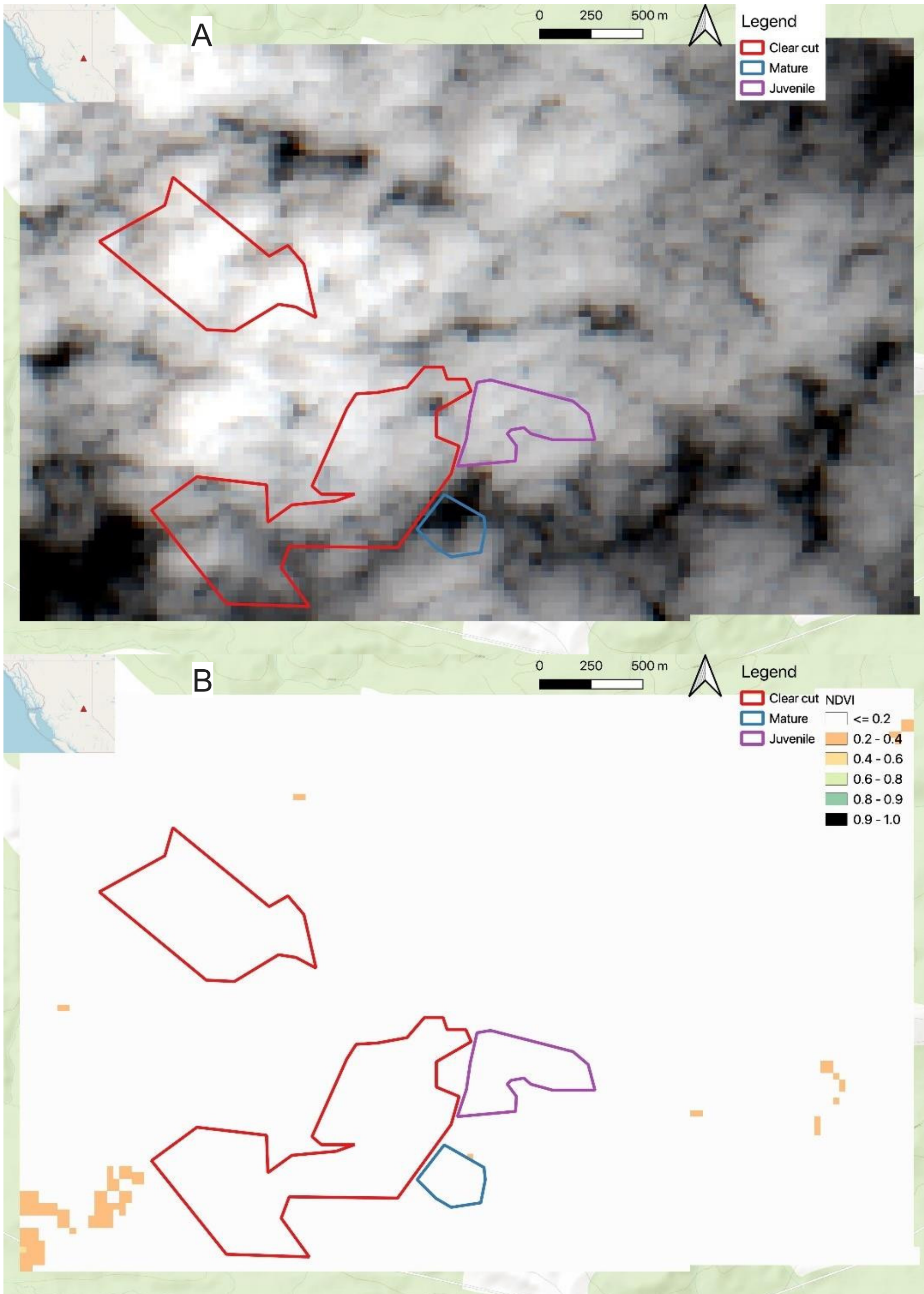

Appendix 8: A) Cloud true colour image, and B) NDVI for the North Fraser site, image captured on June 9th, 2022, centred at 54.252924 N, 122.499171 W.

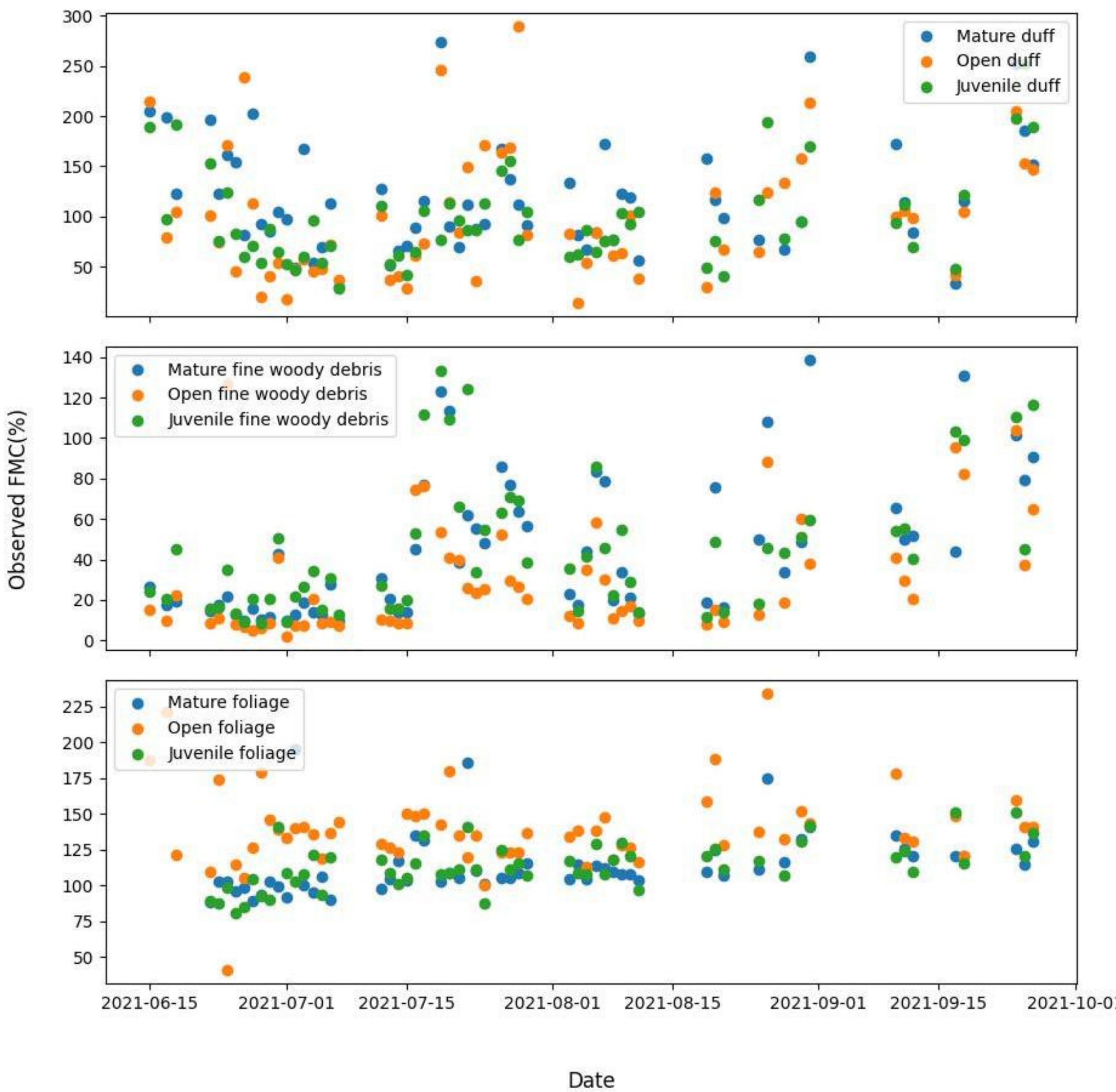

Appendix 9: Daily averaged FMC in 2021 for different stands and fuel types at the Prince George and Smithers study locations. The number of observations averaged to create each point varies between 3 and 15, depending on the number of sites visited.